How to compute consistent nuclear-physics inputs for neutron-star structure and dynamics?

Nicolas Chamel

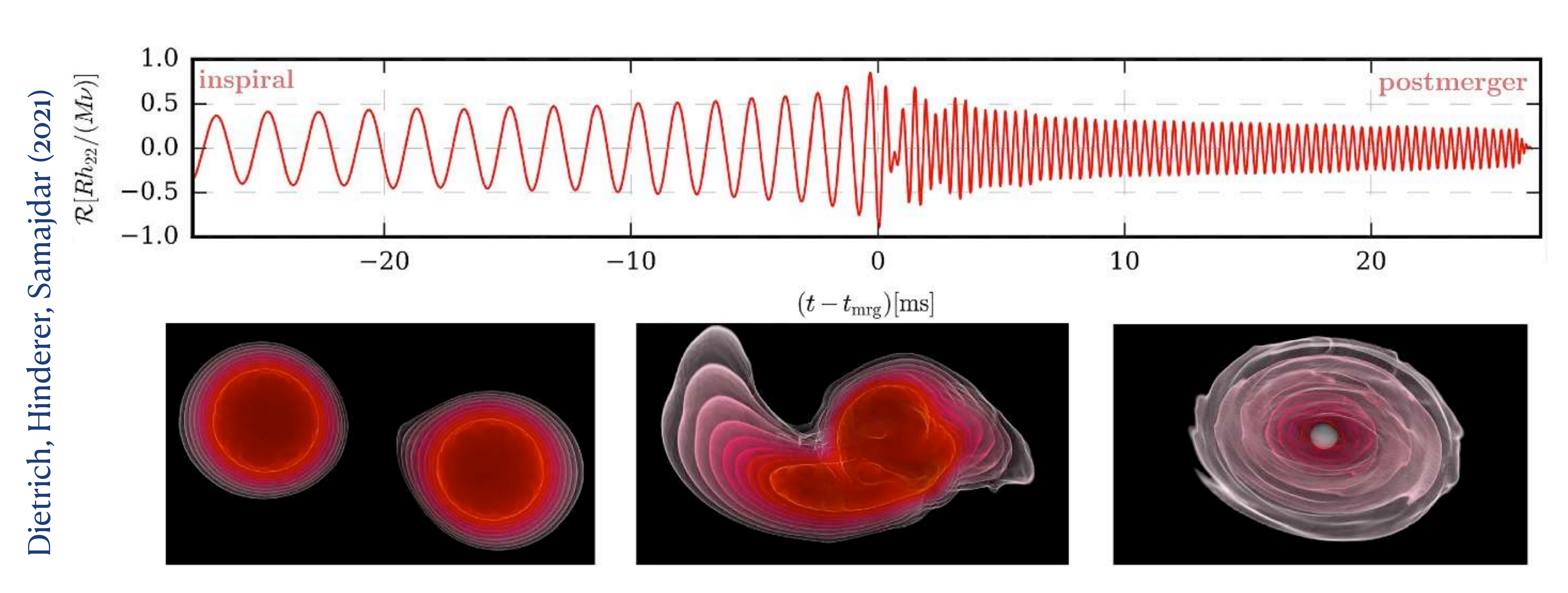








Nuclear physics laboratories



Inspiral

Maximum mass

 Equation of state of cold catalysed matter

Late inspiral

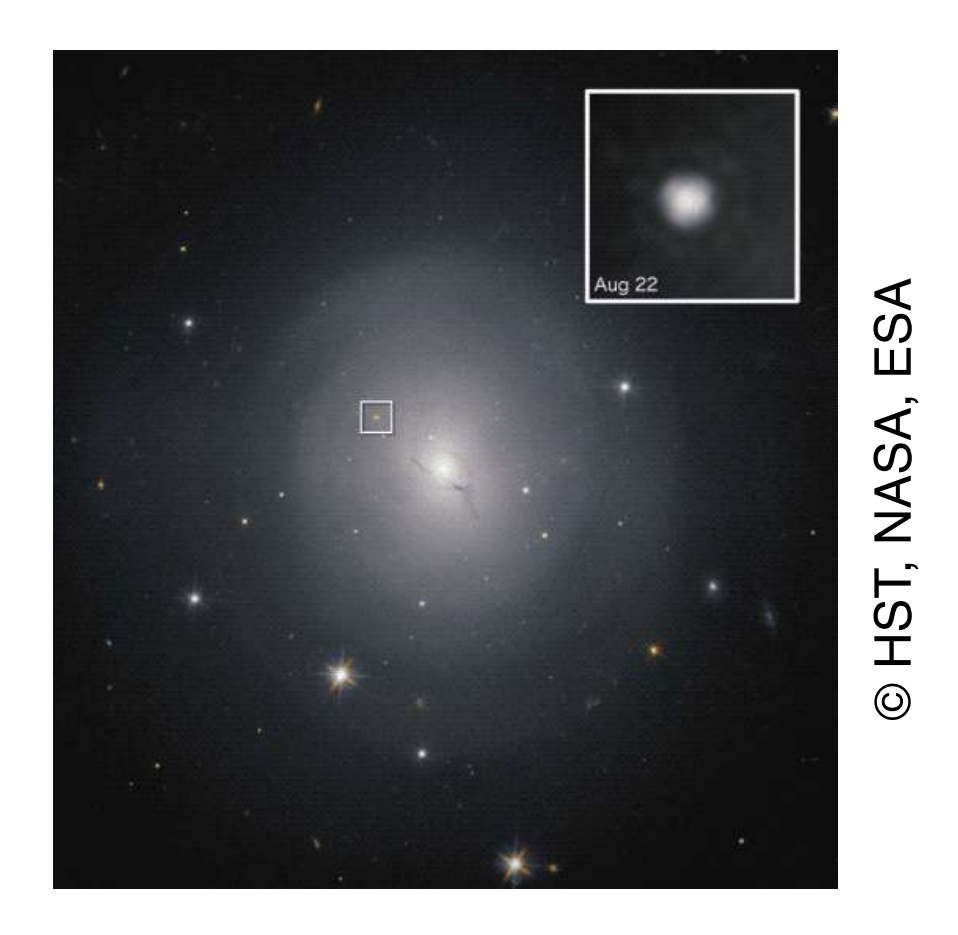
Radius, static & dynamic tides

- Composition
- Elastic constants
- Superfluid properties

Merger and post-merger

Full magnetohydrodynamics

- Equation of state of hot (strongly magnetised?) dense matter off equilibrium
- Electrical and thermal conductivities
- Bulk viscosity, neutrino opacity





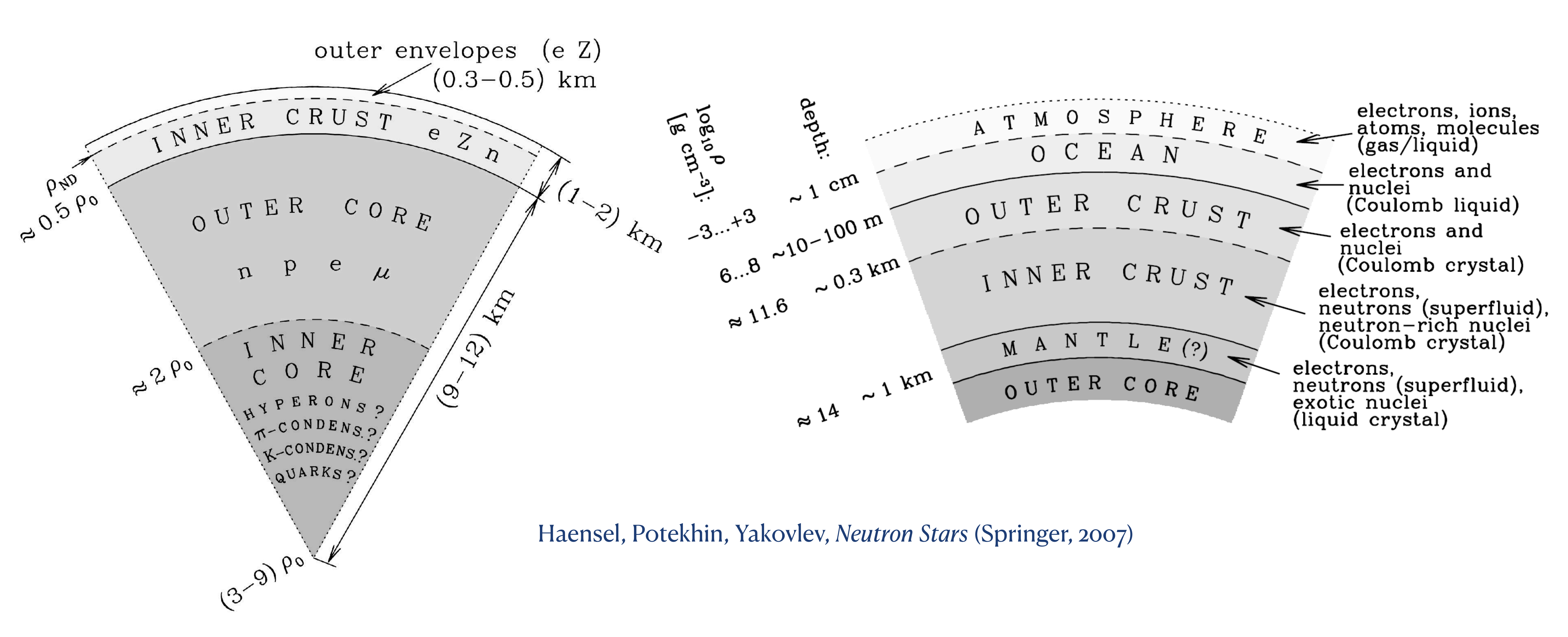
© NASA Goddard Space Flight Center/CI Lab

Kilonova

R-process nucleosynthesis

- Neutron capture and beta decay rates
- Fission rates and yields
- Nuclear masses

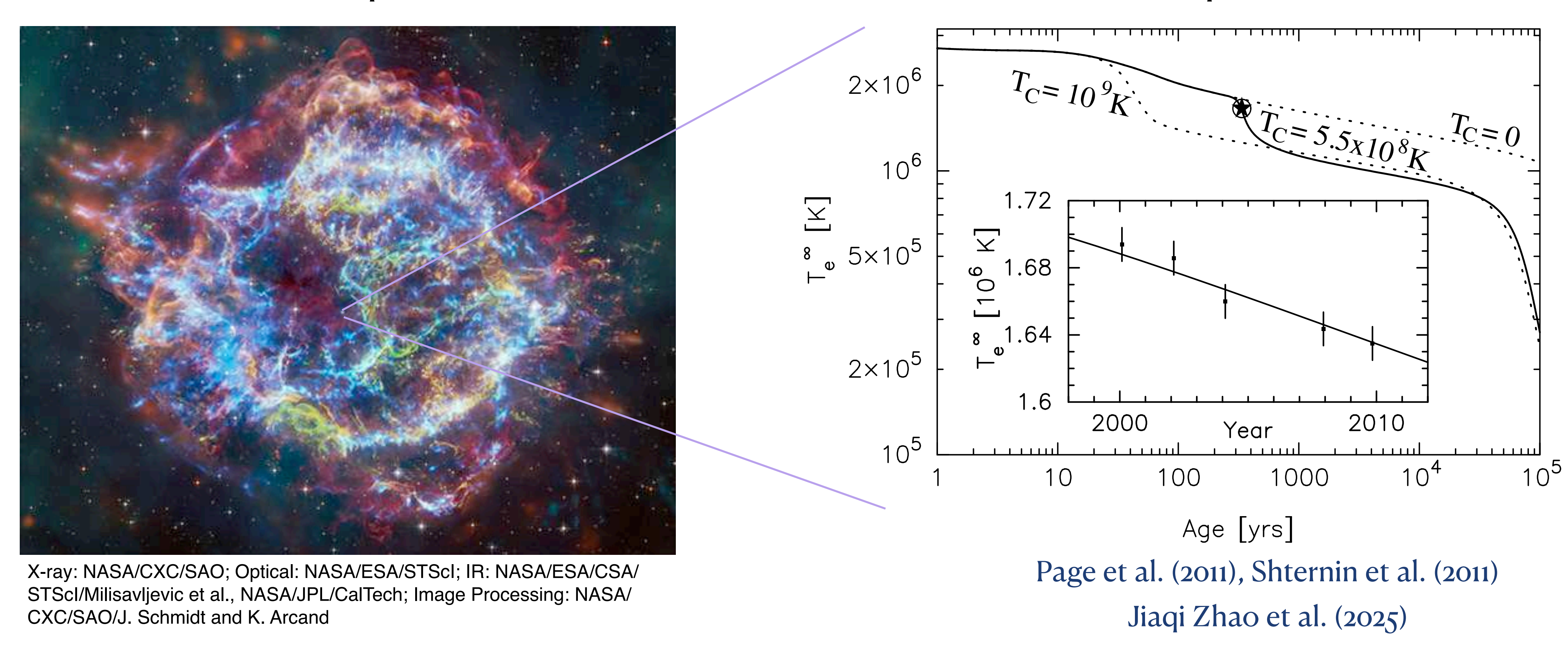
Internal constitution of a neutron star



Describing the interior of a neutron star consistently is very challenging because of the huge range of densities encountered

Cold catalysed matter

Neutron stars are initially very hot ($T\sim 10^{12}$ K) but cool down to 10^9 K within days. The youngest and hottest observed neutron star in Cassiopeia A is about three centuries old and has an internal temperature $T\sim 10^8$ K ($\sim 10^{-2}$ MeV).



Isolated neutron stars are assumed to be at the end point of thermonuclear evolution: their interior is in **full thermodynamic equilibrium at zero temperature** (ground state).

INSTITUT INTERNATIONAL DE PHYSIQUE SOLVAY

XI° CONSEIL DE PHYSIQUE - BRUXELLES 9 - 14 JUIN 1958

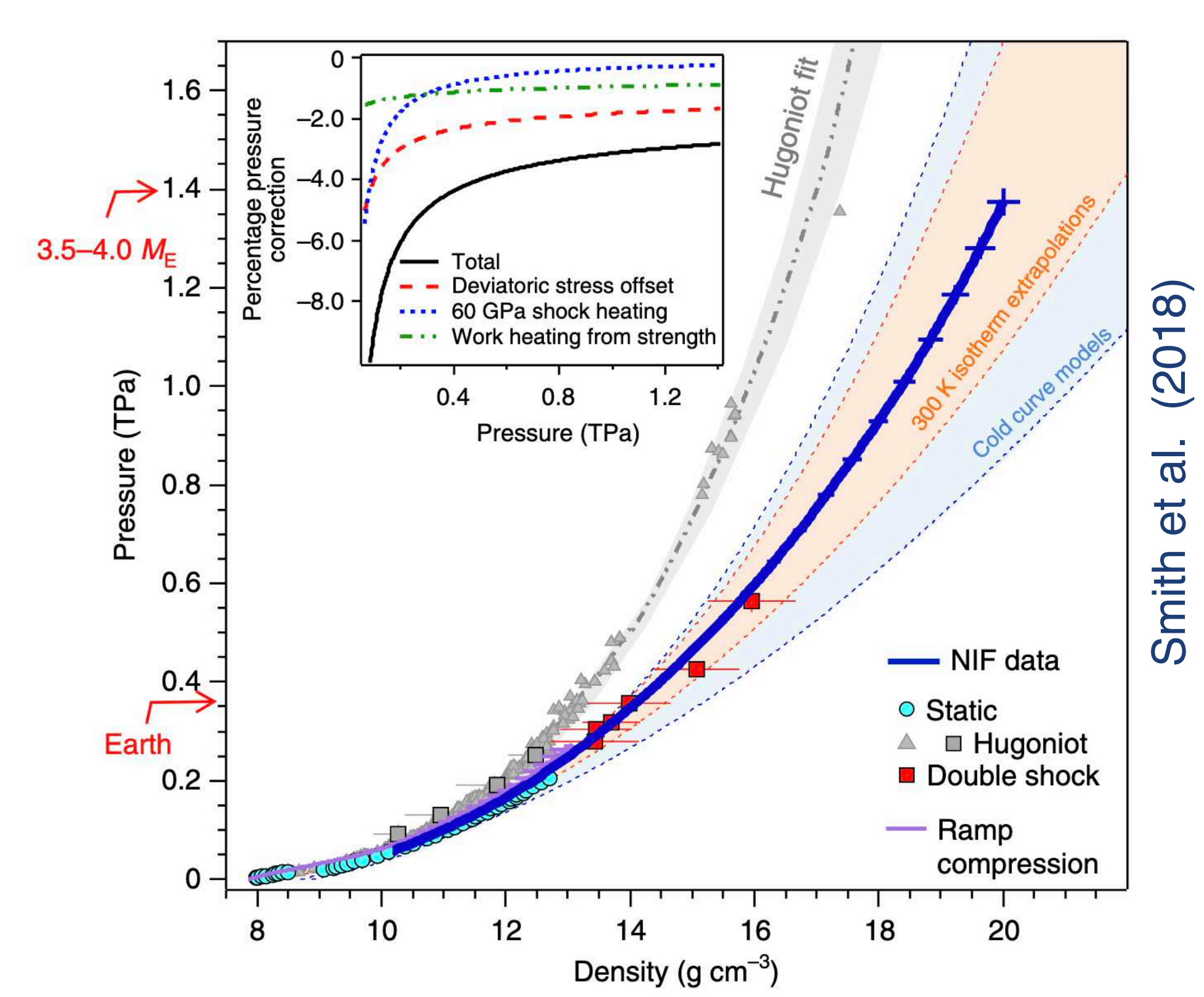


Photo Coopmans, rue du Maquis, 114, Bruxelles.

	F. HOYLE		H. C. van de HULST	A. R. SANDAGE	J. A. WHEELER	н. :	ZANSTRA	L. LEDOUX	
O. S. KLEIN	W. W. MORGAN	B. V. KUKASKIN	M. FIERZ	W. BAADE	H. B	ONDI T. GOLD	L. ROSENFELD	A. C. B. LOYELL	J. GÉHÉNIAU
		V. A. AMBARZUMIAN		E. SCHATZMAN					
W. H. Mc CREA	J. H. OORT	G. LEMAITRE	C. J. GORTER	W. PAULI	SIF W. L. BRAGG	J. R. OPPENHEIMER	C. MØLLEI	R H. SHAPLEY	O. HECKMANN

Neutron star surfaces

The surface of a neutron star is expected to be made of iron, the end product of stellar nucleosynthesis.



Compressed iron can be studied with nuclear explosions and laser-driven shock-wave experiments...

But at pressures corresponding to less than 1 mm below the surface!

Ab initio calculations predict various structural phase transitions: iron is expected to have a **body-centered cubic** (bcc) crystal lattice structure at very high pressures.

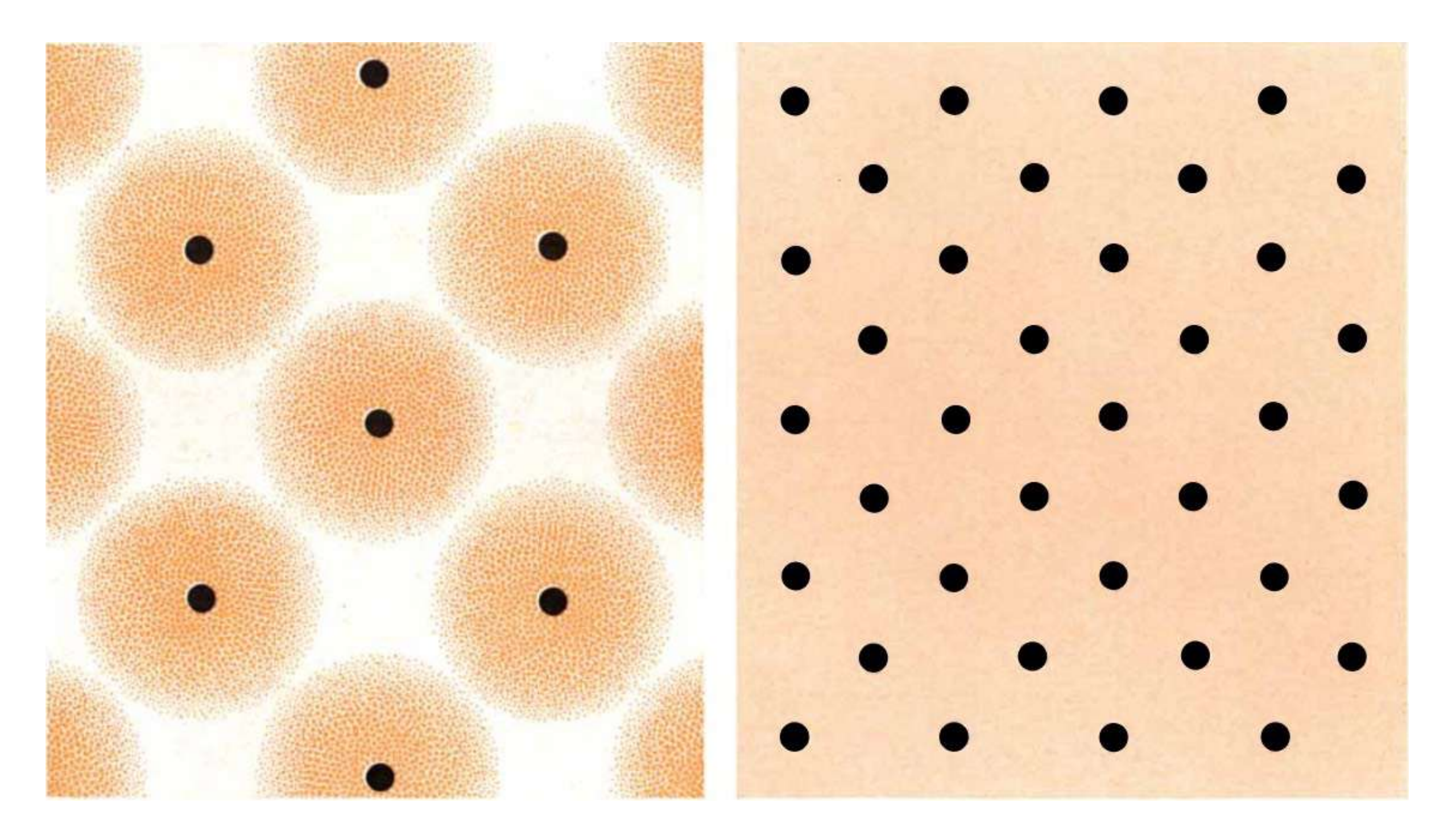
Belonoshko et al. (2017)



Atomium in Brussels, Belgium representing the conventional cubic cell of iron magnified 165 billion times

Coulomb crystal plasma

At a density $\rho_{\rm eip} \approx 2 \times 10^4$ g cm⁻³ (about 22 cm below the surface), the interatomic spacing becomes comparable with the atomic radius.



Ruderman (1971)

At densities $\rho \gg \rho_{\rm eip}$, atoms are crushed into a dense crystal of bare nuclei in a degenerate electron Fermi gas.

Gravitational stratification and matter neutronization

The crust is stratified into pure layers composed of nuclei (Z,A). The pressure is mainly determined by electrons.



At the interface between adjacent layers, the pressure $P \approx P_e(n_e)$ therefore the electron number density n_e must be continuous (hydrostatic equilibrium).

- Electric charge neutrality $n_e = \frac{Z_1}{A_1} \bar{n}_1 = \frac{Z_2}{A_2} \bar{n}_2$
- Le Chatelier-Braun principle $\bar{n}_2 > \bar{n}_1 \Rightarrow \frac{Z_2}{A_2} < \frac{Z_1}{A_1}$
- Electron chemical potential $\mu_e^{1\to 2} > 0 \Rightarrow \frac{M(A_2, Z_2)}{A_2} > \frac{M(A_1, Z_1)}{A_1}$

With increasing depth, **nuclei become more neutron rich** until neutrons "drip" out marking the transition to the inner crust, where nuclei coexist with free neutrons and electrons.

Chamel et al. (2015), Chamel & Fantina (2016)

Description of the outer crust of a neutron star

Traditional approach: numerical minimization of the Gibbs free energy per nucleon at different pressures

Tondeur (1971), BPS (1971)

- layers can be easily missed if δP is not small enough!
- numerically costly (BPS considered 130 even nuclei only vs ~104)

New approach: iterative minimization of the transition pressures between adjacent crustal layers (approximate analytical formulas)

- very accurate and reliable $\delta P/P \sim 10^{-3} \%$
- composition and stratification (depths, abundances) are obtained for free
- ~ 10⁶ times faster

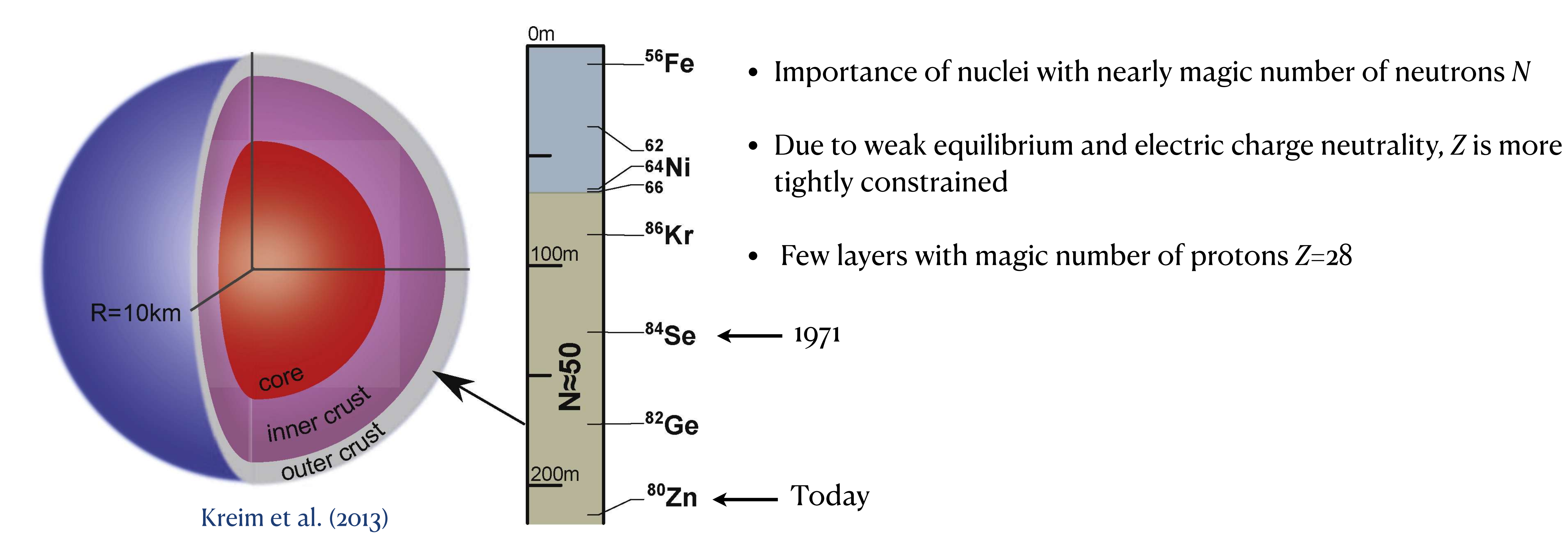
Chamel (2020)

Nuclear-physics inputs: Masses of all atomic nuclei

Freely available computer code: http://doi.org/10.5281/zenodo.3719439

Experimentally determined layers

The composition is completely determined by experimental data down to ~ 200 m for a 1.4 M_{\odot} neutron star with a radius of 10 km.



In 1971, the crust was experimentally known down to the layer of 84 Se at density 8×10^9 g cm⁻³ Today, the limit is at 6×10^{10} g cm⁻³

Plumbing neutron stars to new depths

Precision mass measurements of 82Zn by the ISOLTRAP collaboration at CERN ISOLDE radioactive-beam facility allowed to reach the layer of 80Zn in 2013.

Nuclei in the layers beneath must be such that

- Z/A < 0.375
- M(A,Z)/A>930.848 MeV.

This rules out the doubly magic nuclei 48 Ca, 48 Ni, and 56 Ni (since Z/A = 0.417, 0.583 and 0.5 respectively) but not 78 Ni (Z/A = 0.359).

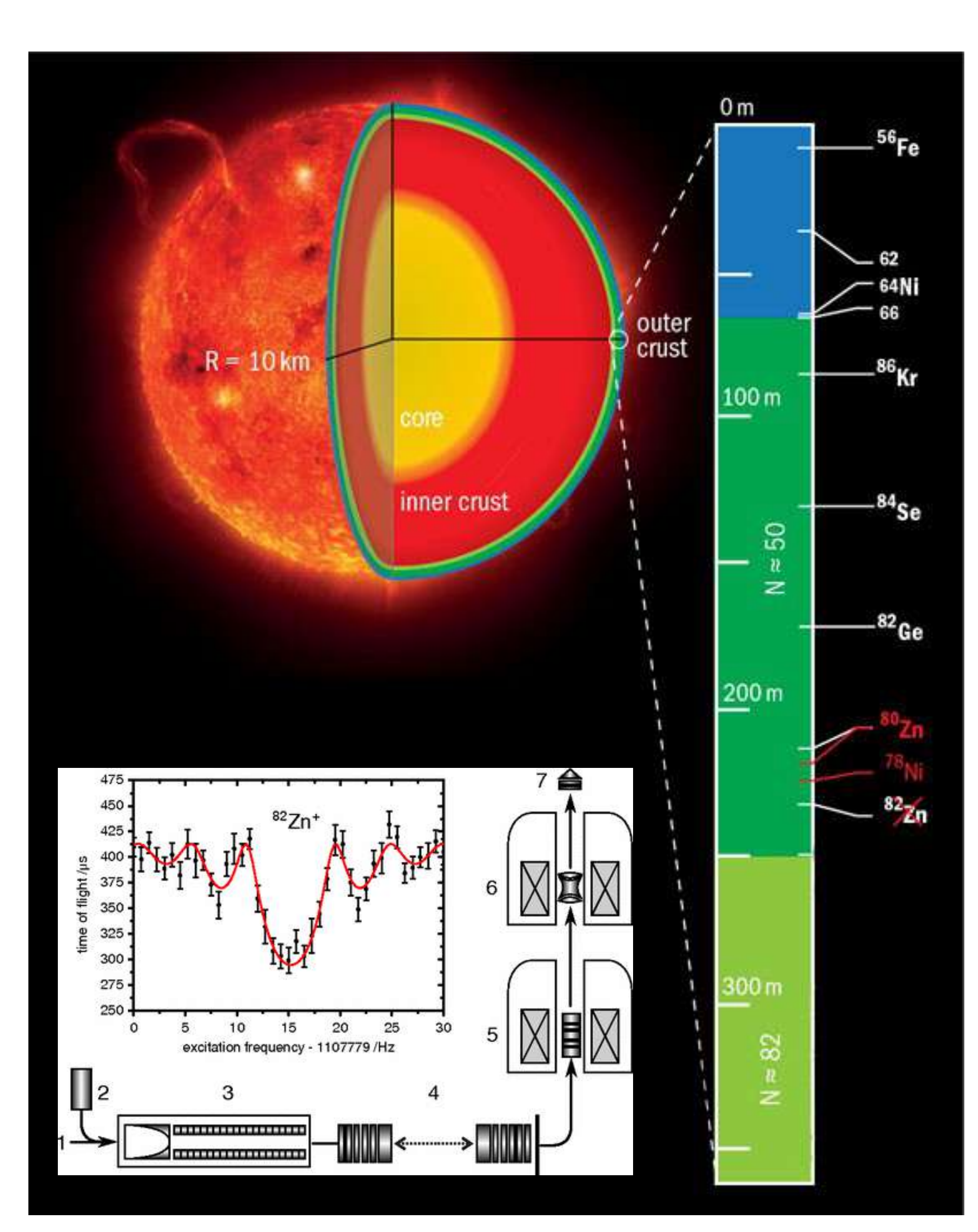
Precision mass measurements of nuclei with $Z\sim40$ and $N\sim82$ are crucially needed!

To drill deeper, nuclear mass models must be used.

Lunney et al. (2003)

Models based on machine learning fit the data very precisely Utama et al. (2016), Shelley & Pastore (2021)

- but their predictions for unmeasured nuclei are not necessarily accurate
- they are not applicable to the inner crust and core

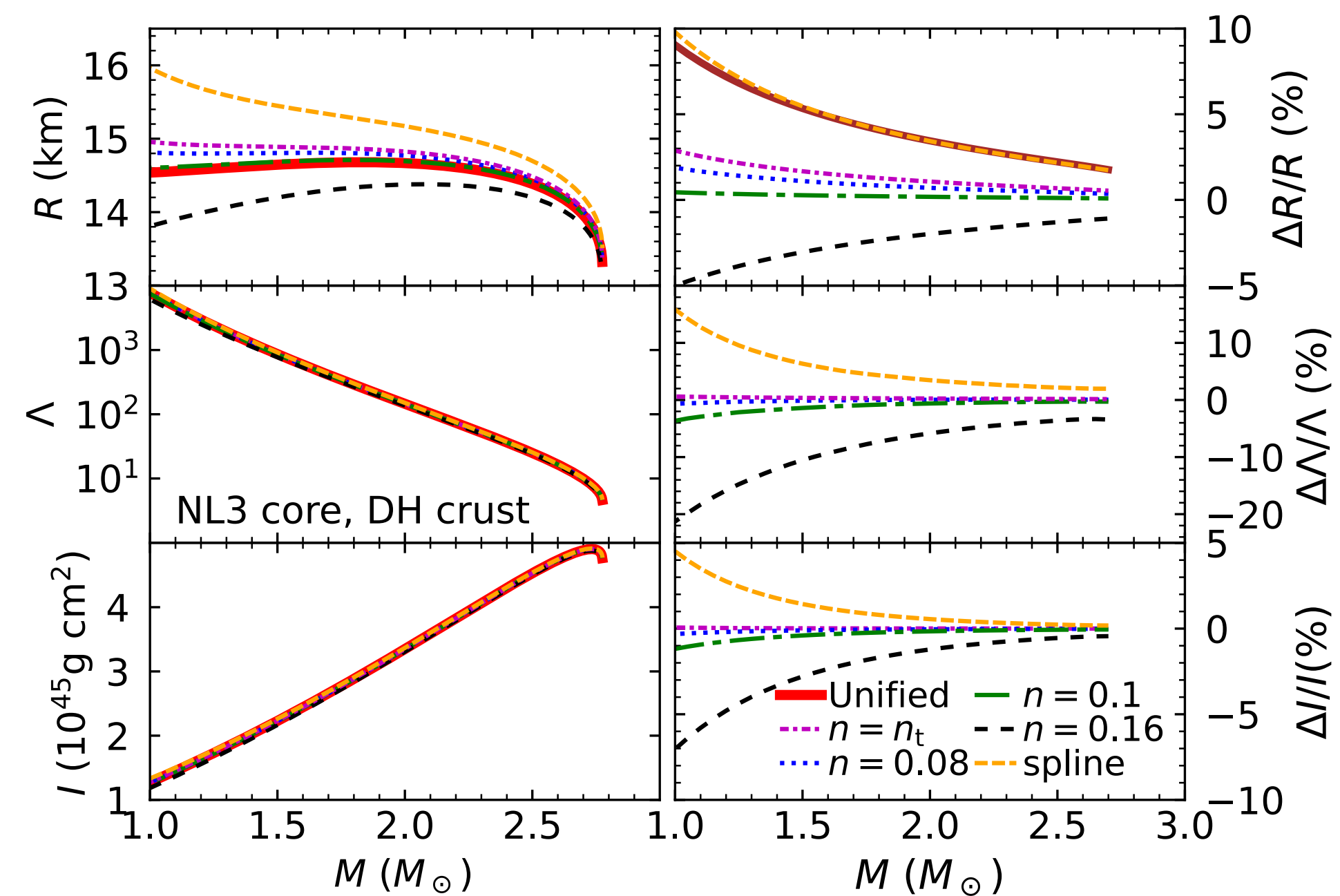


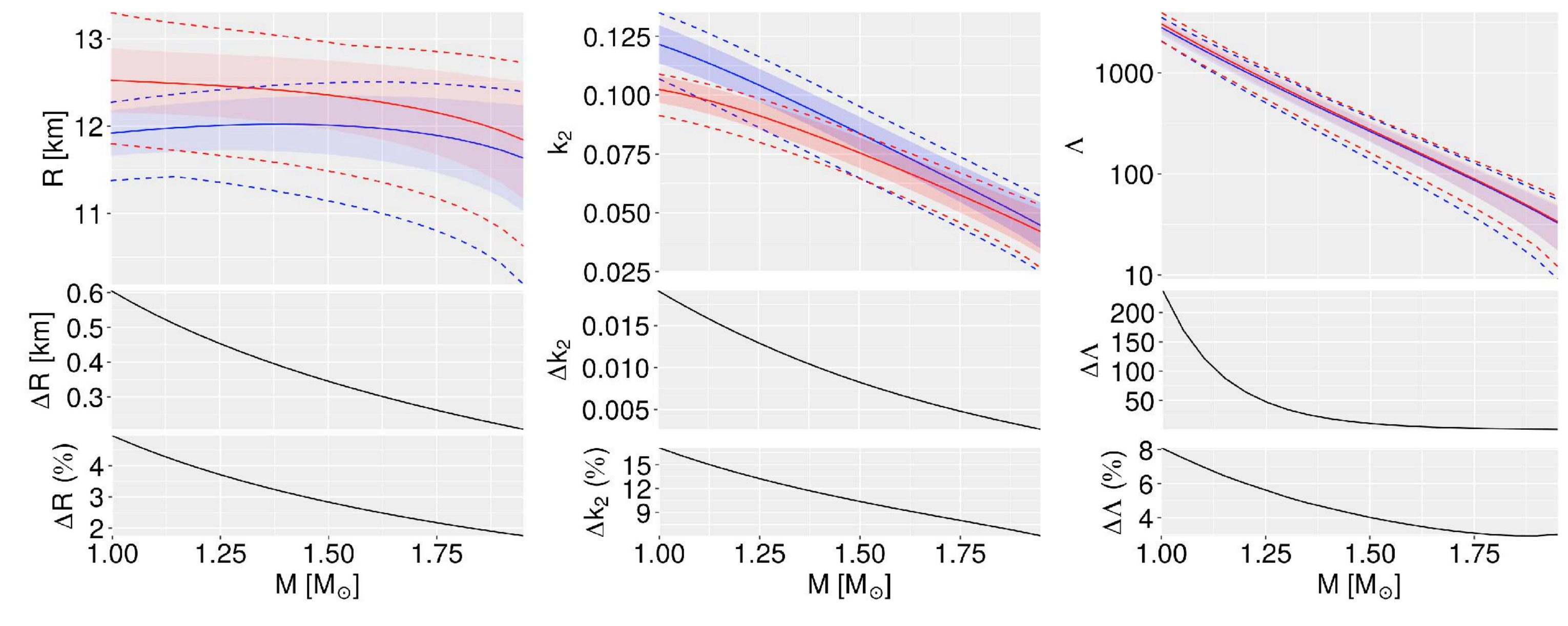
Inconsistencies in the equation of state

Different models for the neutron-star crust and core are usually employed. However, thermodynamic inconsistencies can lead to significant errors on the radius and tidal deformability.

Matching at constant baryon chemical potential vs constant energy density

Ferreira & Providência (2020)





Matching

- at different baryon densities
- using a cubic spline interpolation of pressure vs energy density

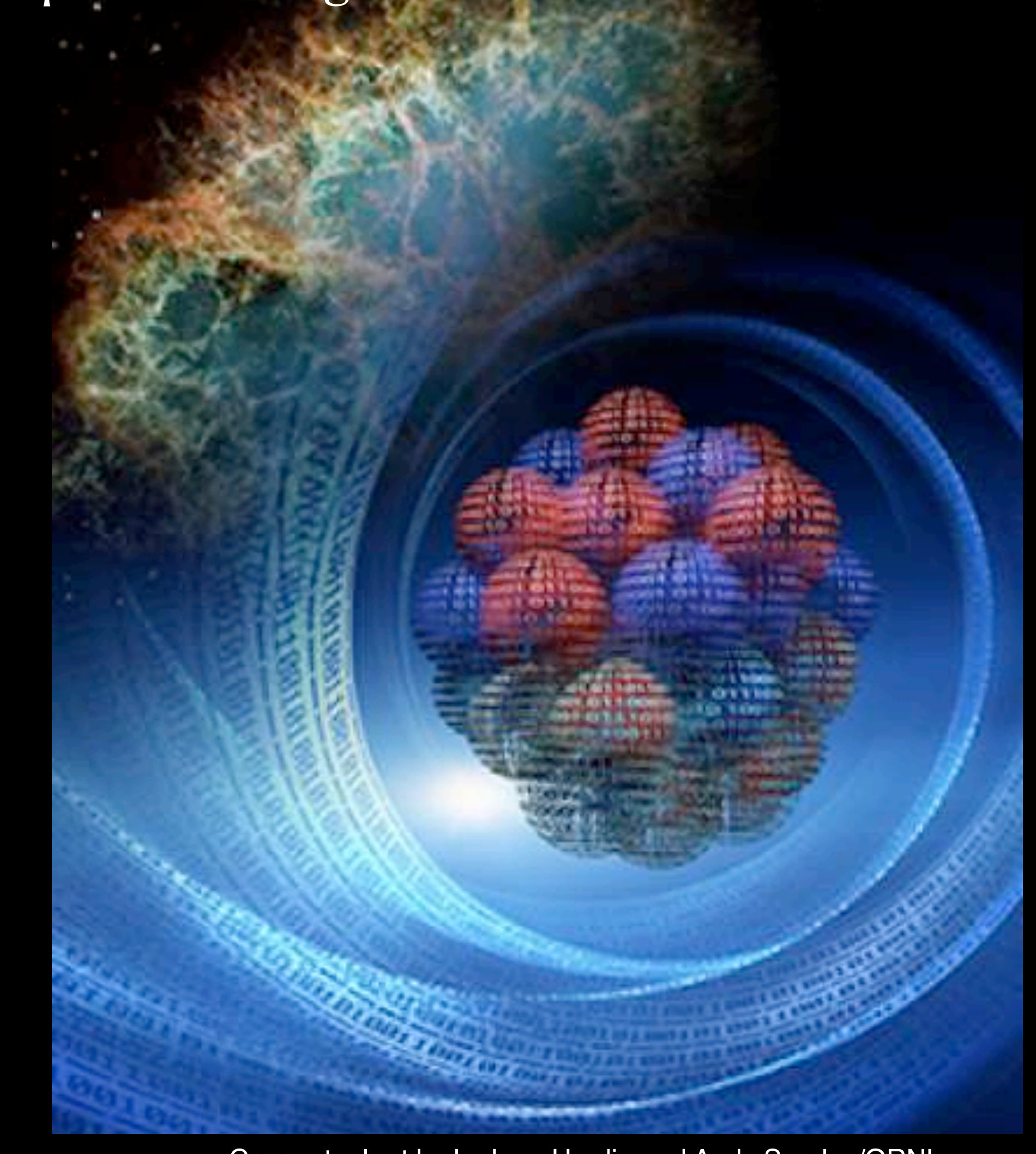
Suleiman et al. (2021)

Errors can reach ~10% for the radius and tidal deformability

Nuclear energy density functional (EDF) theory

This theory allows for a unified and thermodynamically consistent description of all regions of neutron stars

- microscopic: self-consistent quantum approach
- numerically tractable: allows for systematic calculations over a wide range of thermodynamic conditions (temperature, pressure, composition, magnetic fields)
- not restricted to nucleons: possibility to include hyperons
- time-dependent extension: quantum dynamics
- versatile: not only for the equation of state, but also transport properties, reaction rates, neutrino opacity, etc.

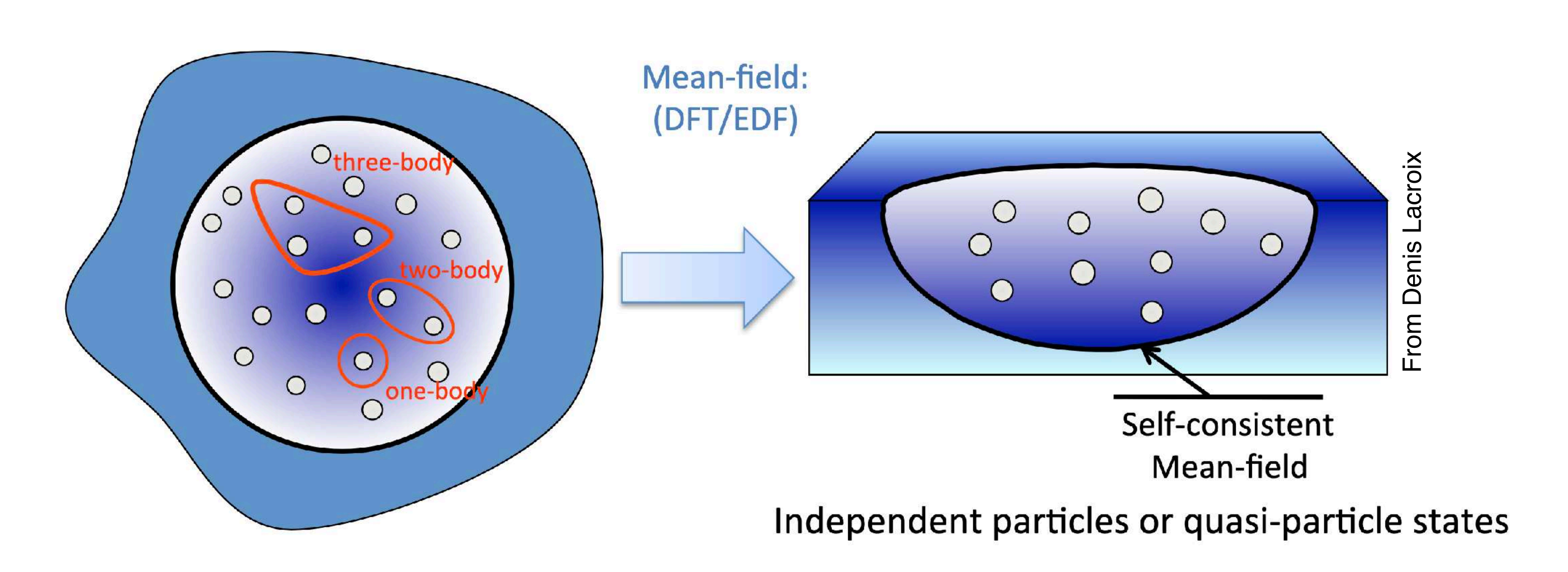


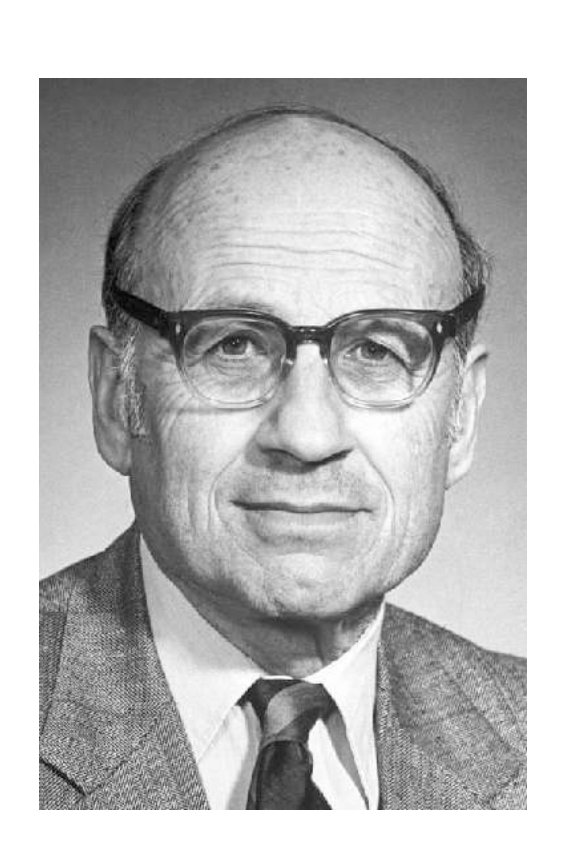
Nuclear energy density functional (EDF) theory

The density functional theory (DFT) was developed in the 1960's for electrons in molecules and solids...

...and independently in the 1970's for nucleons in atomic nuclei

The many-body problem reduced to an effective one-body problem (Kohn-Sham equations)





Walter Kohn Nobel Prize 1998

For historical reason, the nuclear DFT is often referred to as a "mean field method" even though it includes beyond mean field effects with respect to the underlying realistic nucleon-nucleon interactions

Nuclear energy density functional (EDF) theory

In practice, one must solve the coupled **Hartree-Fock-Bogoliubov** (HFB) equations for both neutrons and protons (q=n,p):

$$i\hbar \frac{\partial}{\partial t} \begin{pmatrix} \psi_1^{(q)}(\mathbf{r}, \sigma) \\ \psi_2^{(q)}(\mathbf{r}, \sigma) \end{pmatrix} = \sum_{\sigma'} \begin{pmatrix} h_q'(\mathbf{r})_{\sigma\sigma'} & \Delta_q(\mathbf{r})\delta_{\sigma\sigma'} \\ \Delta_q(\mathbf{r})^* \delta_{\sigma\sigma'} & -\sigma\sigma' h_q'(\mathbf{r})^*_{-\sigma-\sigma'} \end{pmatrix} \begin{pmatrix} \psi_1^{(q)}(\mathbf{r}, \sigma') \\ \psi_2^{(q)}(\mathbf{r}, \sigma') \end{pmatrix}$$

$$h_q'(\mathbf{r})_{\sigma'\sigma} \equiv \left[-\nabla \cdot \frac{\delta E}{\delta \tau_q(\mathbf{r})} \nabla + \frac{\delta E}{\delta n_q(\mathbf{r})} - \lambda_q \right] \delta_{\sigma\sigma'} - i \frac{\delta E}{\delta \mathbf{J_q}(\mathbf{r})} \cdot \nabla \times \hat{\boldsymbol{\sigma}}_{\sigma'\sigma} + \dots \text{ is an effective single-particle hamiltonian}$$

$$\Delta_q(\mathbf{r}) = 2 \frac{\delta E}{\delta \widetilde{n}_a(\mathbf{r})^*}$$
 is the potential responsible for nucleon pairing and nuclear superfluidity

 $n_q(\mathbf{r})$, $\tau_q(\mathbf{r})$, $J_q(\mathbf{r})$, $\widetilde{n}_q(\mathbf{r})$... are local densities and currents defined from the density matrices

$$n_q(\mathbf{r}, \sigma; \mathbf{r'}, \sigma') = \langle \Psi | c_q(\mathbf{r'}, \sigma')^{\dagger} c_q(\mathbf{r}, \sigma) | \Psi \rangle$$

$$\widetilde{n}_{q}(\mathbf{r},\sigma;\mathbf{r'},\sigma') = -\sigma'\langle\Psi|c_{q}(\mathbf{r'},-\sigma')c_{q}(\mathbf{r},\sigma)|\Psi\rangle$$

which in turn depend on $\psi_{1,2}^{(q)}(\boldsymbol{r},\sigma)$

In principle, the nuclear EDF theory is exact. But the exact functional is unknown! In practice, phenomenological functionals must be used.

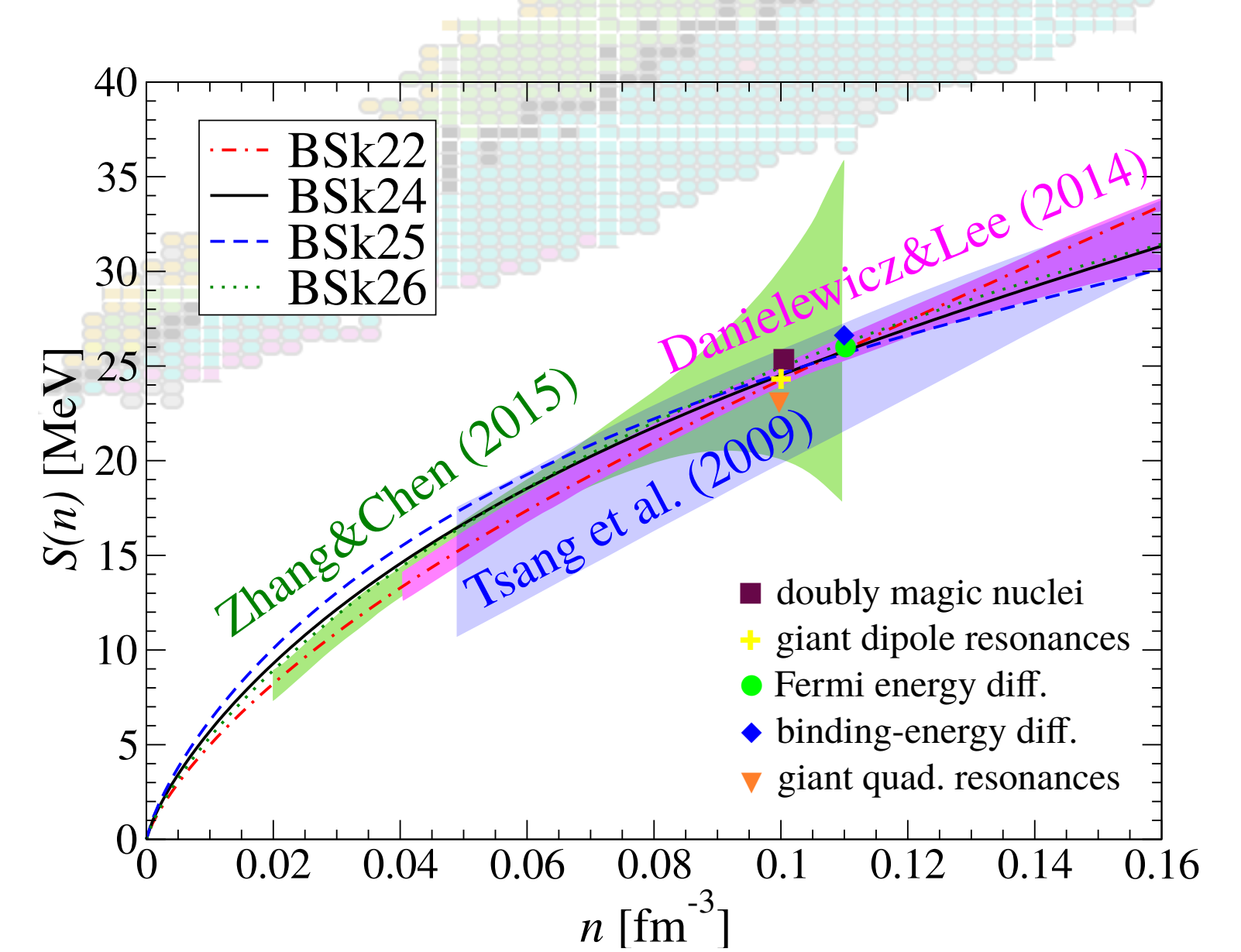
Approaching the exact functional

Brussels functionals have been accurately calibrated to a large set of experimental data

- ~ 2300 atomic masses from the Atomic Mass Evaluation (rms: 0.5-0.6 MeV)
- ~ 900 nuclear charge radii (rms: 0.02-0.03 fm)
 - 45 fission barriers (rms: 0.3-0.5 MeV)

Brussels functionals are based on extended Skyrme interactions:

- Removal of spurious spin-isospin instabilities (BSk18)
- Realistic neutron matter equations of state from soft to stiff (BSk19-21)
- Symmetry energy coefficient varied between 30 and 32 MeV (BSk22-26)
- Generalised spin-orbit coupling (BSk29)
- Realistic ¹S₀ pairing gaps in symmetric matter and neutron matter (BSk30-32)

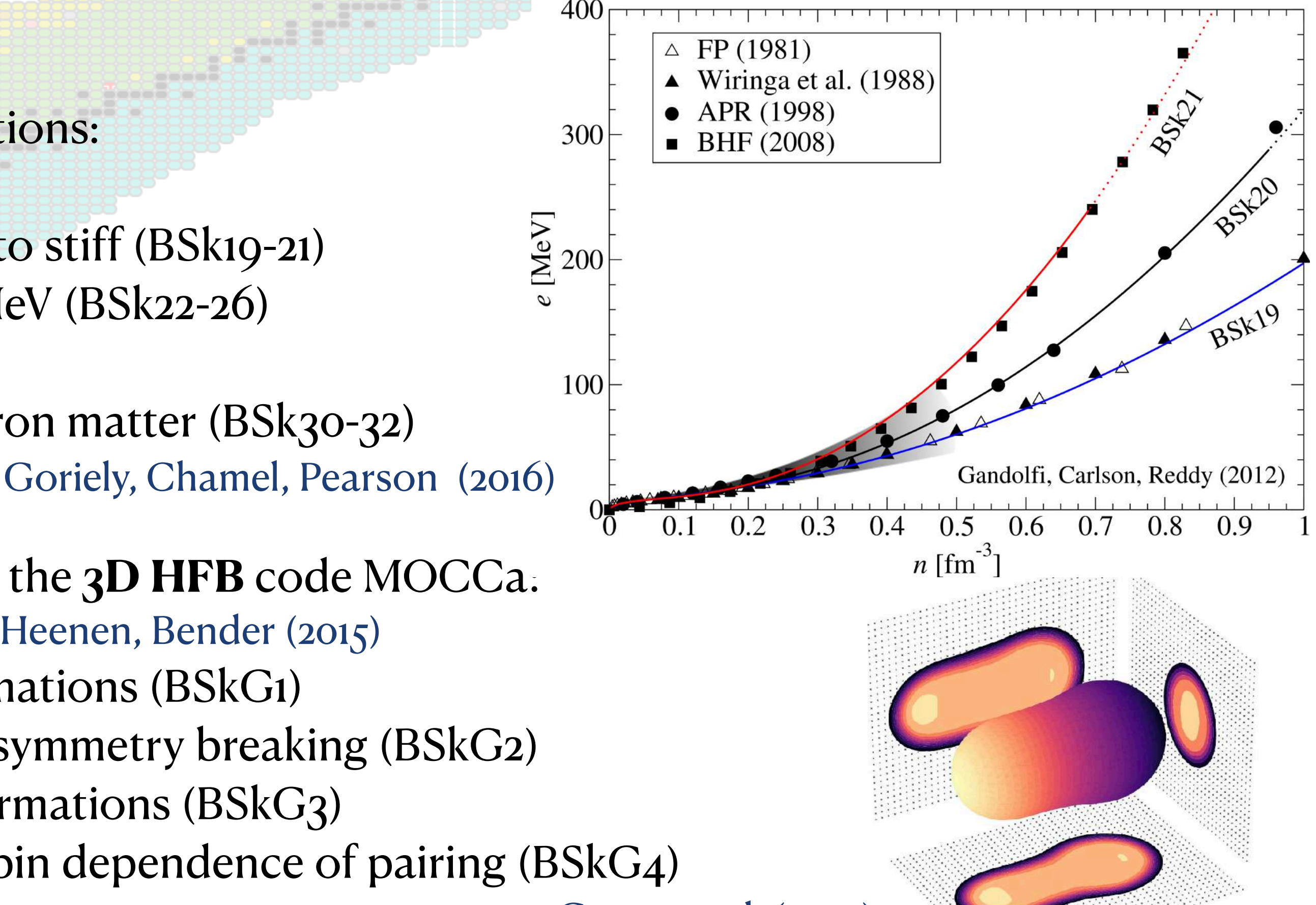


New family using the 3D HFB code MOCCa.

Ryssens, Heenen, Bender (2015)

- Triaxial deformations (BSkG1)
- Time-reversal symmetry breaking (BSkG2)
- Octupole deformations (BSkG3)
- Improved isospin dependence of pairing (BSkG₄)

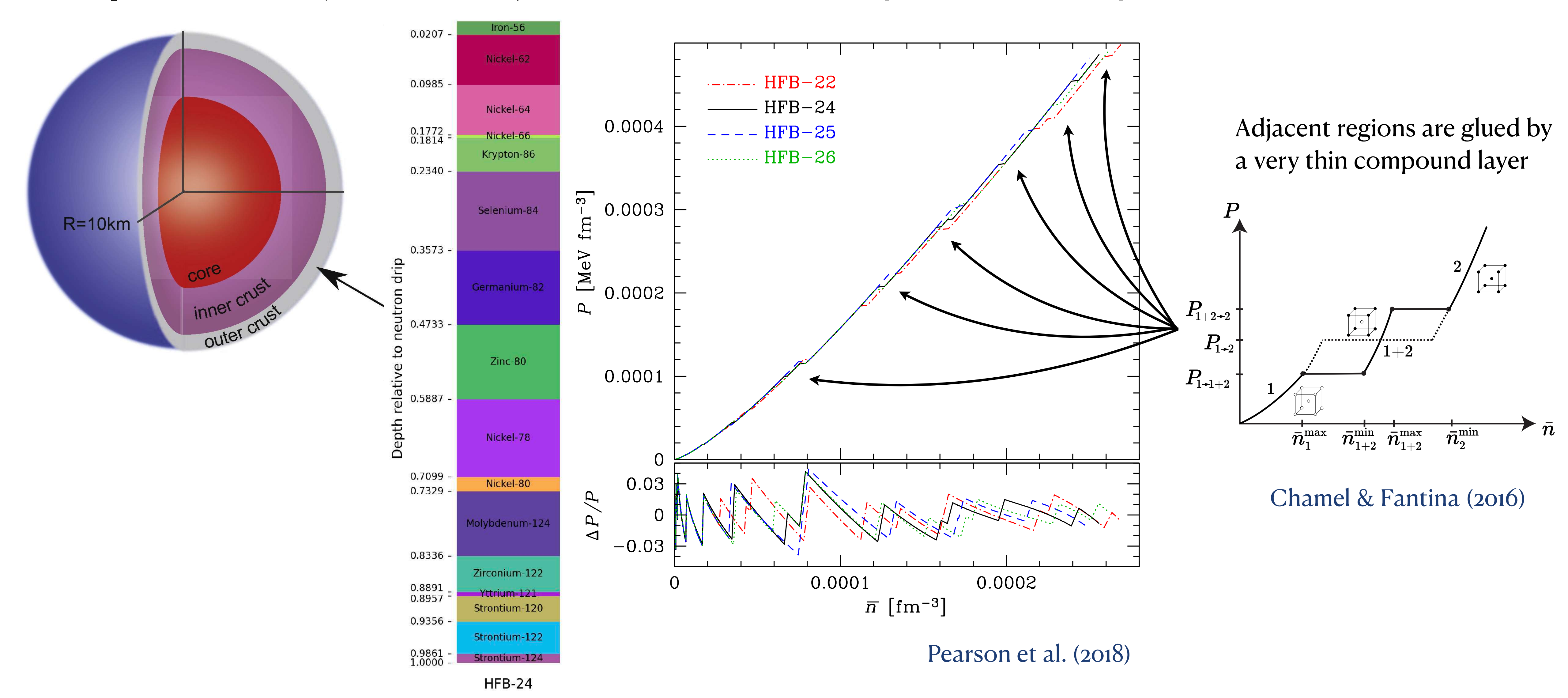
Grams et al. (2025)



Brussels functionals were developed for nucleosynthesis and neutron stars

Outer crust composition and equation of state

The pressure is mainly determined by electrons, and is almost independent of the composition.

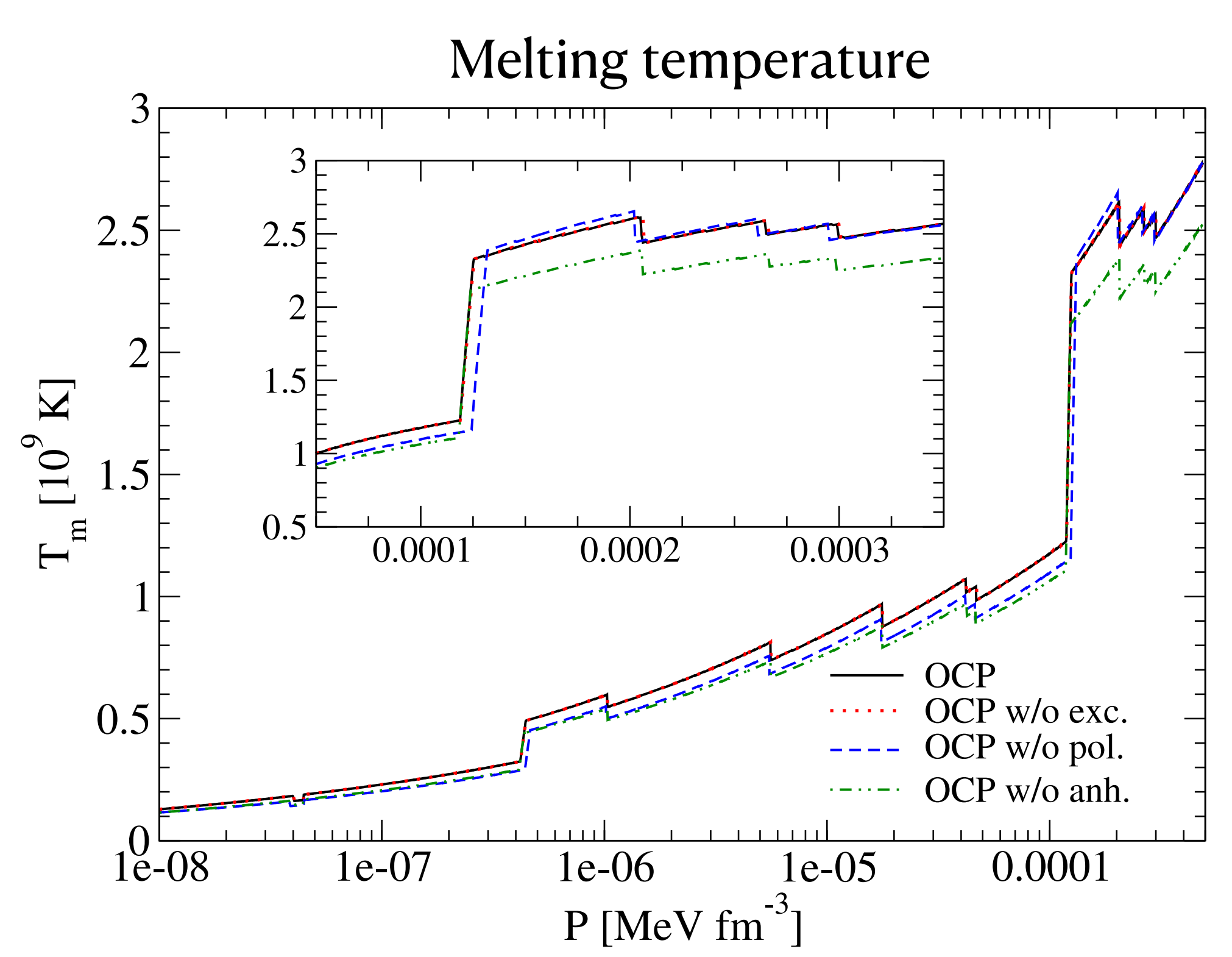


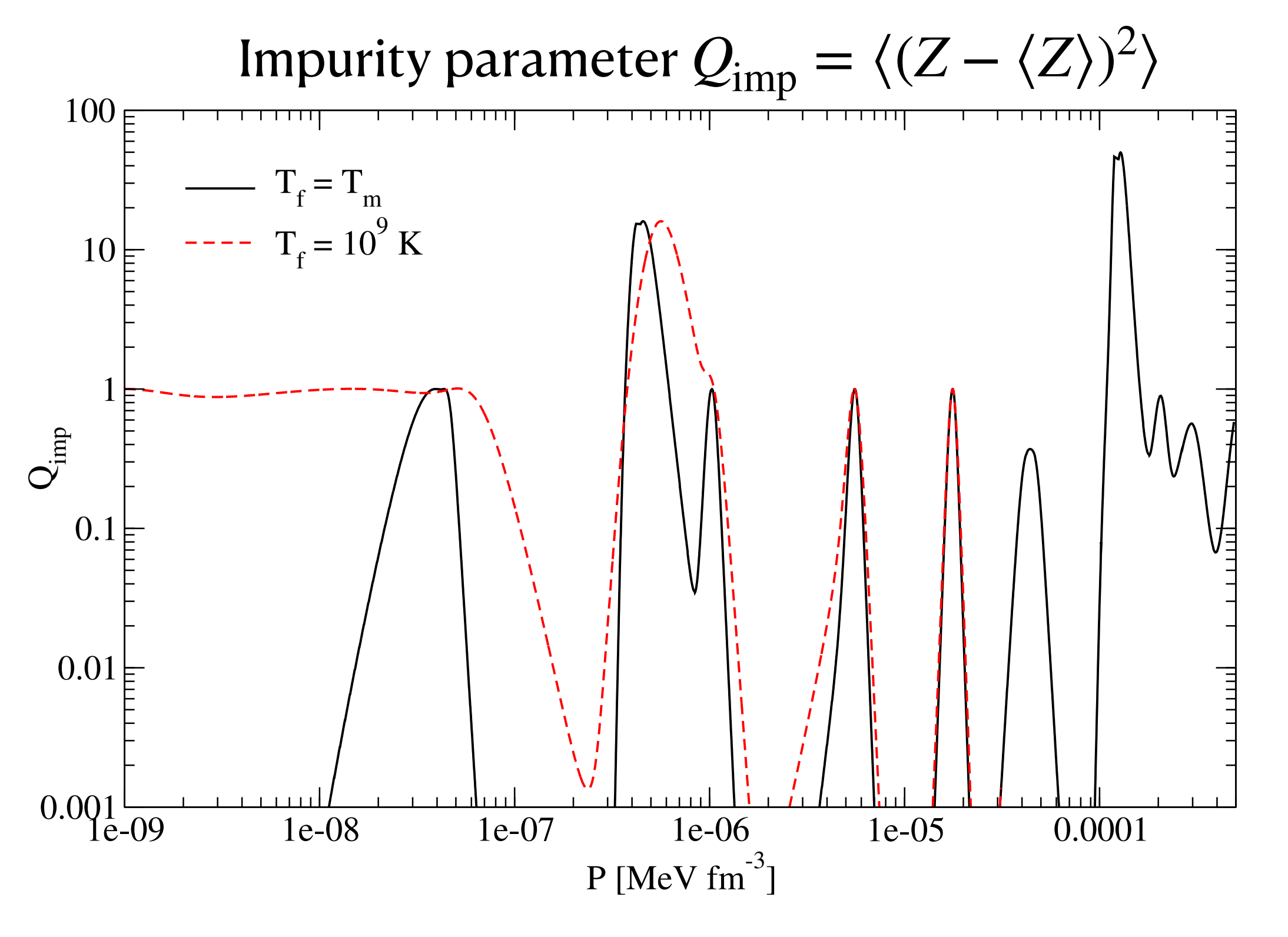
Frozen outer crust

The composition of the crust may be frozen at the time of crystallisation due to the quenching of nuclear reactions.

The nuclear abundances can be calculated by cooling down an initially hot multicomponent plasma of nuclei in equilibrium.

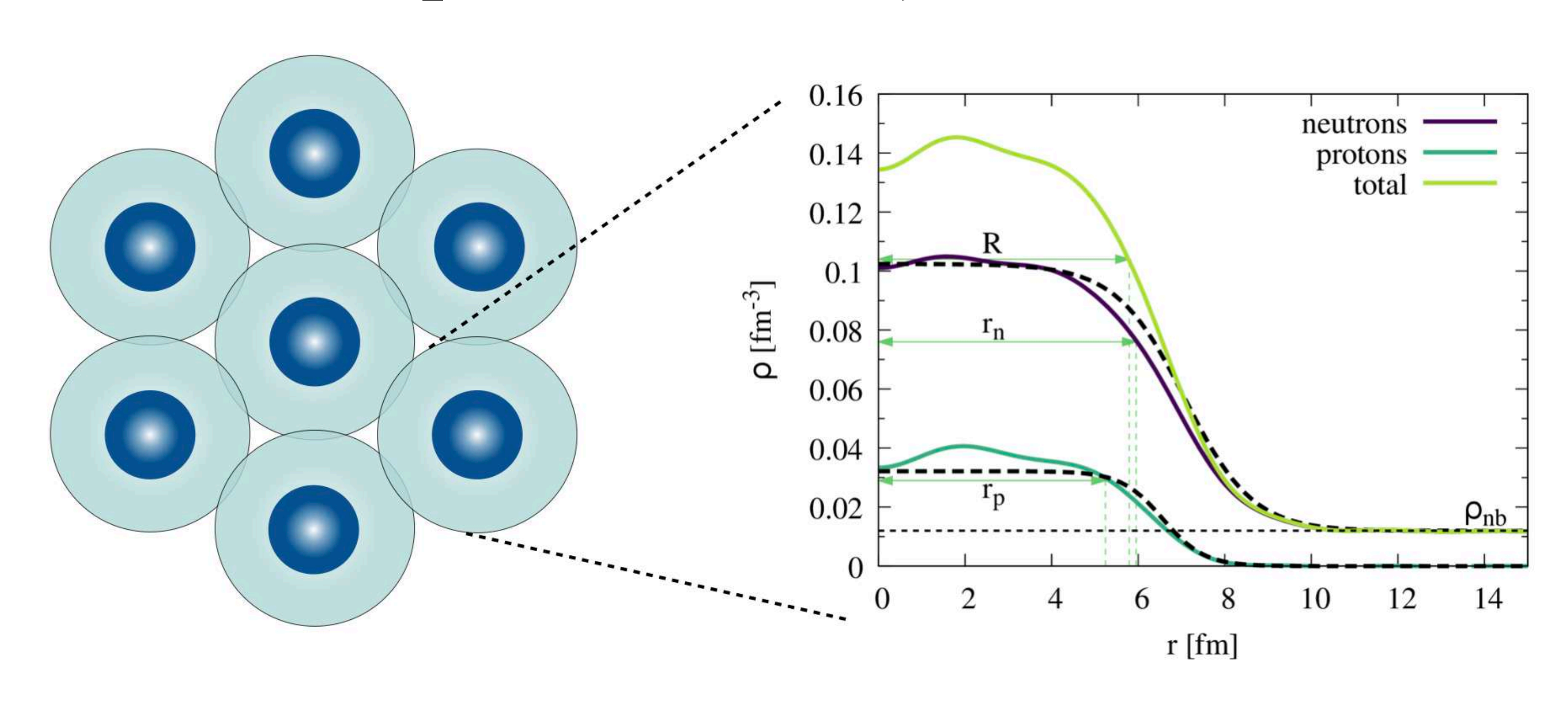
Results for BSk24





The level of impurities is influenced by quantum shell effects

Computationally fast treatment of the inner crust



Wigner-Seitz approximation:

- The crust is decomposed into identical spherical cell of radius *R*
- Each cell is electrically charge neutral

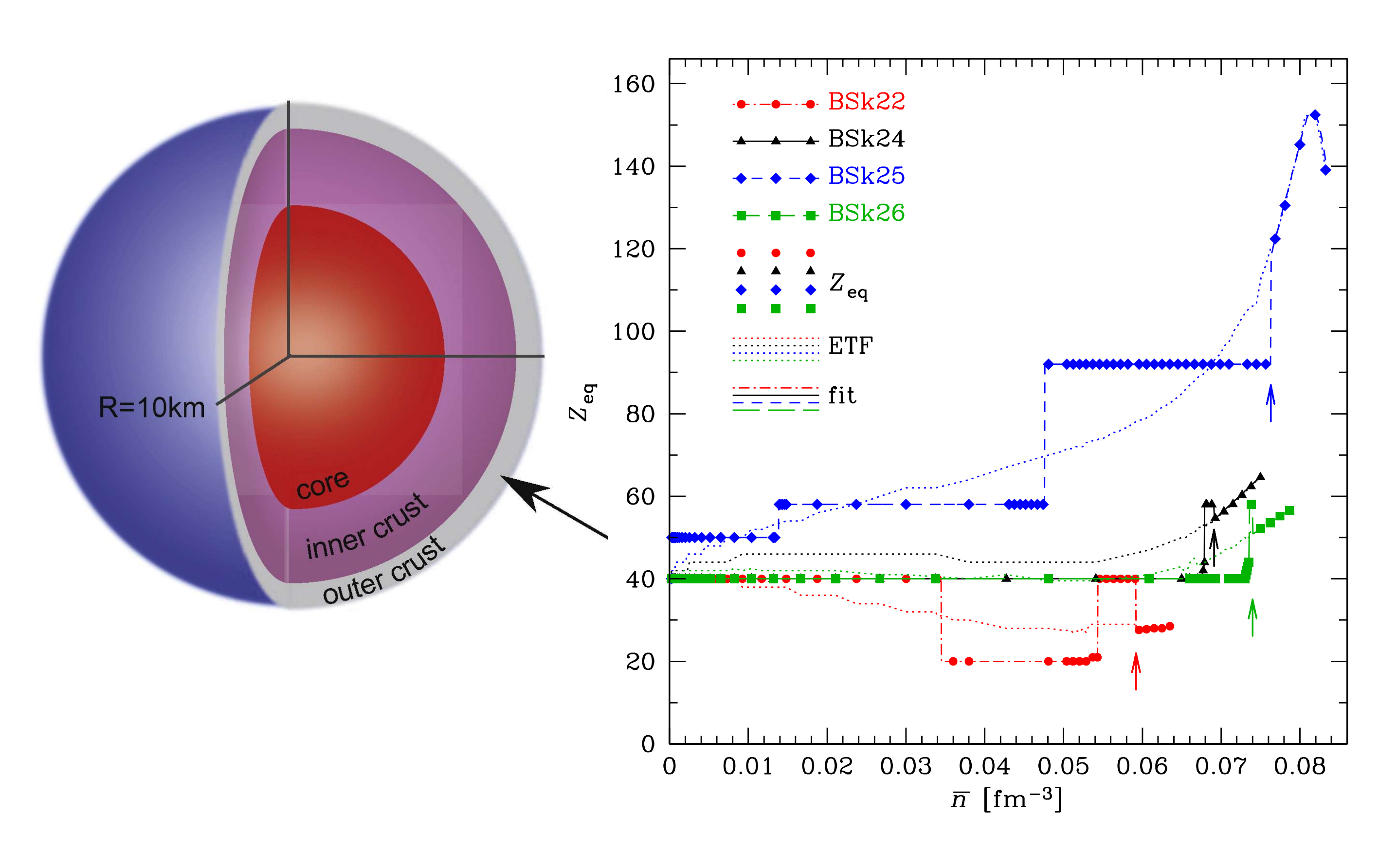
Extended Thomas-Fermi+Strutinsky Integral (ETFSI) approximation to the HFB equations:

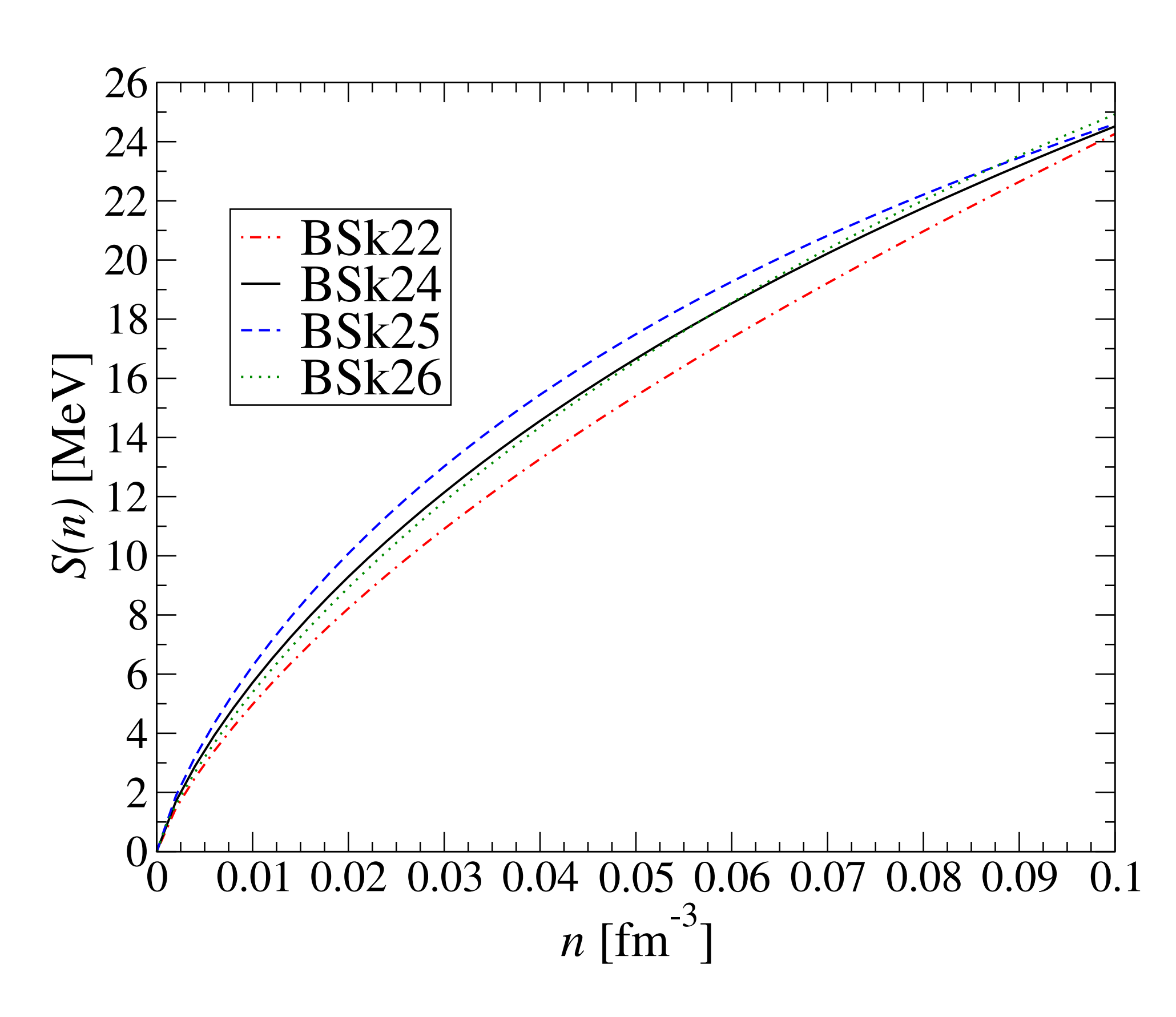
- semiclassical expansion up to \hbar^4 : the energy becomes a functional of $n_q(\mathbf{r})$ and their derivatives only
- proton shell effects are added perturbatively and consistently
- inclusion of BCS pairing for bound protons
- nucleon densities are parametrized as $n_q(r) = n_{\mathrm{B}q} + n_{\Lambda q} f_q(r)$ and $f_q(r) = \frac{1}{1 + \exp\left[\left(\frac{C_q R}{r R}\right)^2 1\right] \exp\left(\frac{r C_q}{a_q}\right)}$ with free parameters $n_{\mathrm{B}q}$, $n_{\Lambda q}$, C_q , a_q

Onsi et al. (2008), Pearson et al. (2012), Pearson et al. (2015), Pearson et al. (2018)

Inner crust composition and equation of state

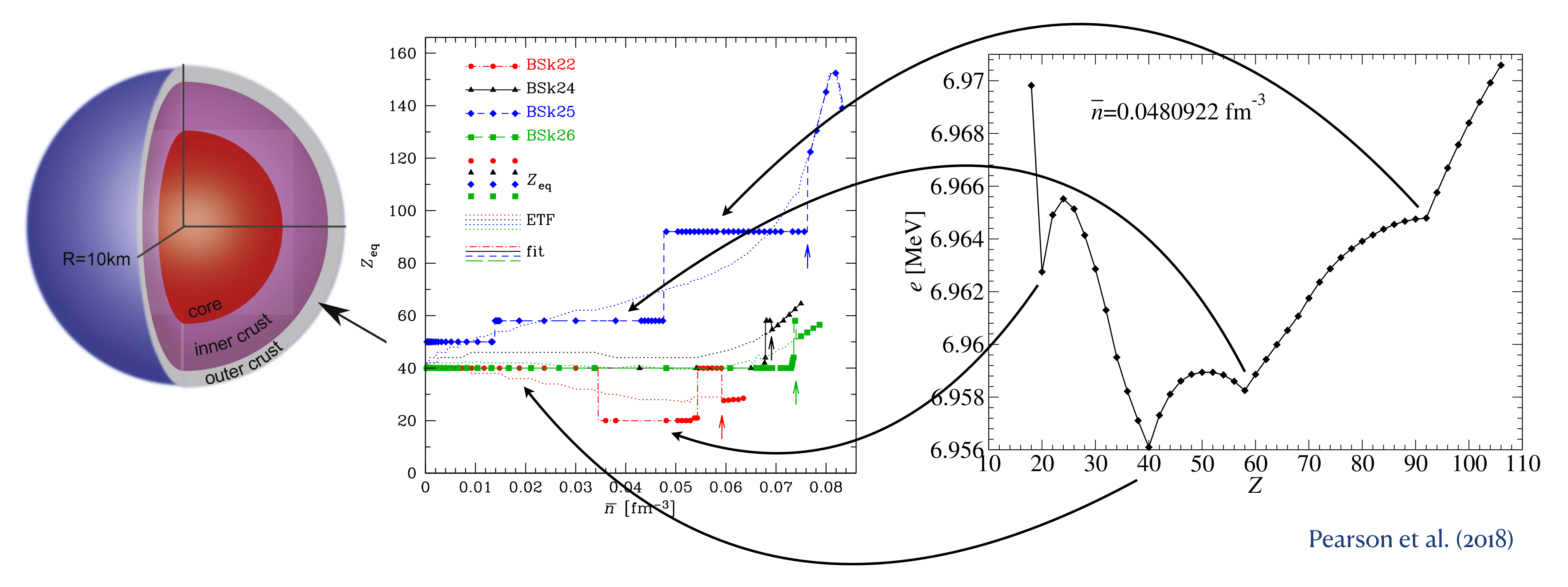
The composition is strongly influenced by the symmetry energy (the lower $S(\bar{n})$, the lower Z)





Inner crust composition and equation of state

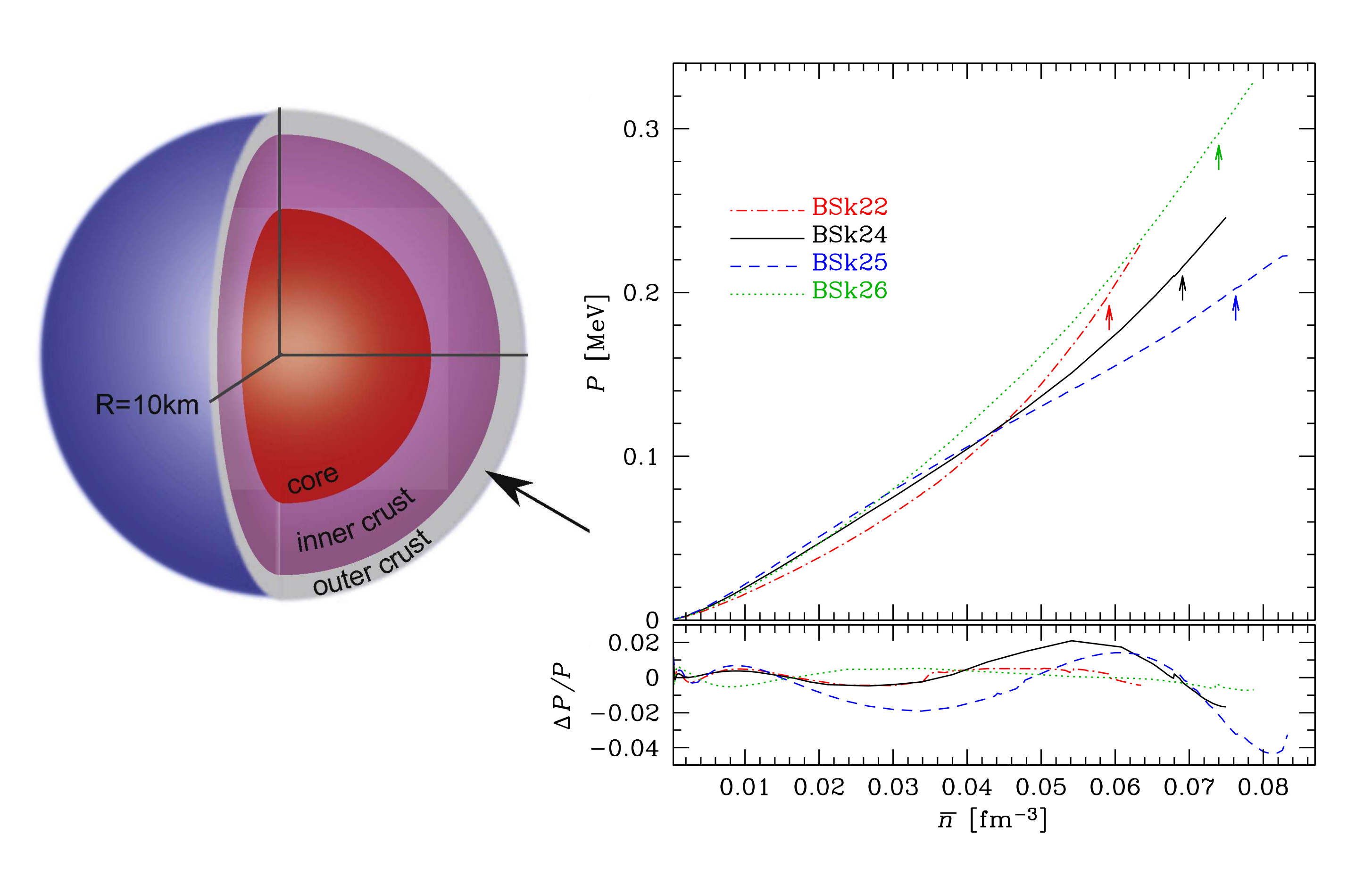
The composition is strongly influenced by the symmetry energy (the lower $S(\bar{n})$, the lower Z) but also by **shell effects**

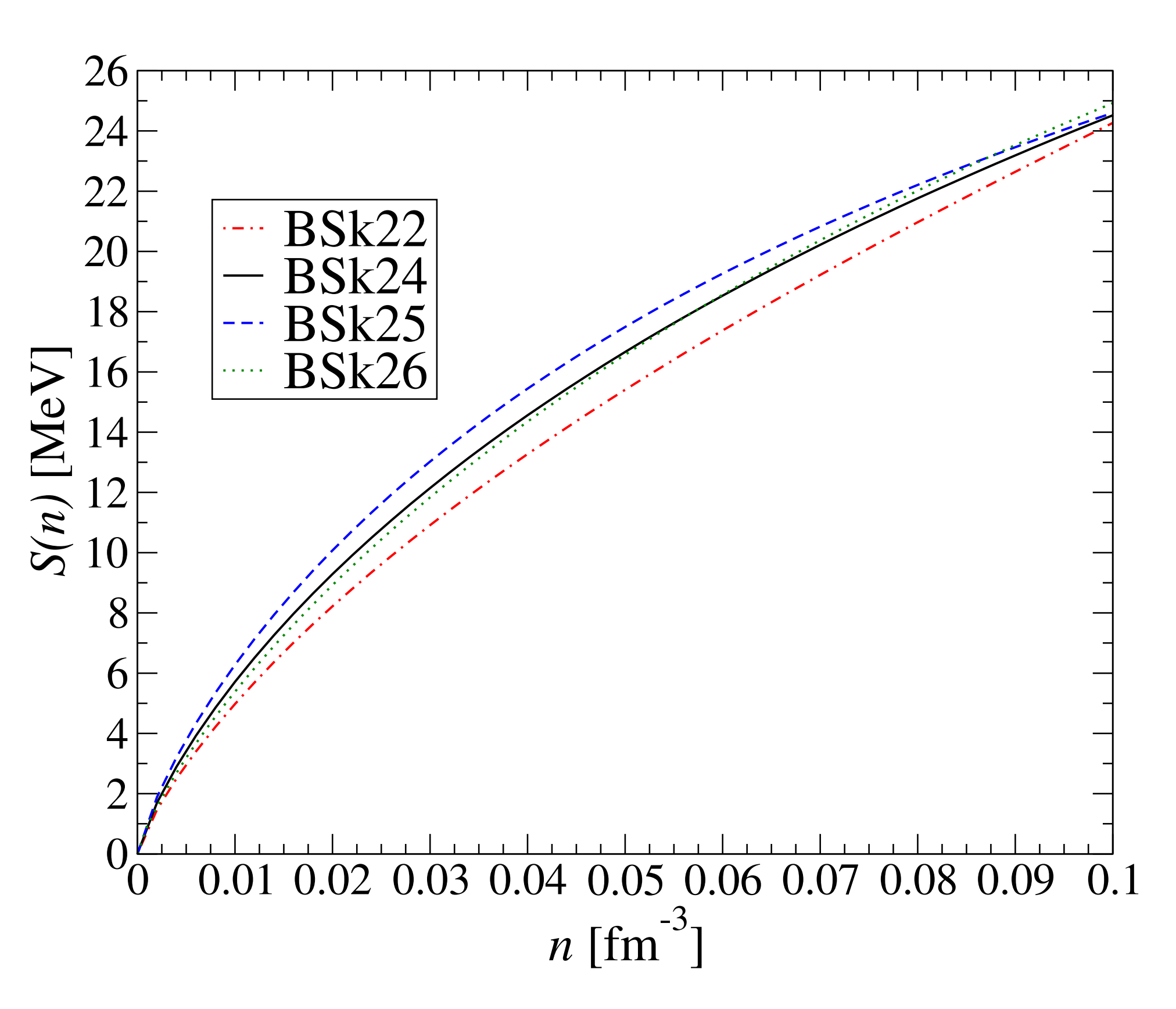


Electrical and thermal conductivities in the outer and inner crusts have been calculated by Alexander Potekhin: https://www.ioffe.ru/astro/conduct/index.html

Inner crust composition and equation of state

The pressure is directly governed by the density-dependence of the symmetry energy $P \sim \bar{n}^2 S'(\bar{n})$

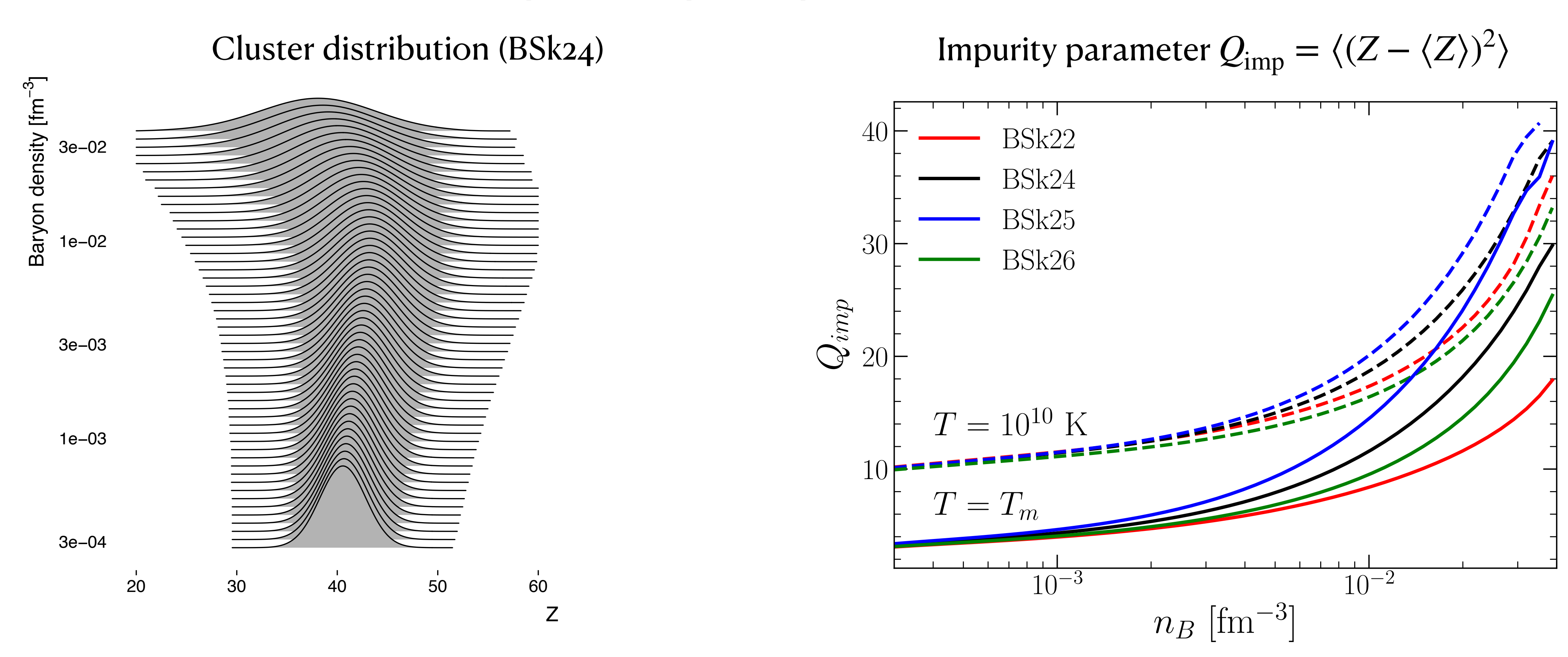




Frozen inner crust

The composition of the crust may be frozen at the time of crystallisation due to the quenching of nuclear reactions.

Nuclear abundances estimated from a compressible liquid-drop model:



Deep layers are more impure because of higher crystallisation temperatures

Refinements of the ETFSI approach

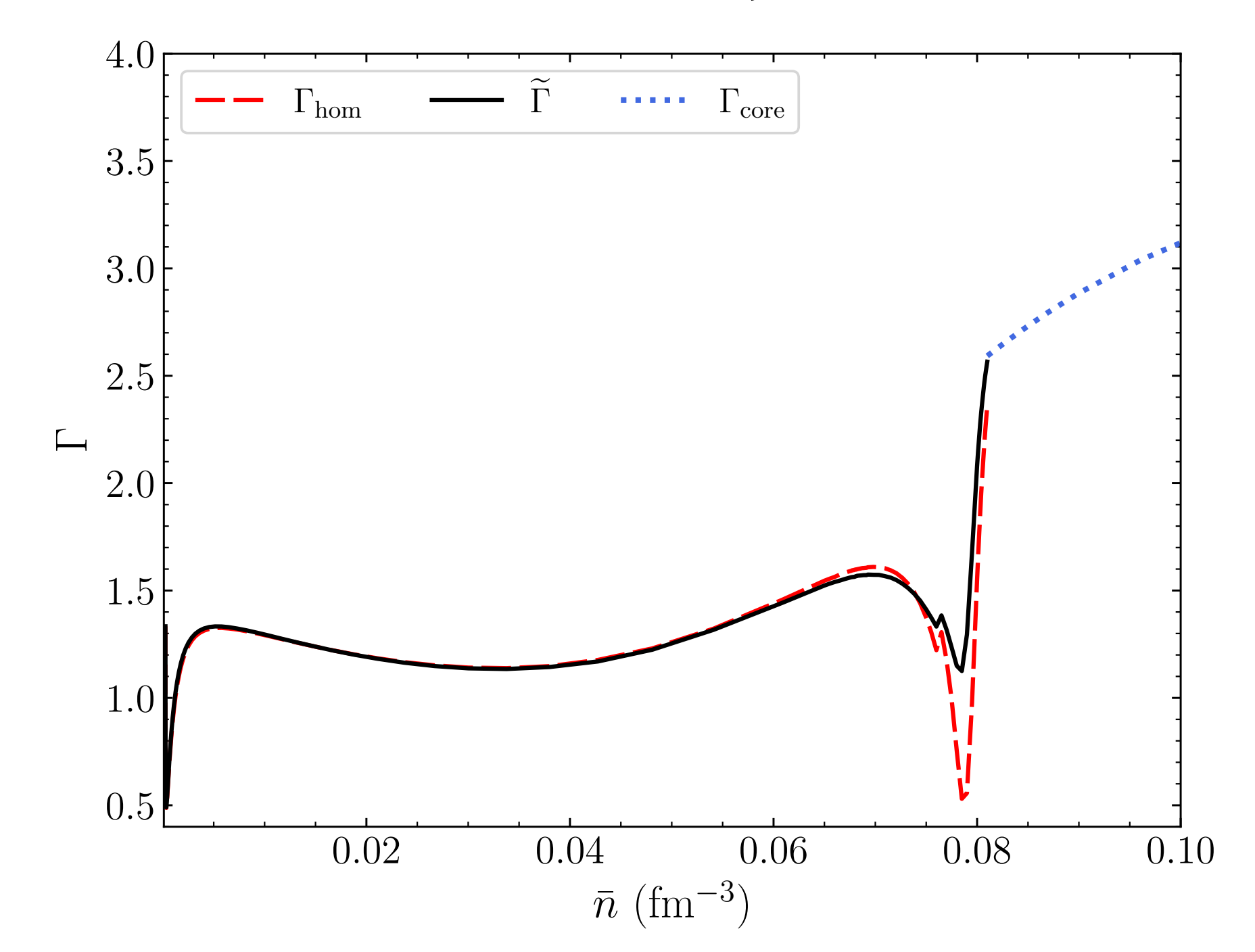
Improved treatment of pairing for nucleons:

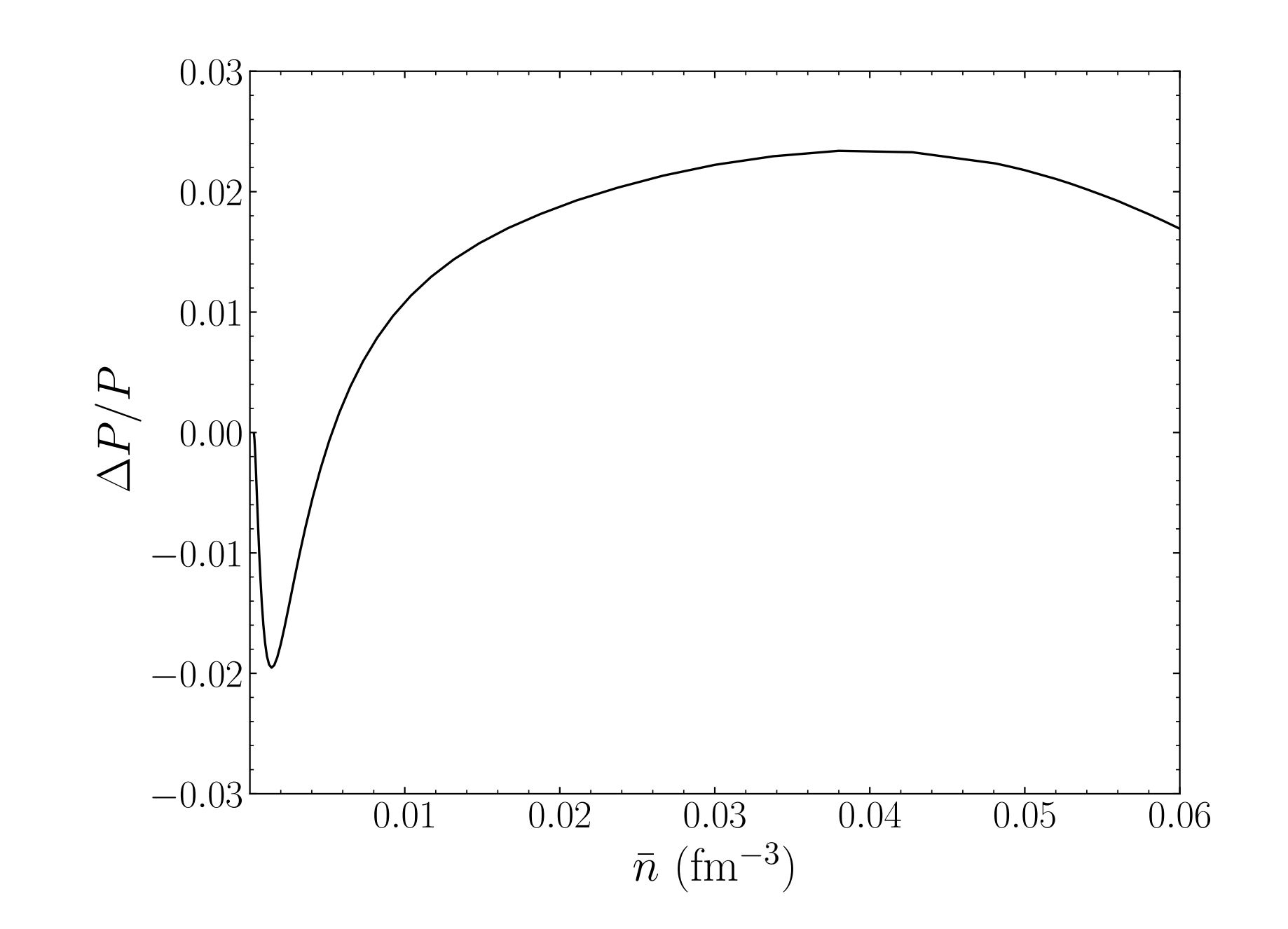
- corrections to the pressure amount to a few %
- composition remains unchanged

Chamel, Pearson, Shchechilin (2024)

Analytical formulas for chemical potentials and pressure:

- lattice correction (better matching to outer crust),
- corrections due to the use of parametrized density profiles,
- corrections due to boundary conditions.





A few % correction on the pressure *P*

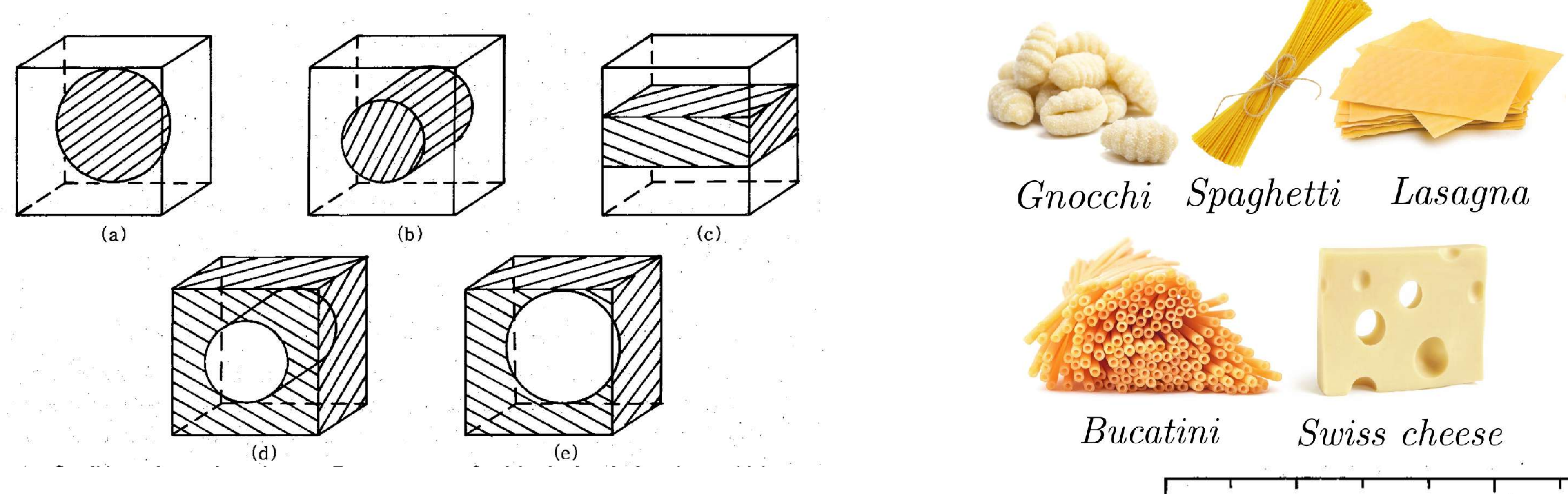
Larger correction on the adiabatic index $\Gamma \equiv \frac{\bar{n}}{P} \frac{dP}{d\bar{n}}$

Impact on oscillation modes?

Chamel, Shchechilin, Chugunov (2025)

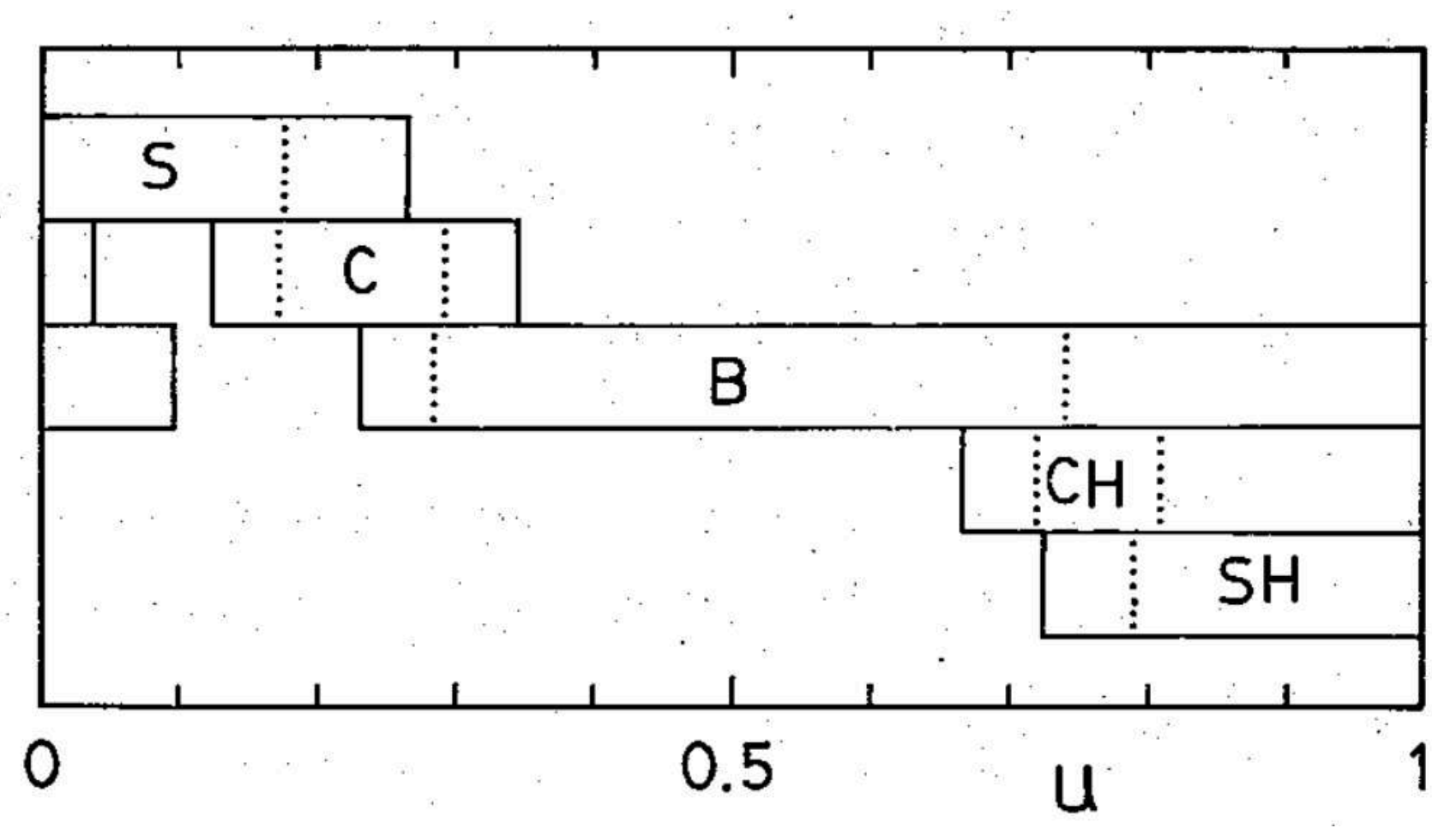
Nuclear pasta mantle

In 1984, Hashimoto, Seki and Yamada showed within the **compressible liquid-drop approach** that nuclear pasta generically appear when the filling fraction *u* exceeds ~20% independently of the nuclear interactions



With increasing filling fraction: gnocchi (S), spaghetti (C), lasagna (B), bucatini (CH), and Swiss cheese (SH).

This was independently confirmed by Ravenhall, Pethick and Wilson.



Nuclear pasta mantle

Pasta could represent ~50% of the crust mass

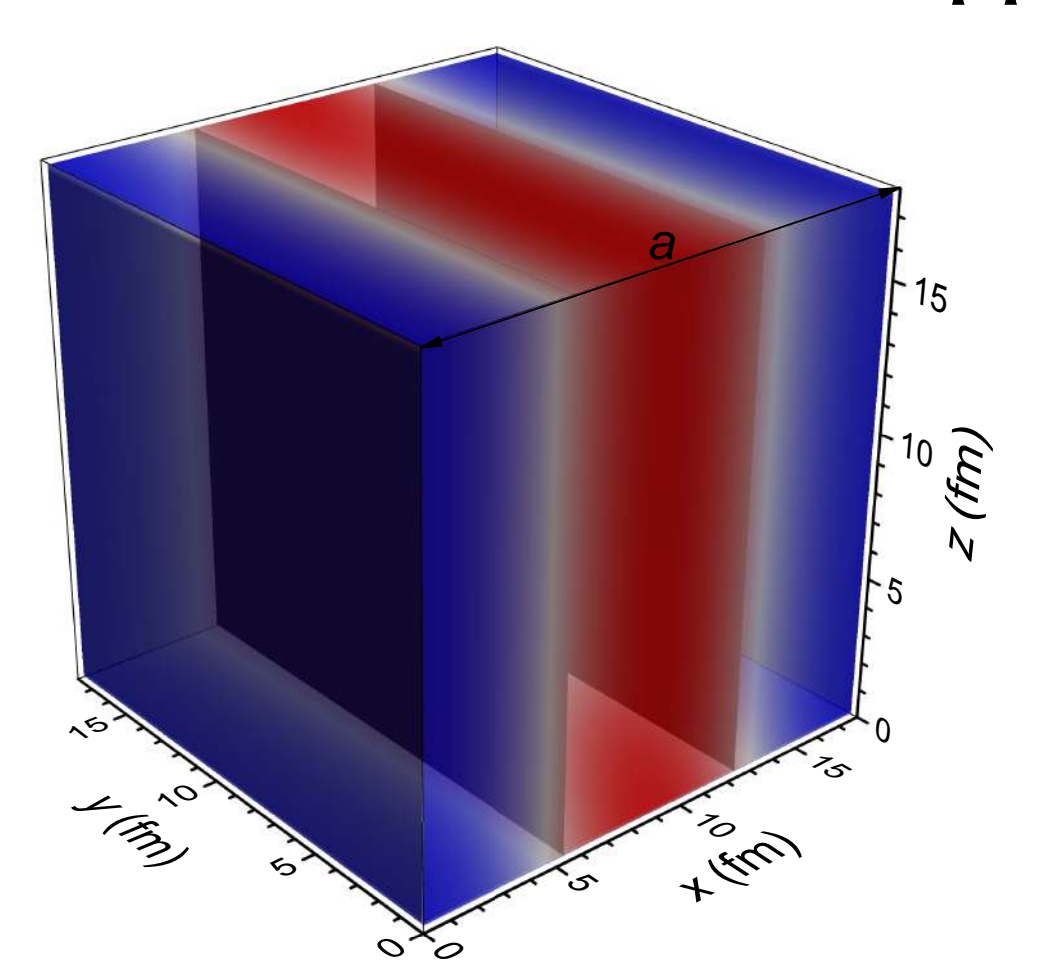
Dinh Thi et al. (2021), Newton et al. (2022)

and have implications for the dynamical and magnetothermal evolution of neutron stars

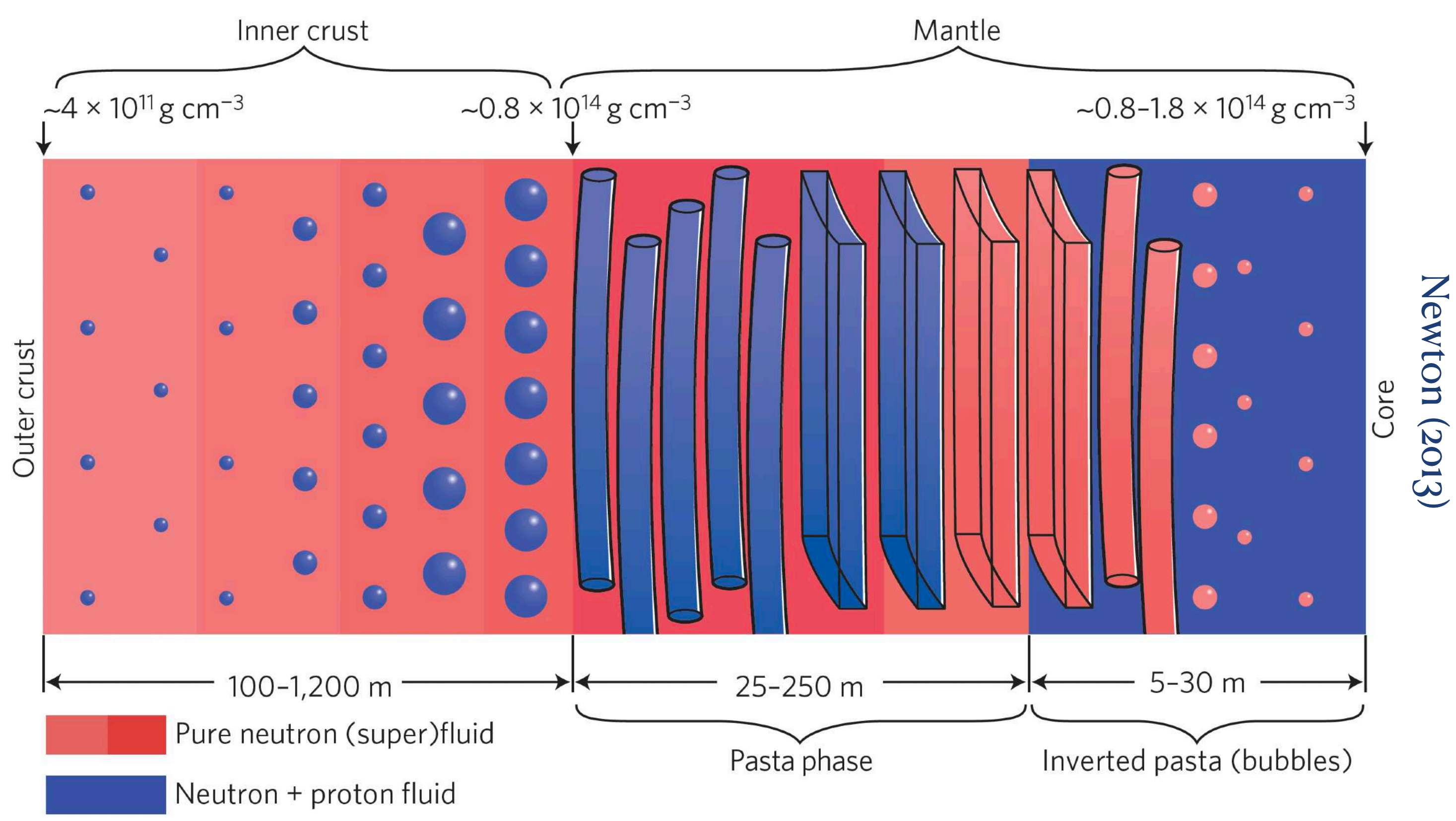
Gusakov et al. (2004), Pons et al. (2013), Horowitz et al. (2015)

However, predictions are very sensitive to nuclear surface corrections (curvature, neutron skin) ignored in the first liquid-drop models!

Pasta have been studied within the more realistic Thomas-Fermi (TF) approximation



Cheng-Jun Xia et al. (2021)



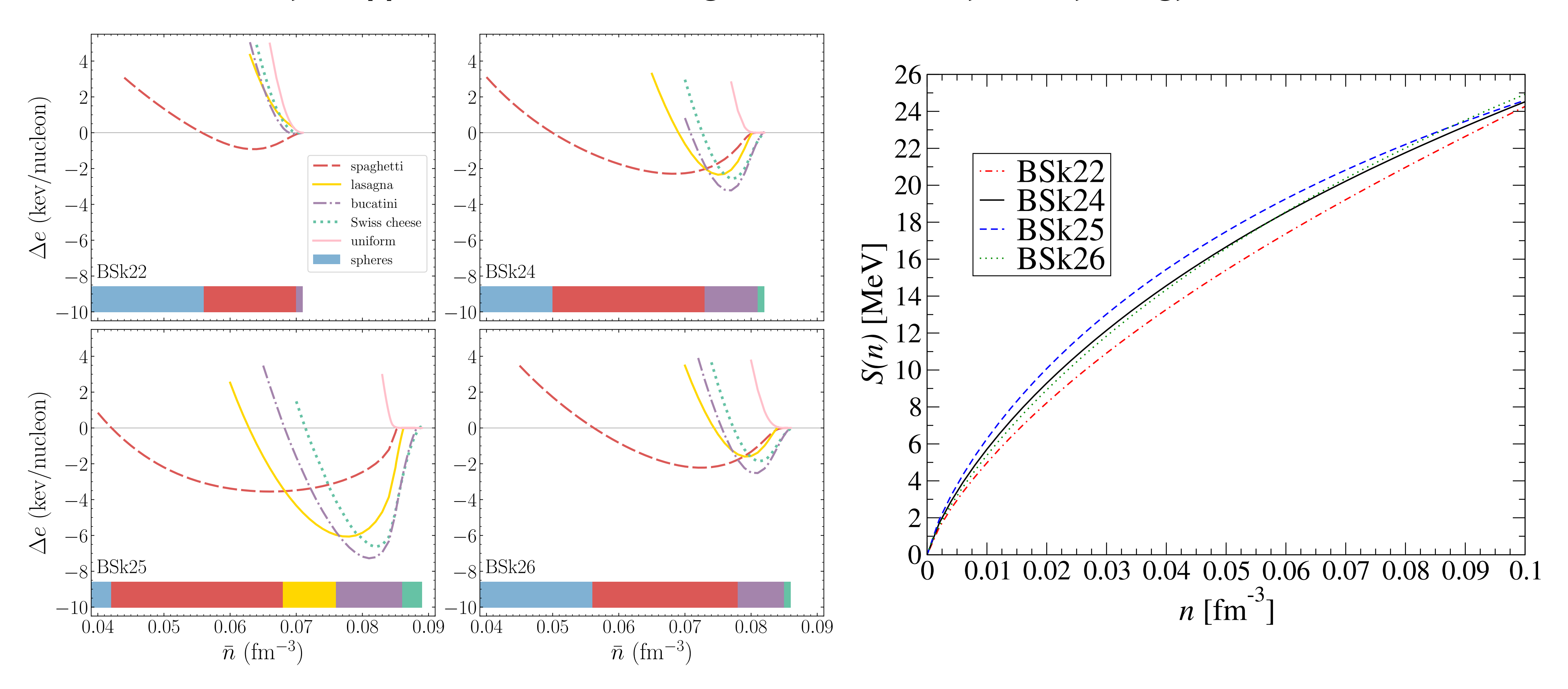
We have adapted the ETFSI method to allow for pasta:

- better treatment of nuclear surface (4th order)
- inclusion of shell effects and pairing

Pearson & Chamel (2020,2022)

Classical pasta recipe (ETF)

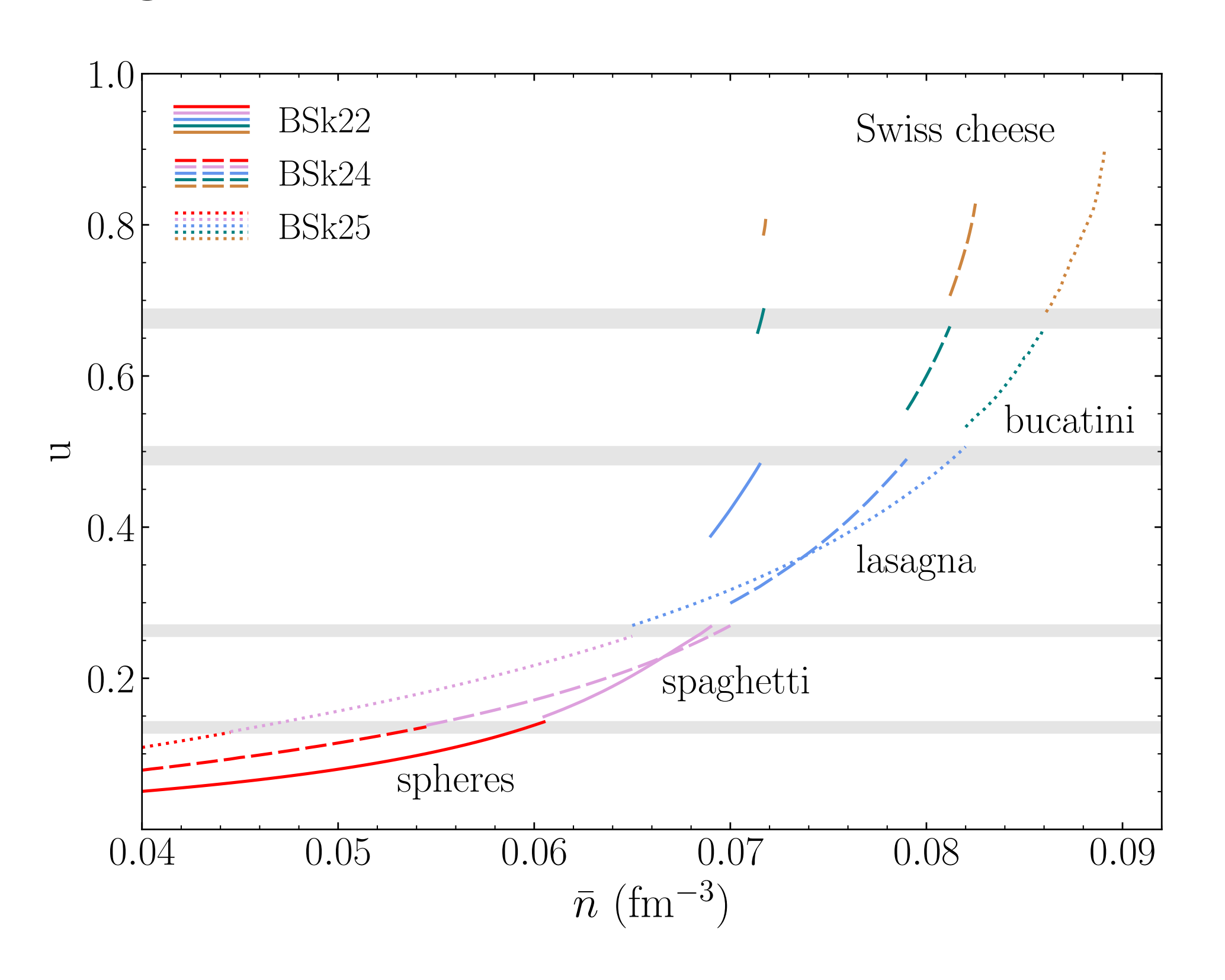
Pasta are more likely to appear for models with higher values of the symmetry energy at relevant densities

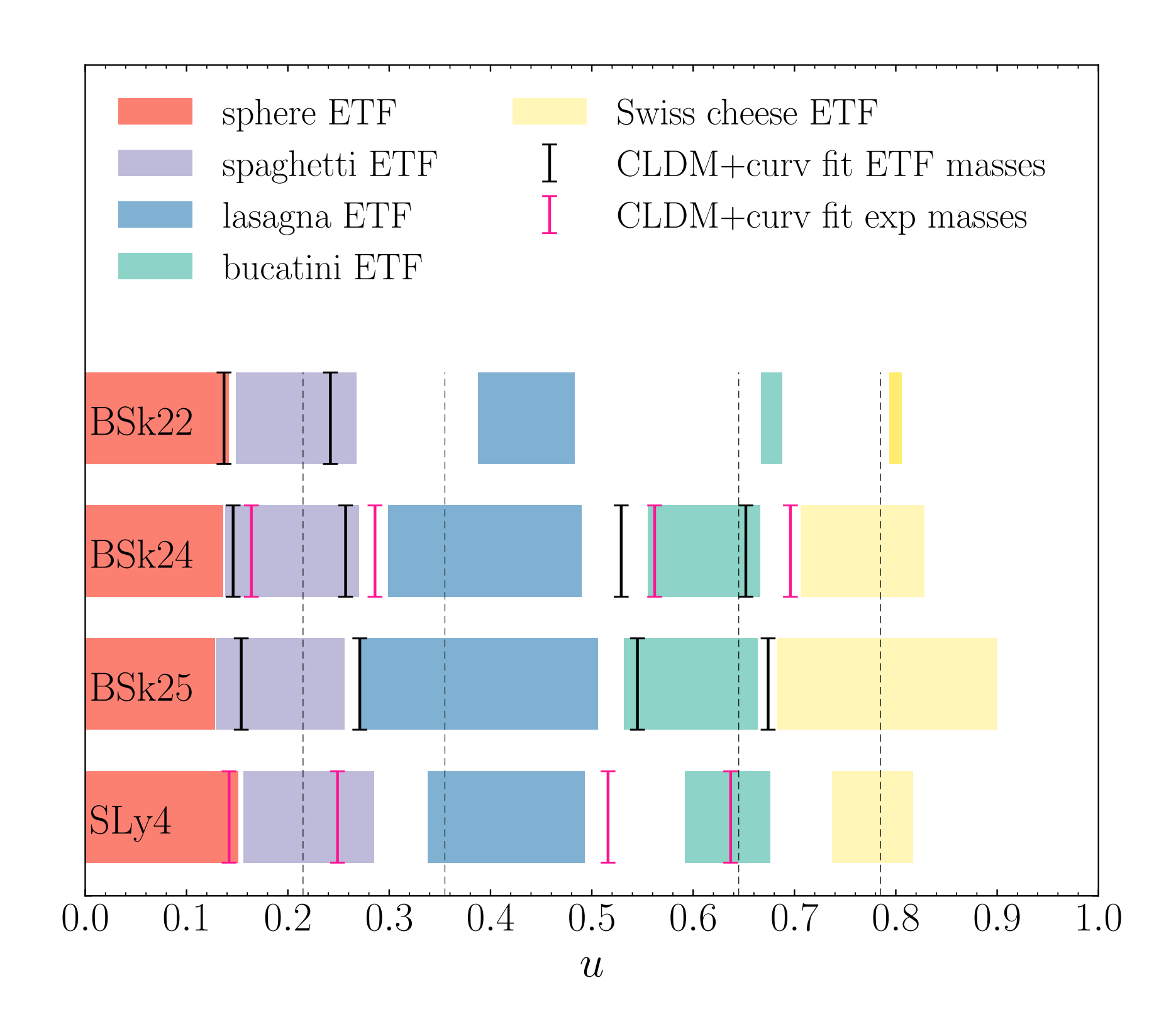


Shchechilin, Chamel, Pearson (2023)

Quasi universal pasta transitions

The filling fractions for the different transitions are found to be quasi-universal:

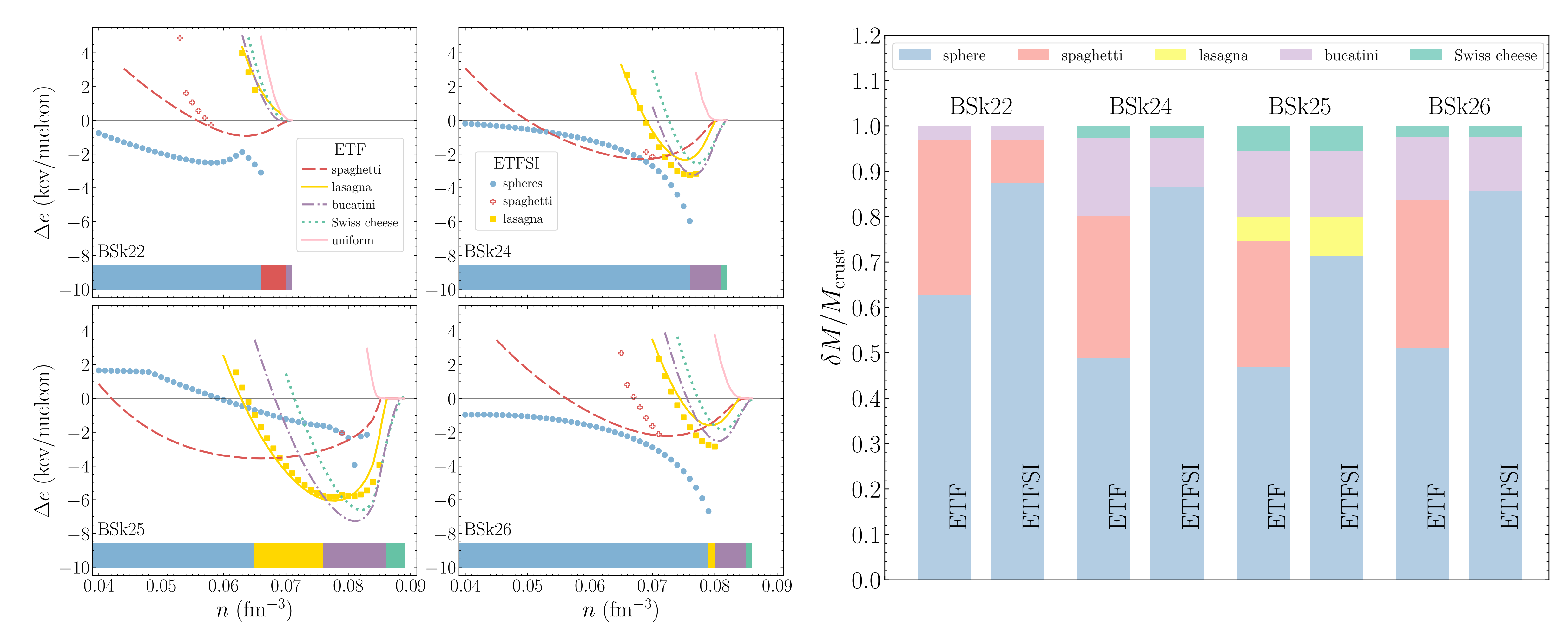




Pasta appear for a **lower filling fraction** $u \gtrsim 0.13$ than predicted by Hashimoto et al. within the liquid-drop model. This is because of **curvature corrections** ignored in their stability analysis

Quantum pasta recipe (ETFSI)

Pasta occupy a much narrower range of densities, and correlations with symmetry energy vanish!



Refinement of the ETFSI approach for pasta

Above $\bar{n} \approx 0.07$ fm⁻³, results are very sensitive to the adopted parametrization of the nuclear shapes

The popular ansatz
$$f_q^{\text{FD}}(r) = \frac{1}{1 + \exp\left(\frac{r - C_q}{a_a}\right)}$$
 does not satisfy the boundary condition $\frac{dn_q}{dr}(r = R) = 0$

This condition is satisfied by our ansatz
$$f_q^{\text{StrD}}(r) = \frac{1}{1 + \exp\left[\left(\frac{C_q - R}{r - R}\right)^2 - 1\right] \exp\left(\frac{r - C_q}{a_q}\right)}$$
 but all derivatives vanish

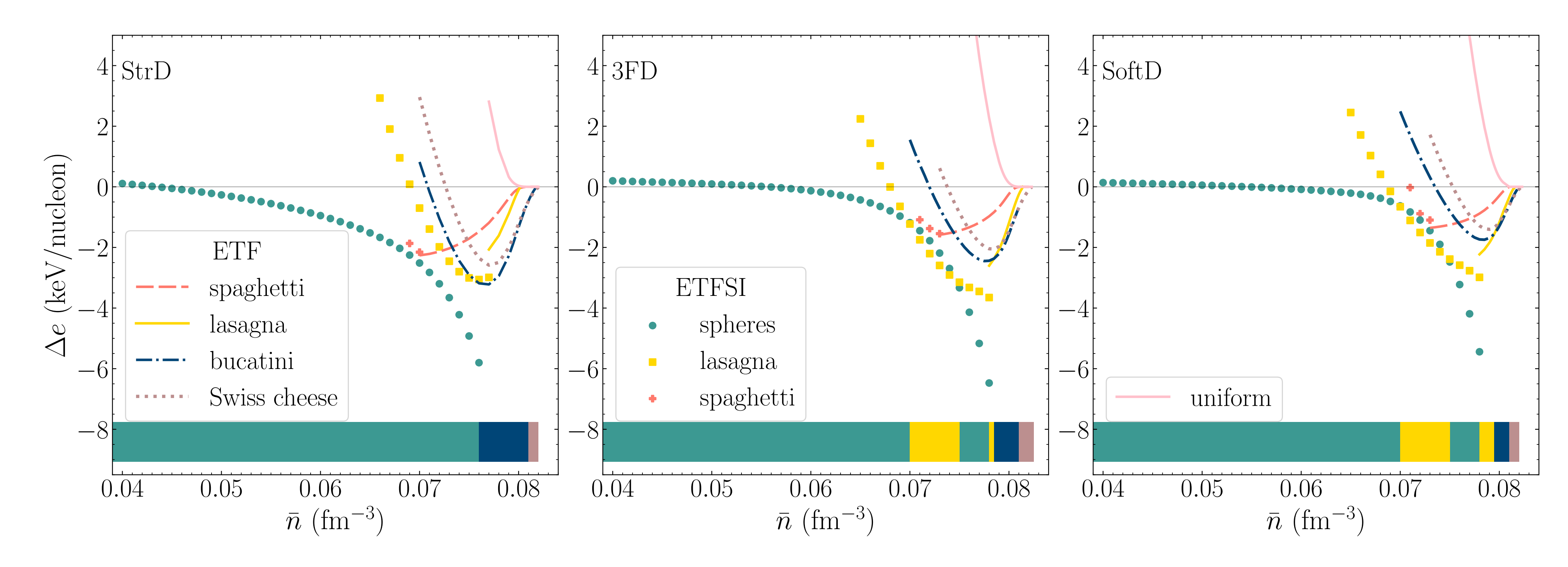
We propose two new parametrizations:

•
$$f_q^{\text{SoftD}}(r) = \frac{1}{1 + \left(\frac{C_q - R}{C_q}\right)^2 \left(\frac{r}{r - R}\right)^2 \exp\left(\frac{r - C_q}{a_q}\right)}$$

•
$$f_q^{3\text{FD}}(r) = f_q^{\text{FD}}(-r) + f_q^{\text{FD}}(r) + f_q^{\text{FD}}(2R - r) - f_q^{\text{FD}}(-R) - 2f_q^{\text{FD}}(R)$$

Refinement of the ETFSI approach for pasta

- The two new parametrizations yield more stable configurations (lower energies)
- Both predict the existence of gnocchi among lasagna
- The equation of state is hardly changed



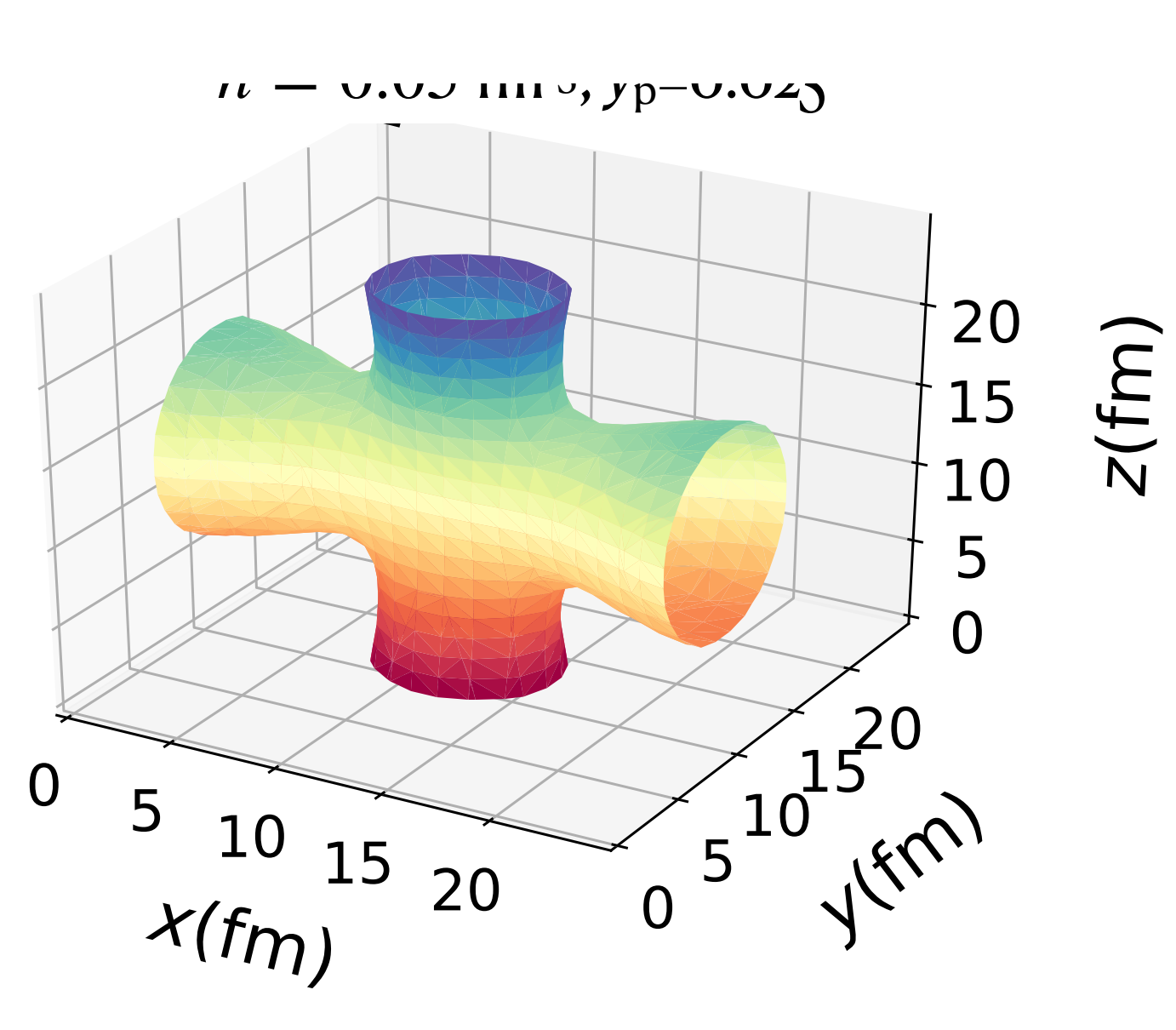
Caveats:

- Pasta shapes restricted to spheres, cylinders, slabs
- Neglect of neutron shell effects
- Not fully self-consistent

Pasta: from small to large scales

The formation of nuclear pasta has been explored within different approaches:

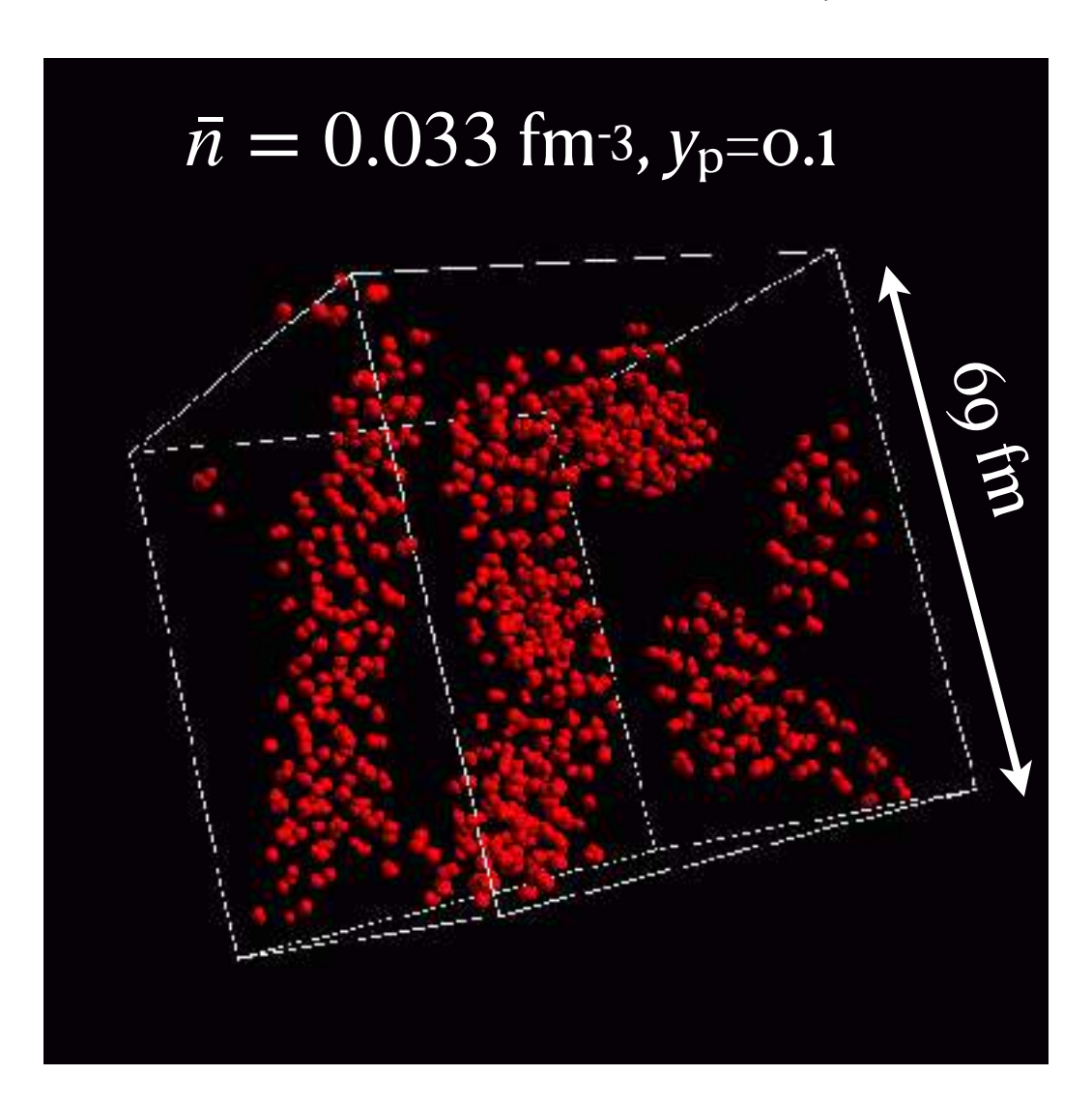
3D Hartree-Fock (+BCS)



Newton et al. (2022)

- Fully quantum approach
- Realistic conditions
- Small scale N~103

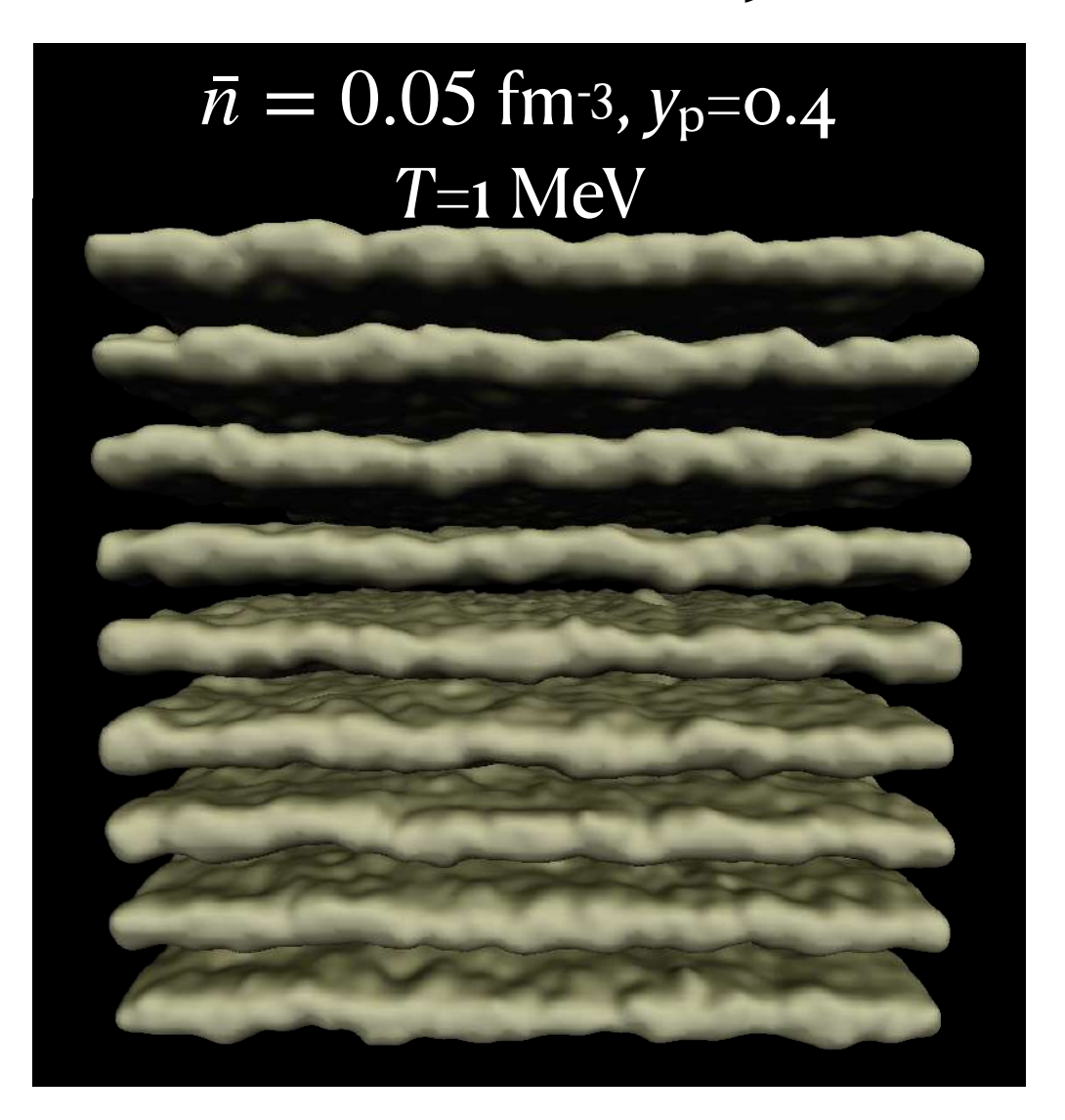
Quantum molecular dynamics



Watanabe et al. (2003)

- Partly quantum approach
- Less realistic conditions
- Intermediate scale N~104

Classical molecular dynamics



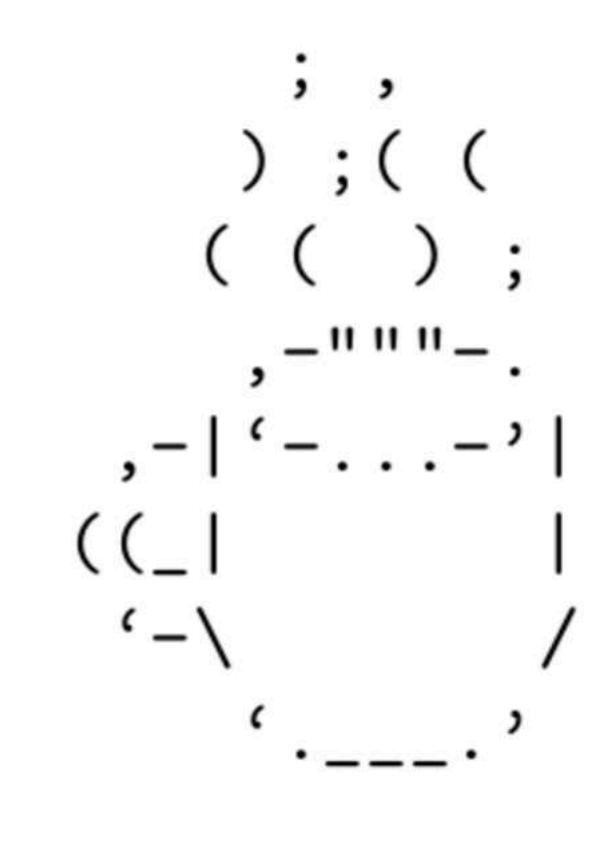
Zidu Lin et al. (2020)

- Classical approach
- Hot and proton rich matter
- Large scale N~105

Cooking pasta

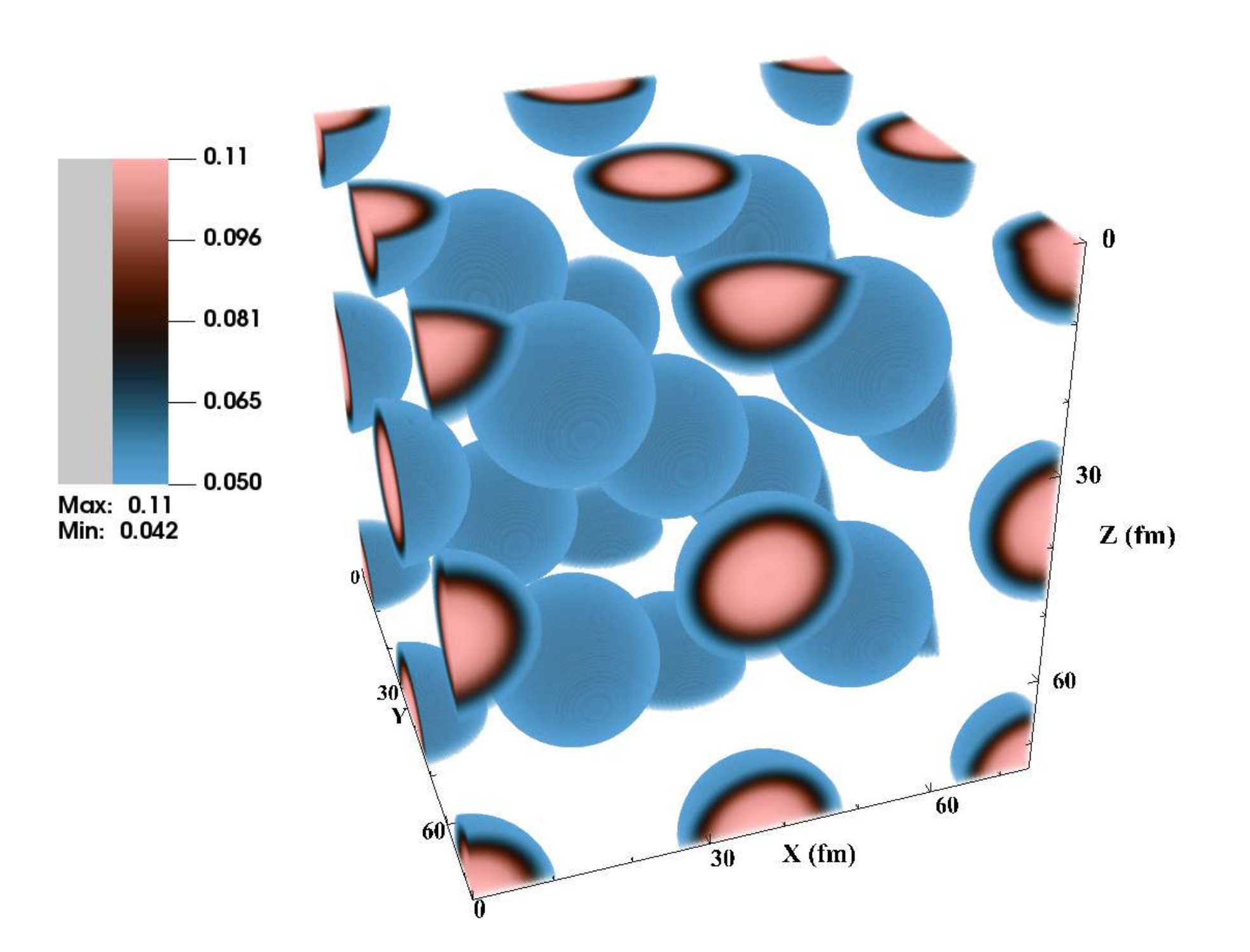
Fully self-consistent 3D Hartree-Fock + BCS calculations using MOCCa code originally developed for isolated atomic nuclei

Ryssens, Heenen, Bender (2015)





Wouter Ryssens



Adapted for the extreme astrophysical environment of neutron stars:

- Degenerate electron background
- Cuboid supercell up to ~100 fm
- Periodic boundary conditions
- No symmetry restrictions
- Up to ~50 ooo nucleons

Calculations performed using **BSkG4** with ETFSI solution as initial guess

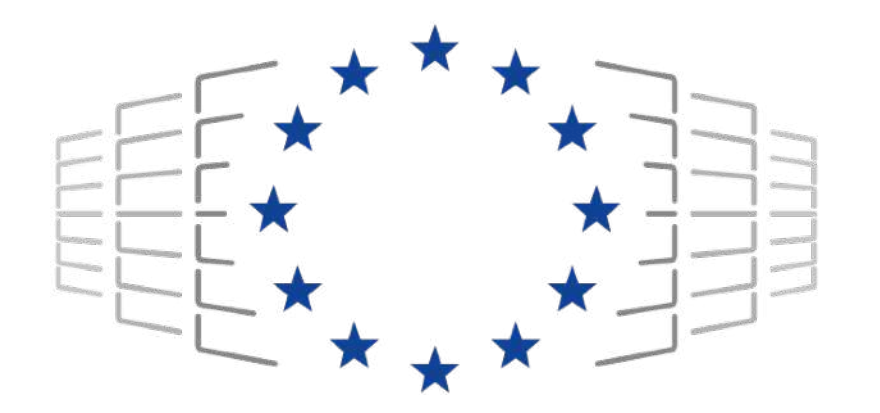


Nikolai Shchechilin

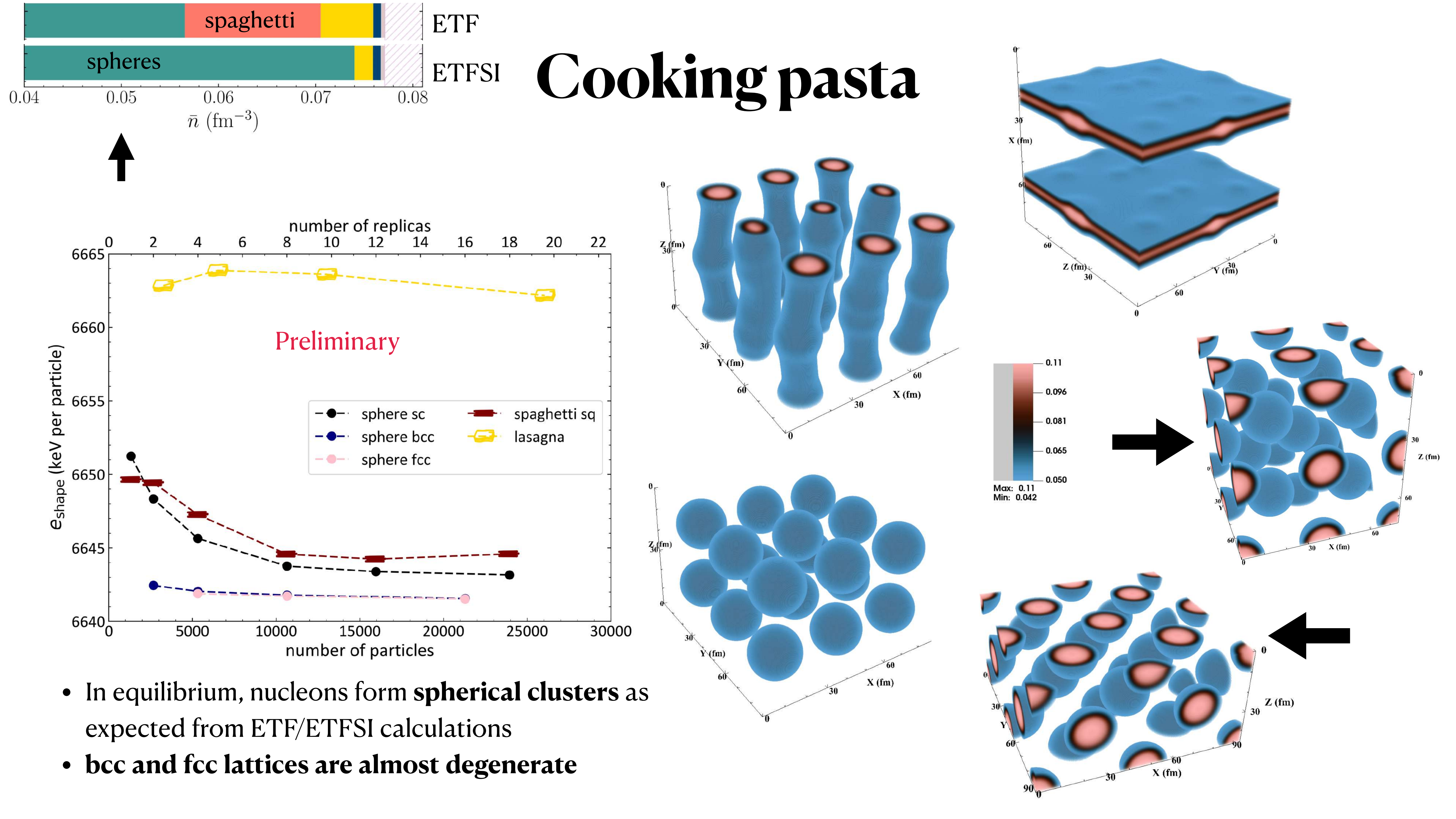
To ensure proper convergence to the true solution:

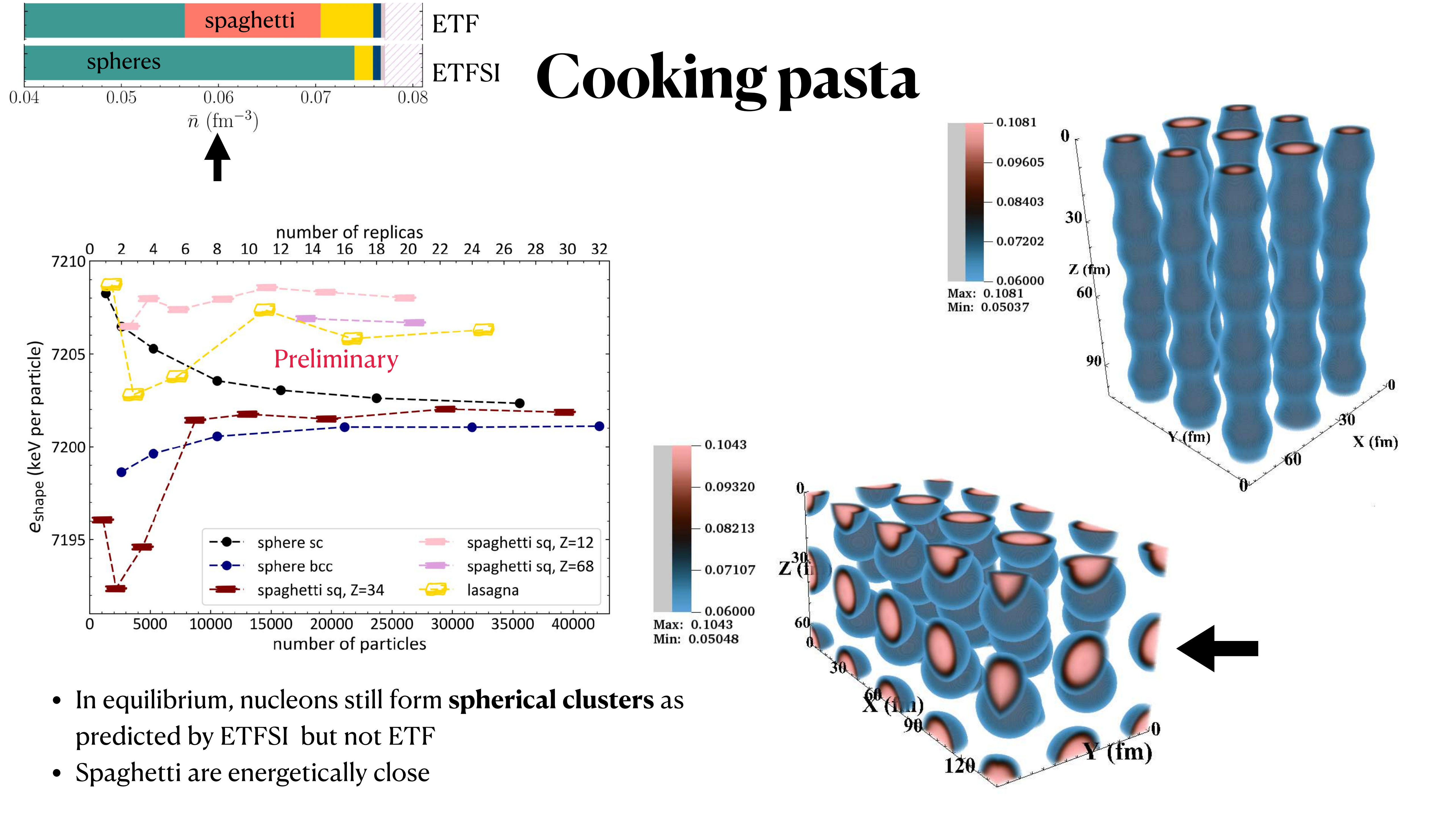
- The supercell must be large enough
- Different initial shapes must be considered

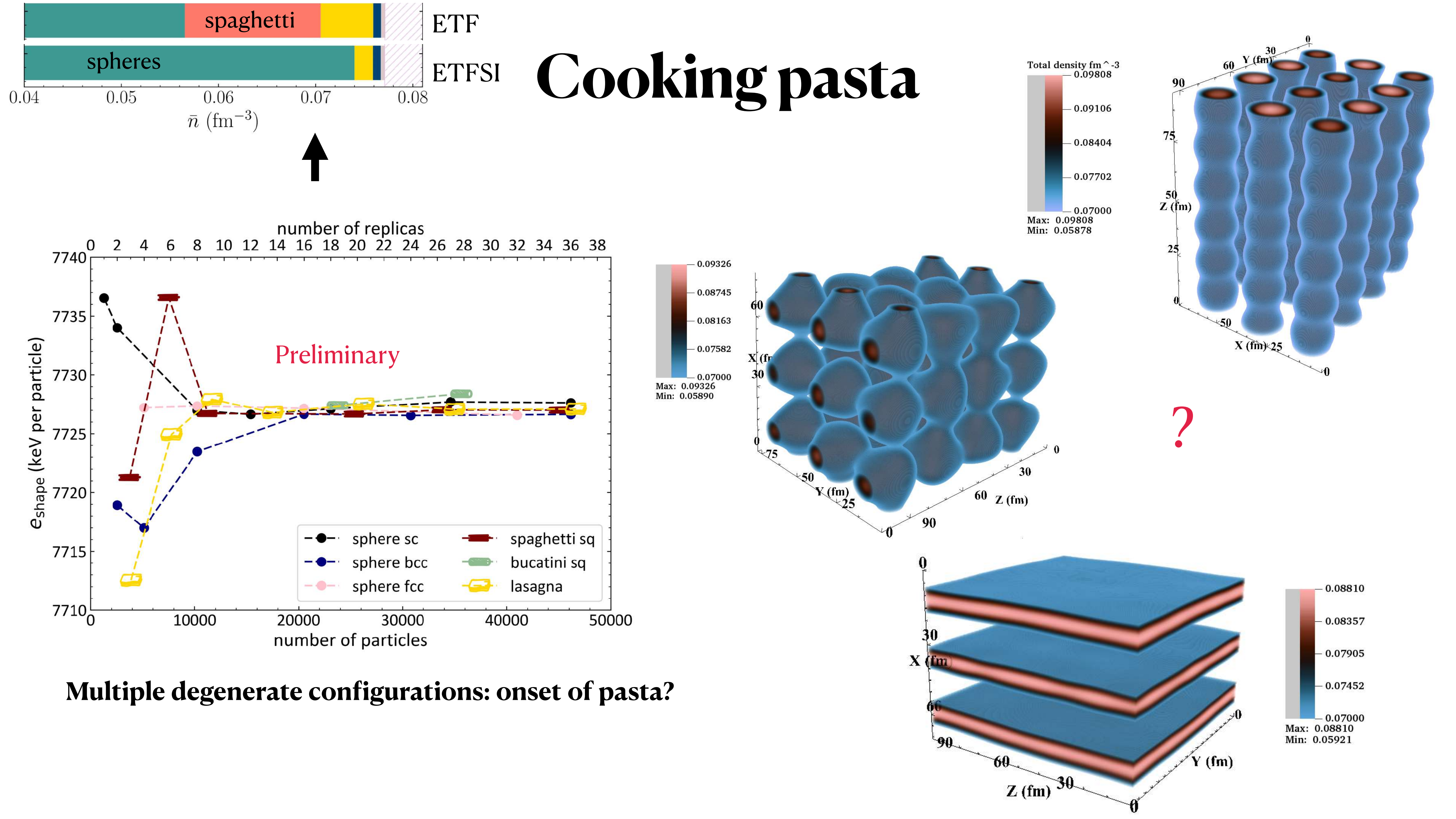


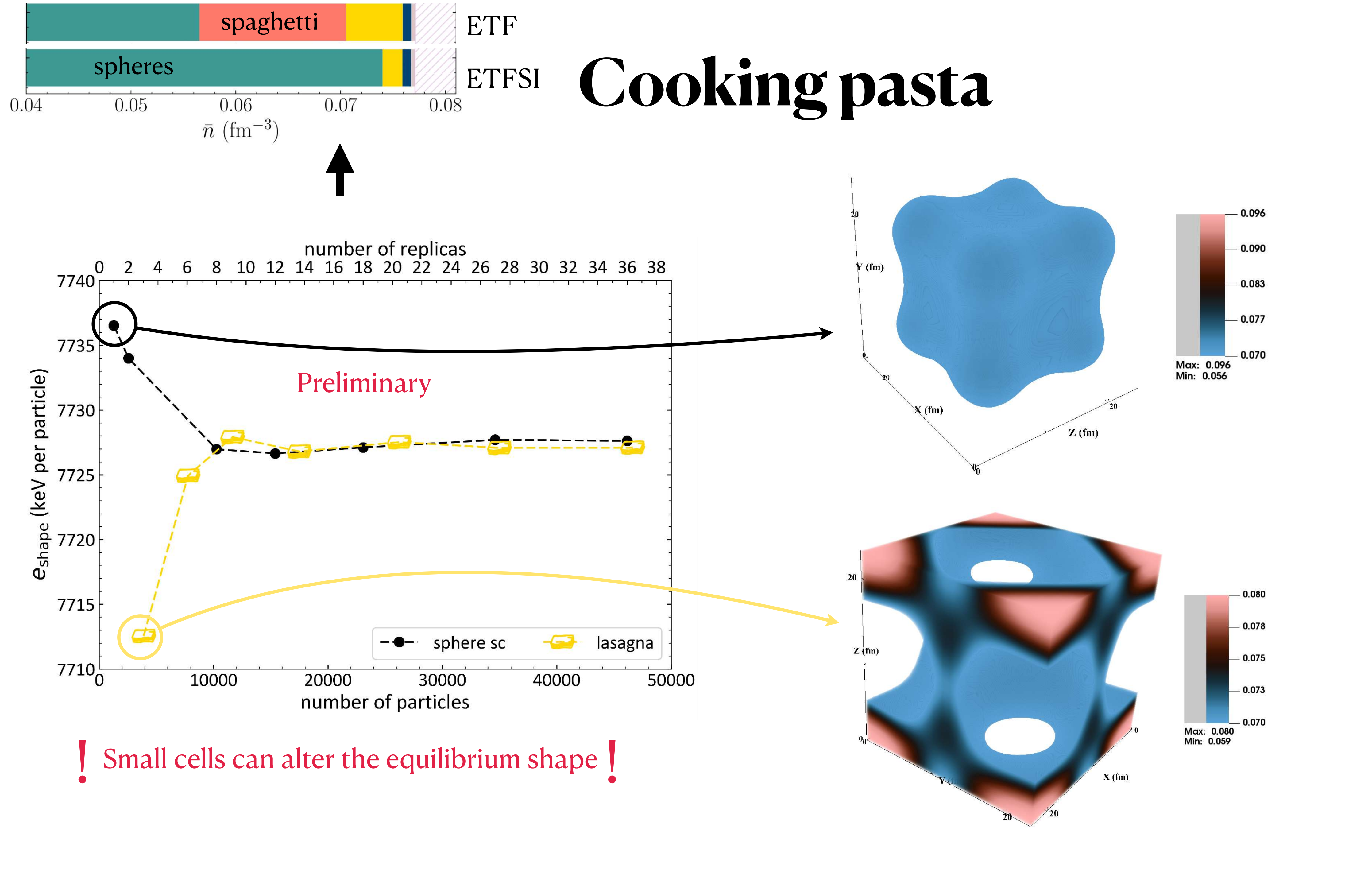


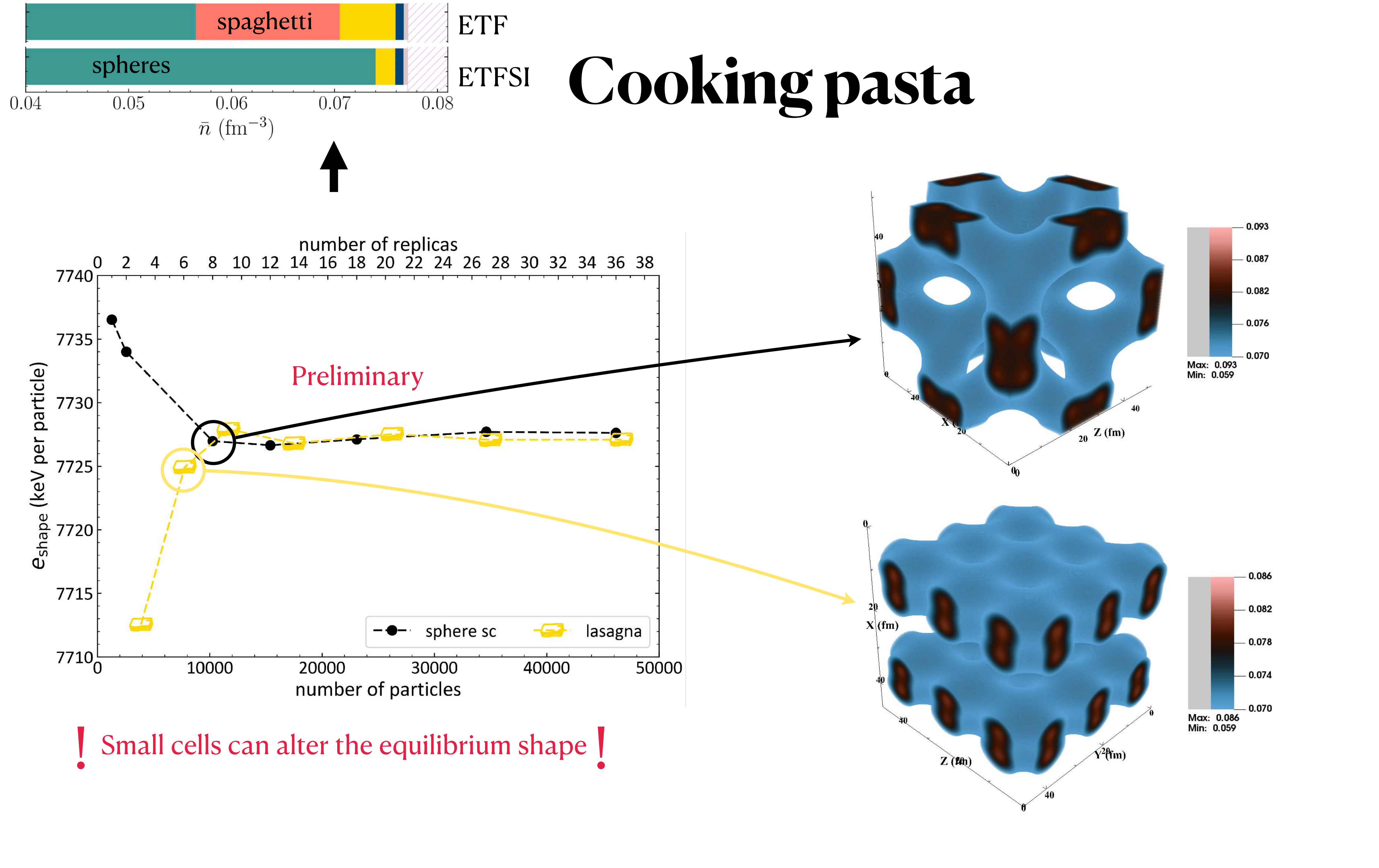


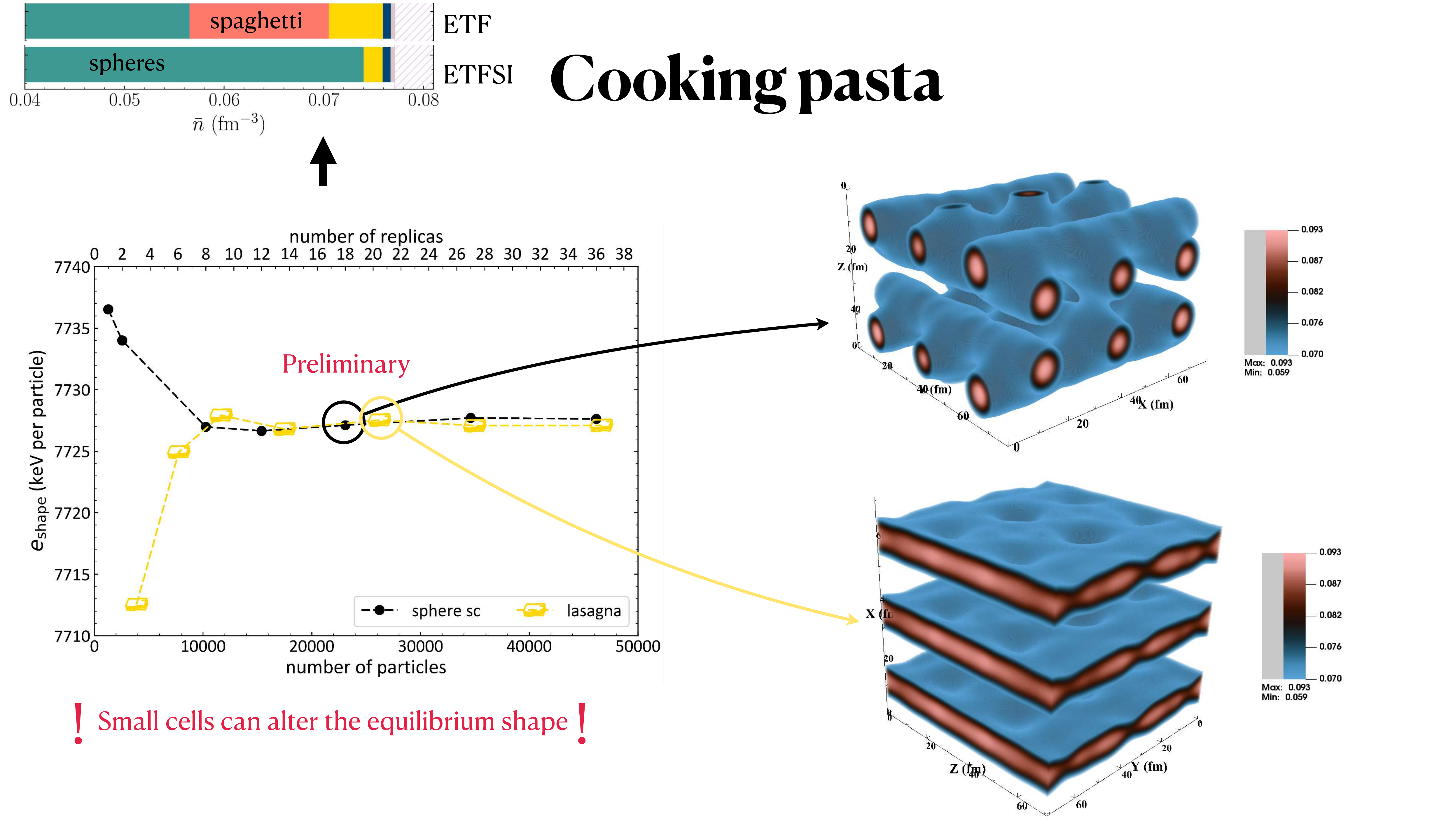


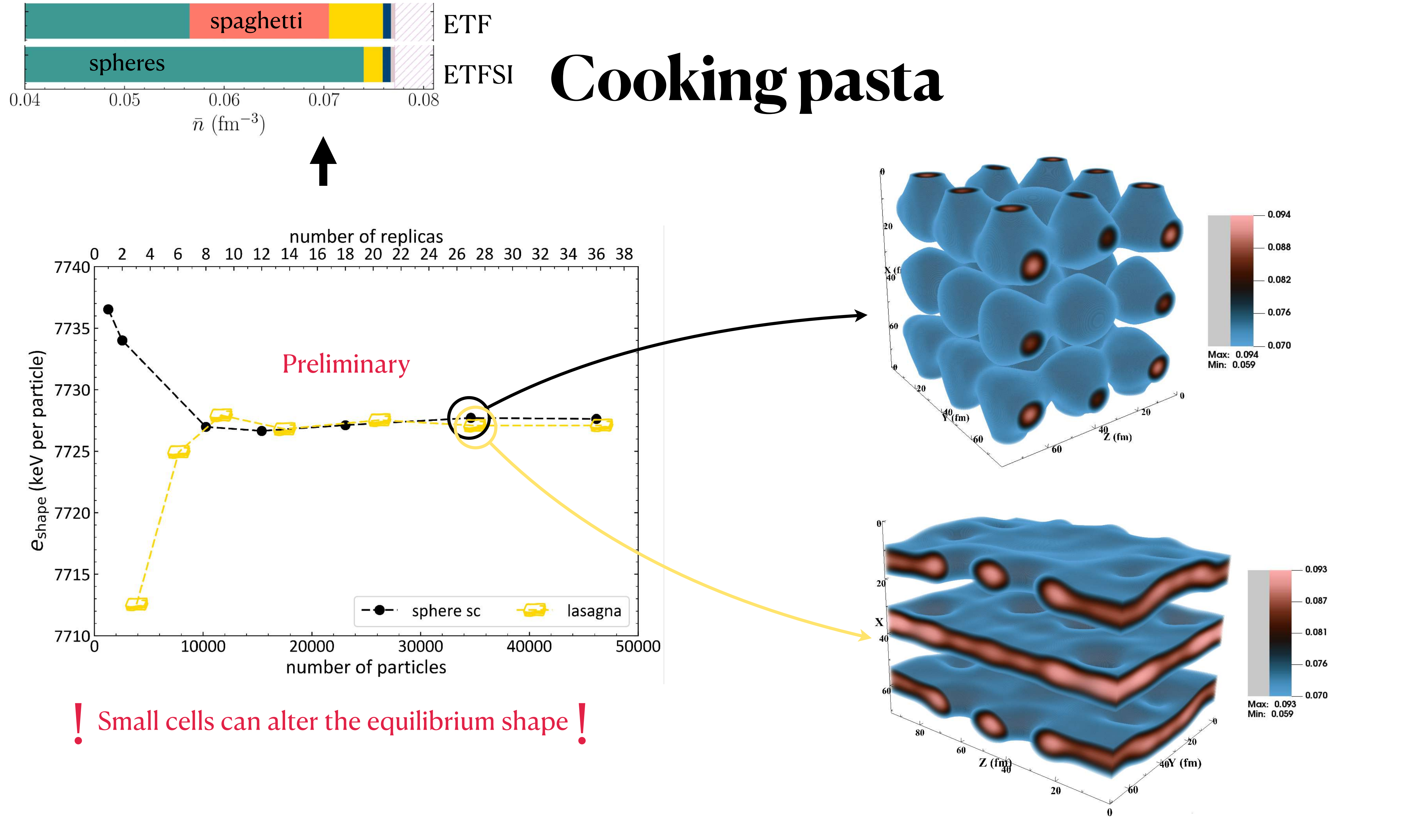


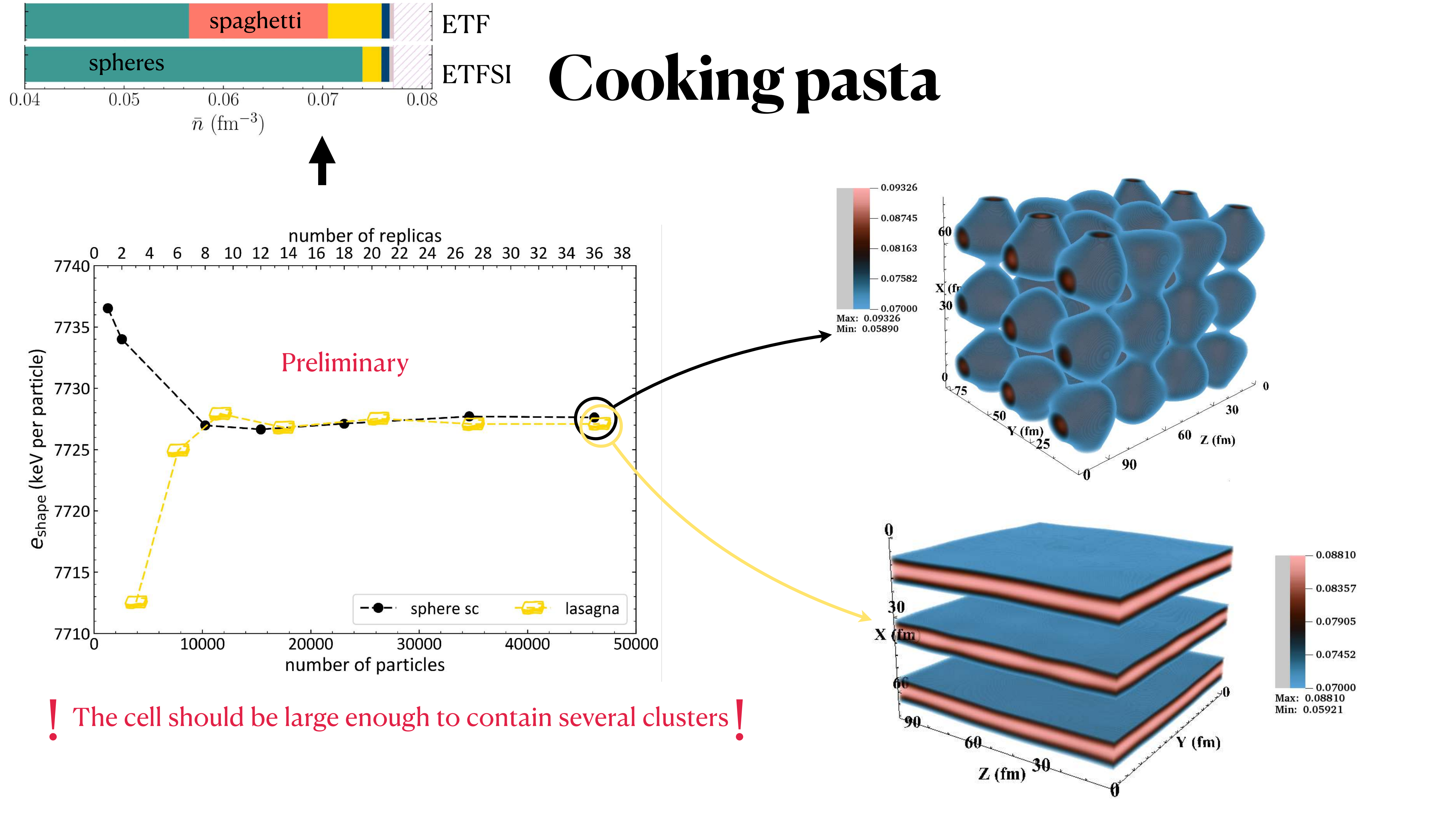


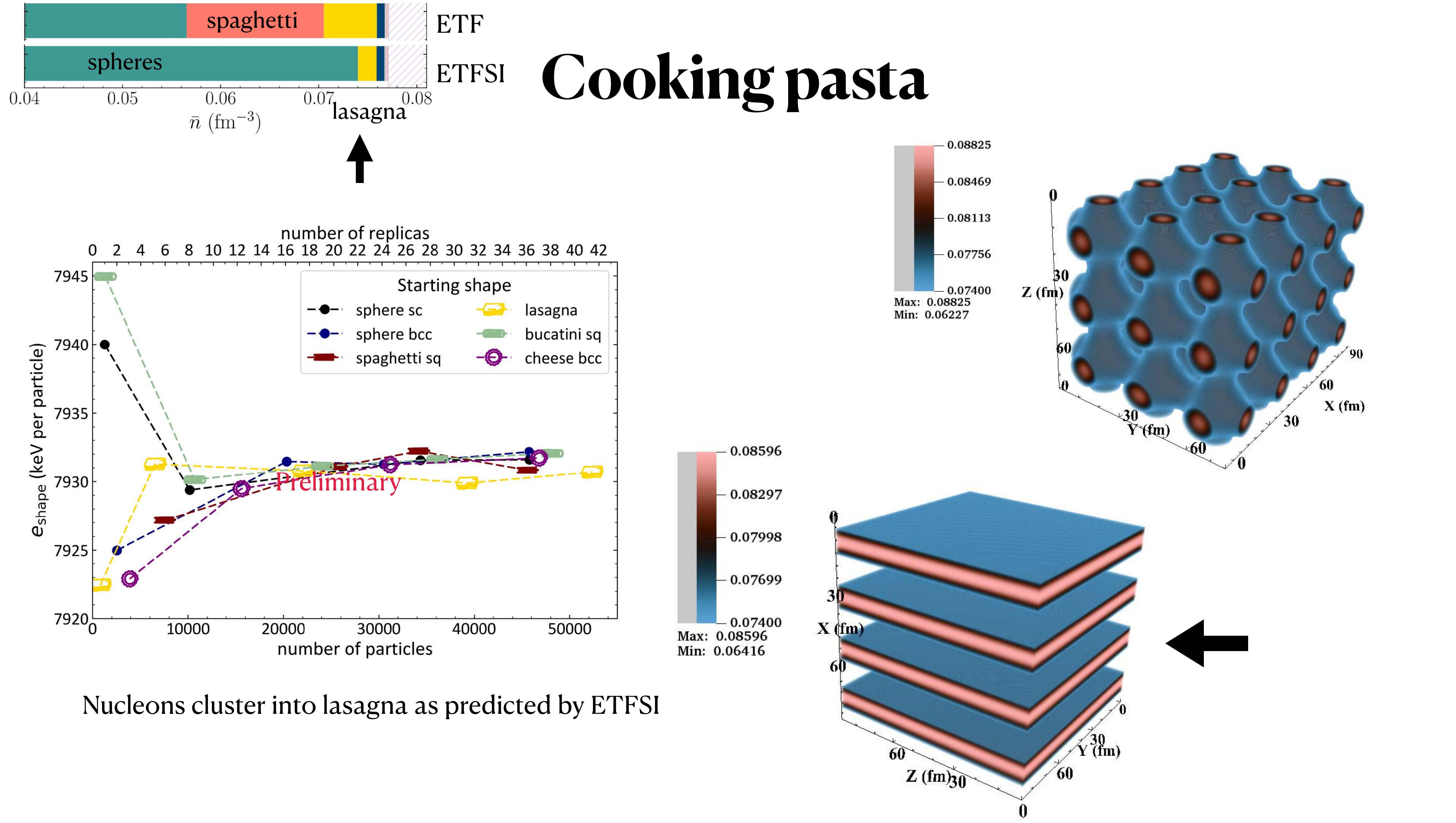


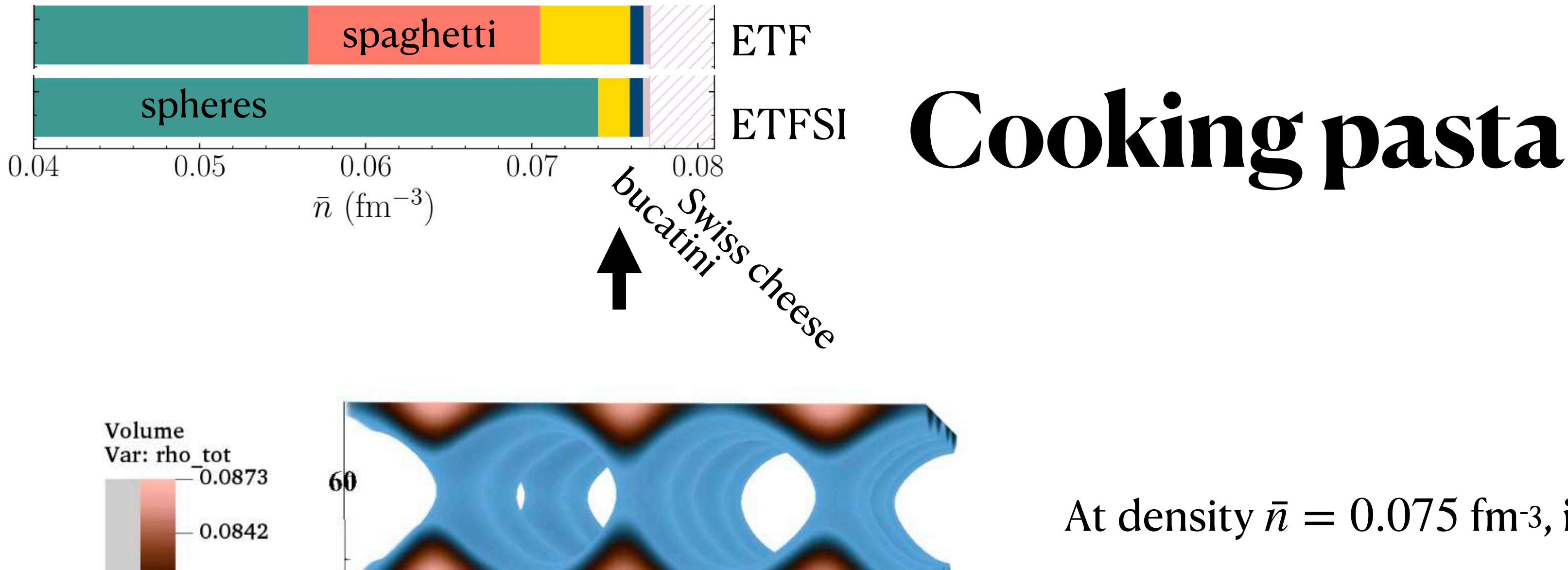












-0.0812

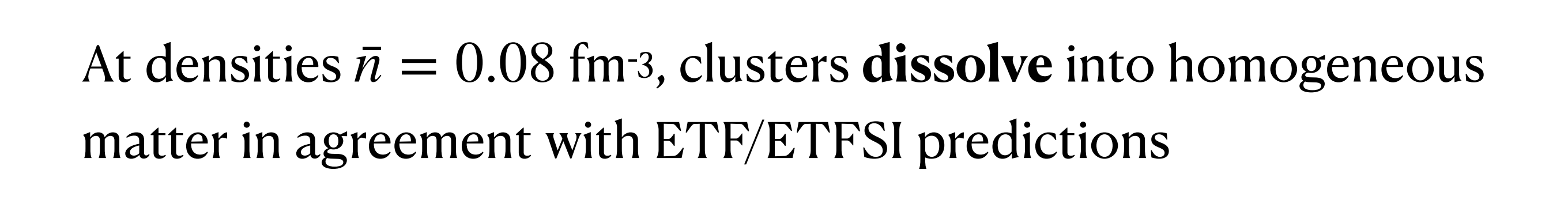
-0.0781

0.0750

Max: 0.0873 Min: 0.0634 Y (fm)

At density $\bar{n} = 0.075$ fm⁻³, intermediate "hollow" structures appear



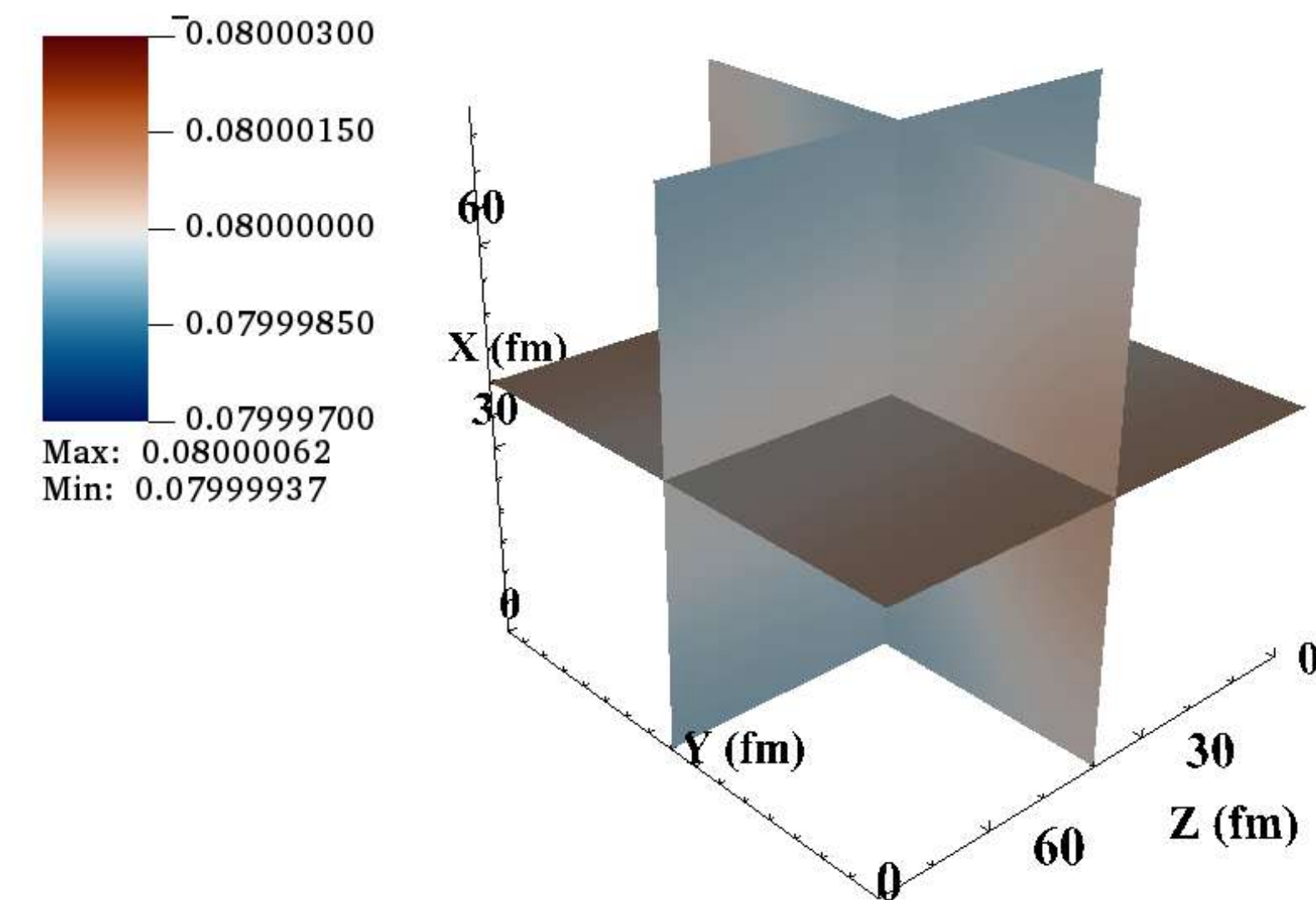


25

50

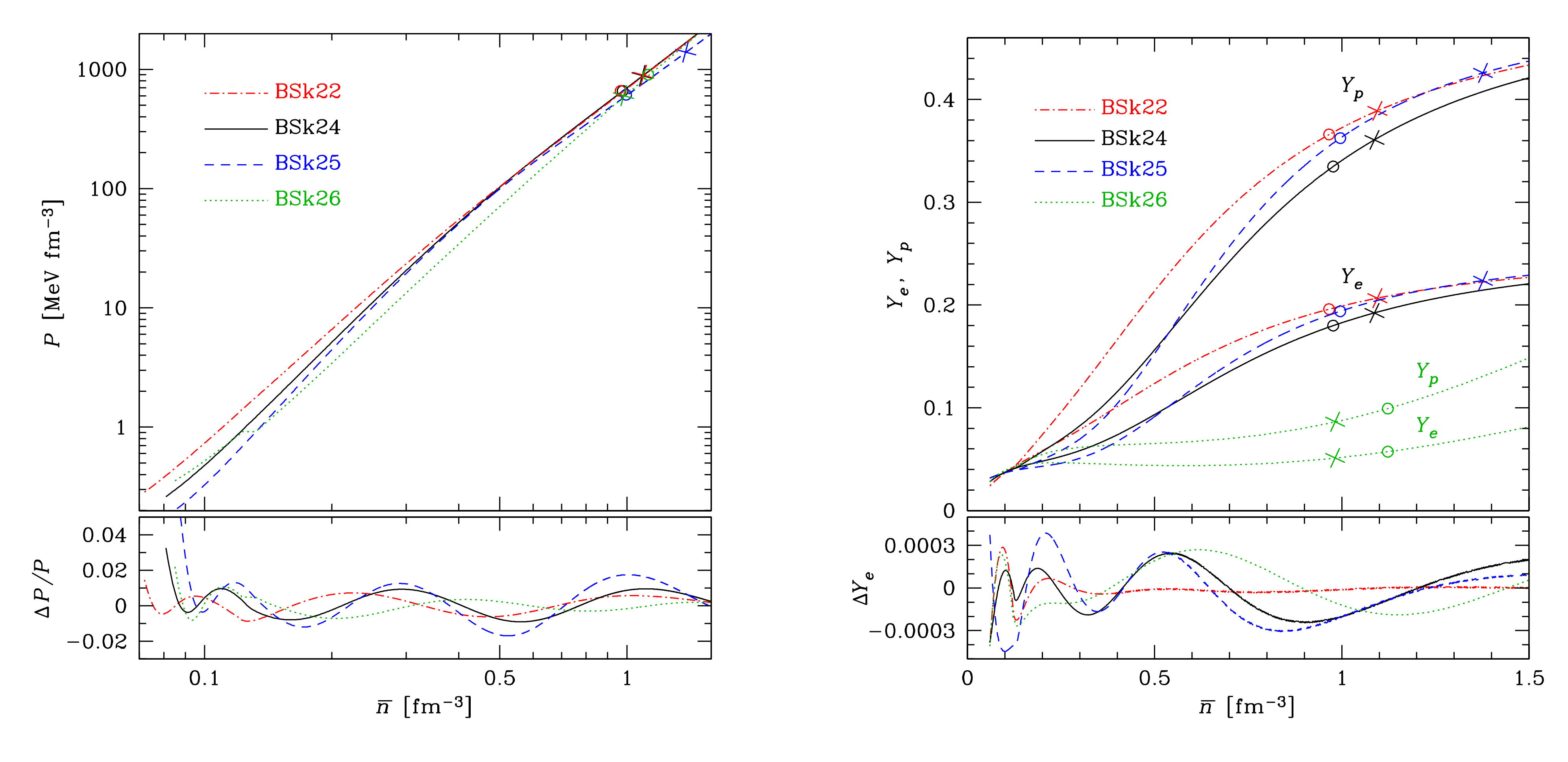
X (fm)

 $50^{\text{Z (fm)}}$



Core composition and equation of state

The EDF approach can be used to compute the properties of the core assuming n, p, e, μ matter:



Tables are available on CompOSE: https://compose.obspm.fr PCP(BSk22-26)

Fits of all thermodynamic variables and composition (including density profiles in the crust)

Observational constraints on the composition

The very fast direct Urca (dUrca) cooling process

$$n \rightarrow p + e^- + \bar{\nu}_e$$
 , $p + e^- \rightarrow n + \nu_e$

is required to explain

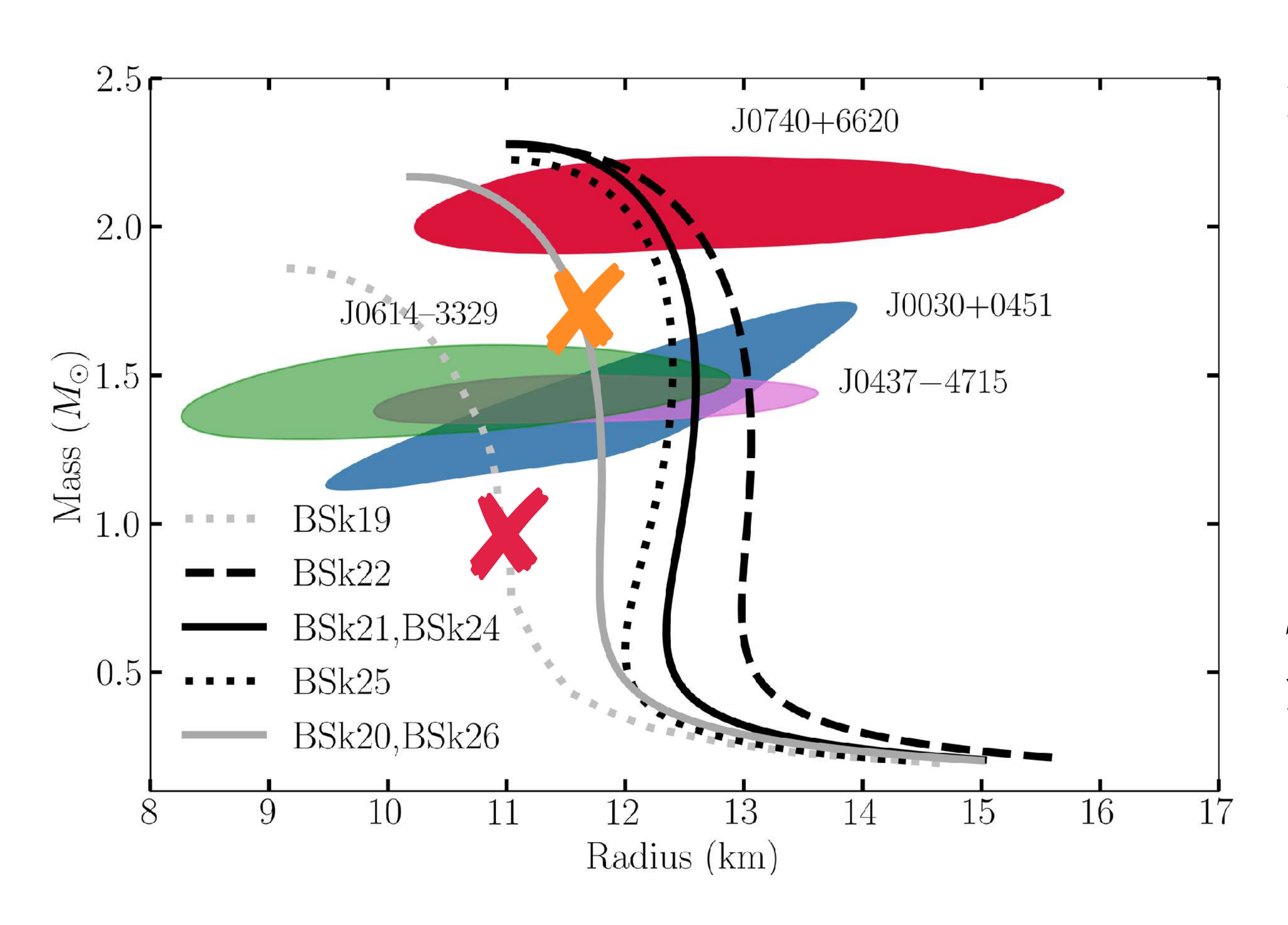
- the thermal luminosities of some accreting neutron stars (e.g. SAX J1808.4-3658)
- the cooling of cold young isolated neutron stars.

Marino et al. (2024)

	$n ({\rm fm}^{-3})$	$ ho$ (g cm $^{-3}$)	$M_{ m DU}/M_{\odot}$
BSk22	0.33	5.88×10^{14}	1.15
BSk21/24	0.45	8.25×10^{14}	1.60
BSk25	0.47	8.56×10^{14}	1.61
BSk19/20/26	s 8	·	

- The dUrca process is allowed in all models but BSk19/20/26.
- The low value for $M_{\rm DU}$ predicted by BSk22 implies that dUrca would operate in most neutron stars at variance with observations, but could be suppressed by superfluidity.

NICER and XMM observations



Latest analyses of NICER and XMM Newton observations:

- PSR Joo30+0451 Vinciguerra et al. (2024)
- PSR~J0437-4715 Choudhouri et al. (2024)
- PSR~J0740+6620 Salmi et al. (2024)
- PSR~Jo614-3329
 Mauviard et al. (2025)

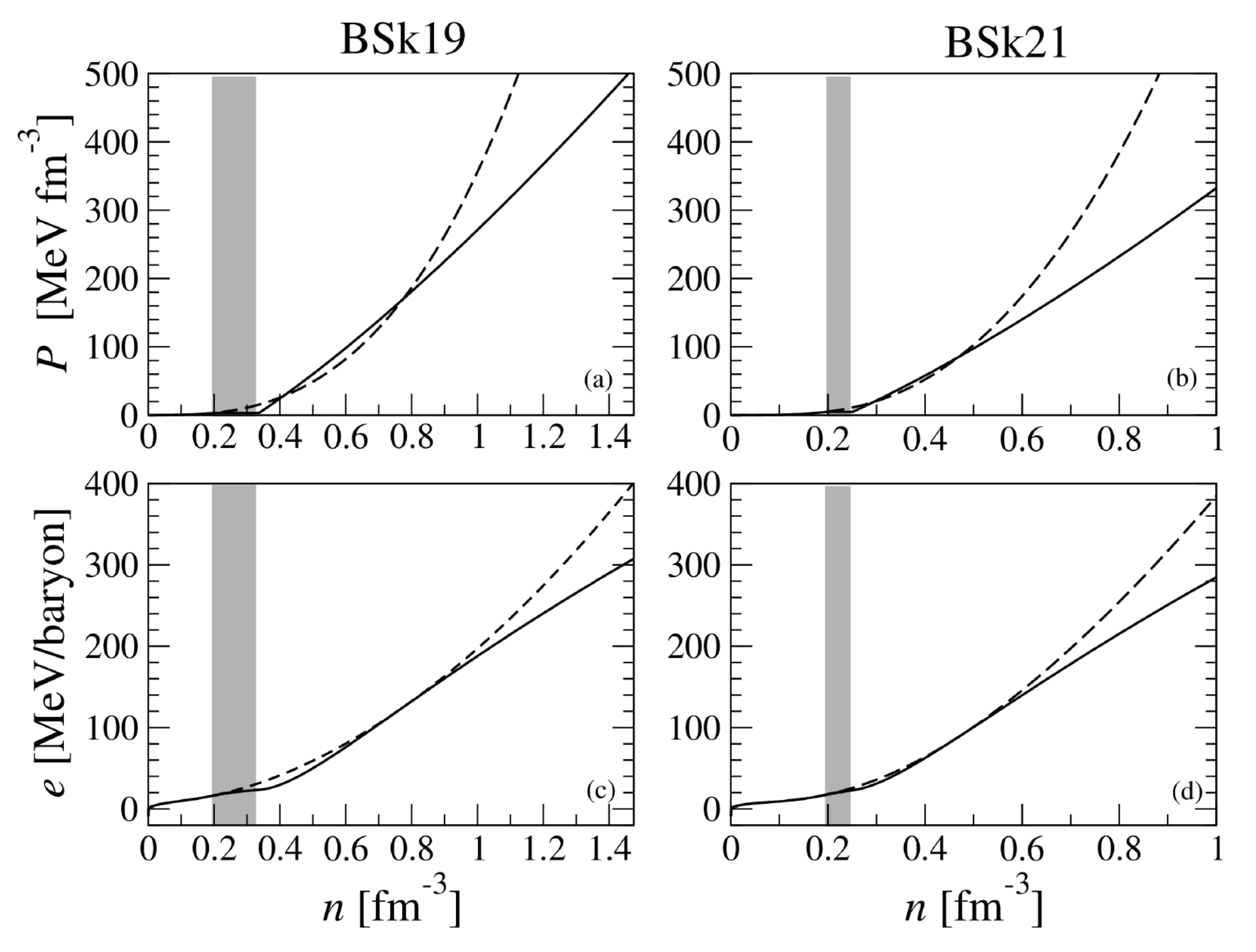
The mass and radius of PSR J1231-1411 and HESS J1731-347 have been measured but their analyses are less reliable

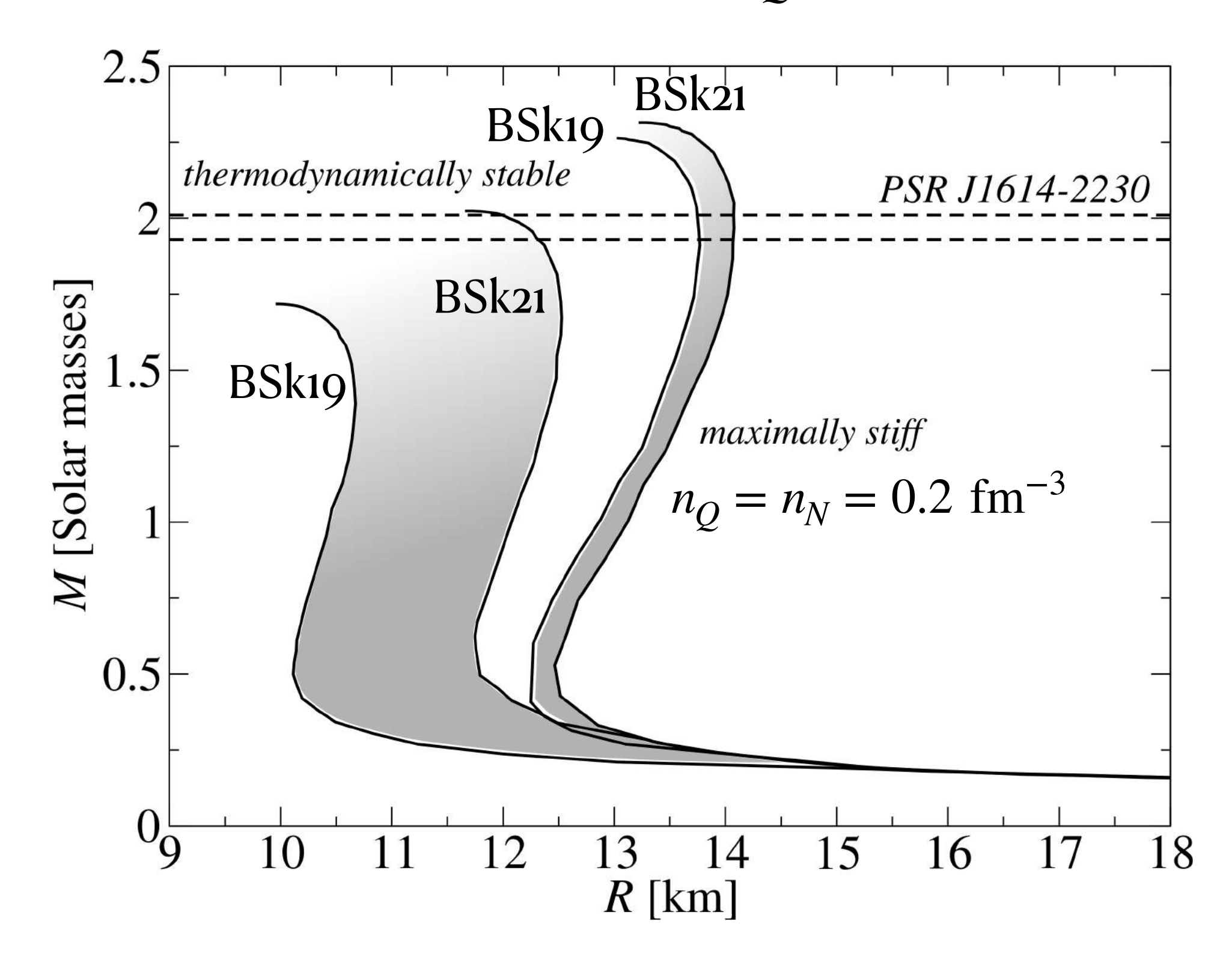
- BSk19 is too soft to support PSR Jo740+6620
- BSk20,BSk26 are compatible with all measurements but do not allow for the dUrca process

Phase transitions in neutron-star core

Soft nucleonic equations of state are not necessarily ruled out if quark matter is present in the inner core.

1st order phase transition: nucleonic matter for $n < n_N$ + MIT bag model for $n > n_Q$

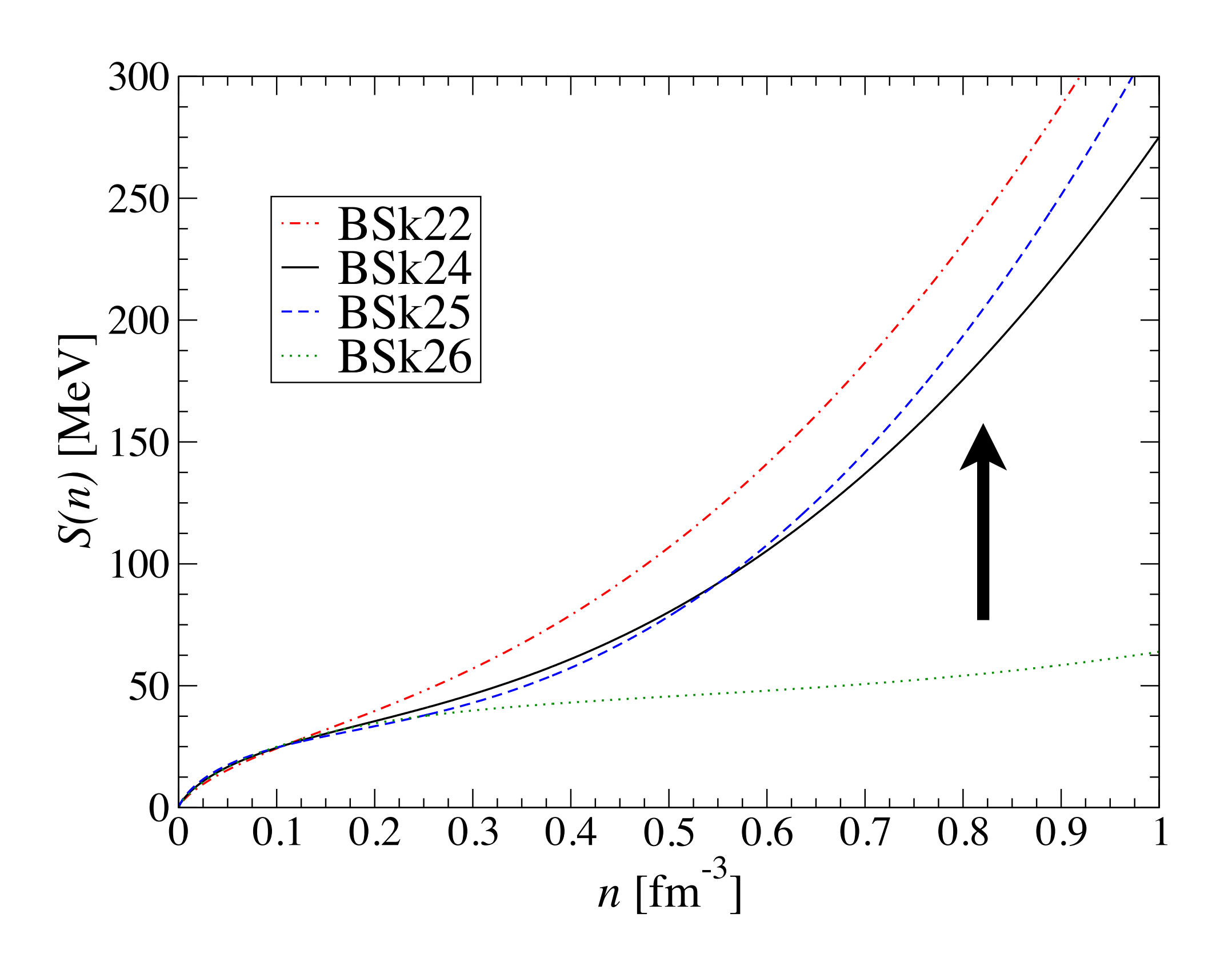


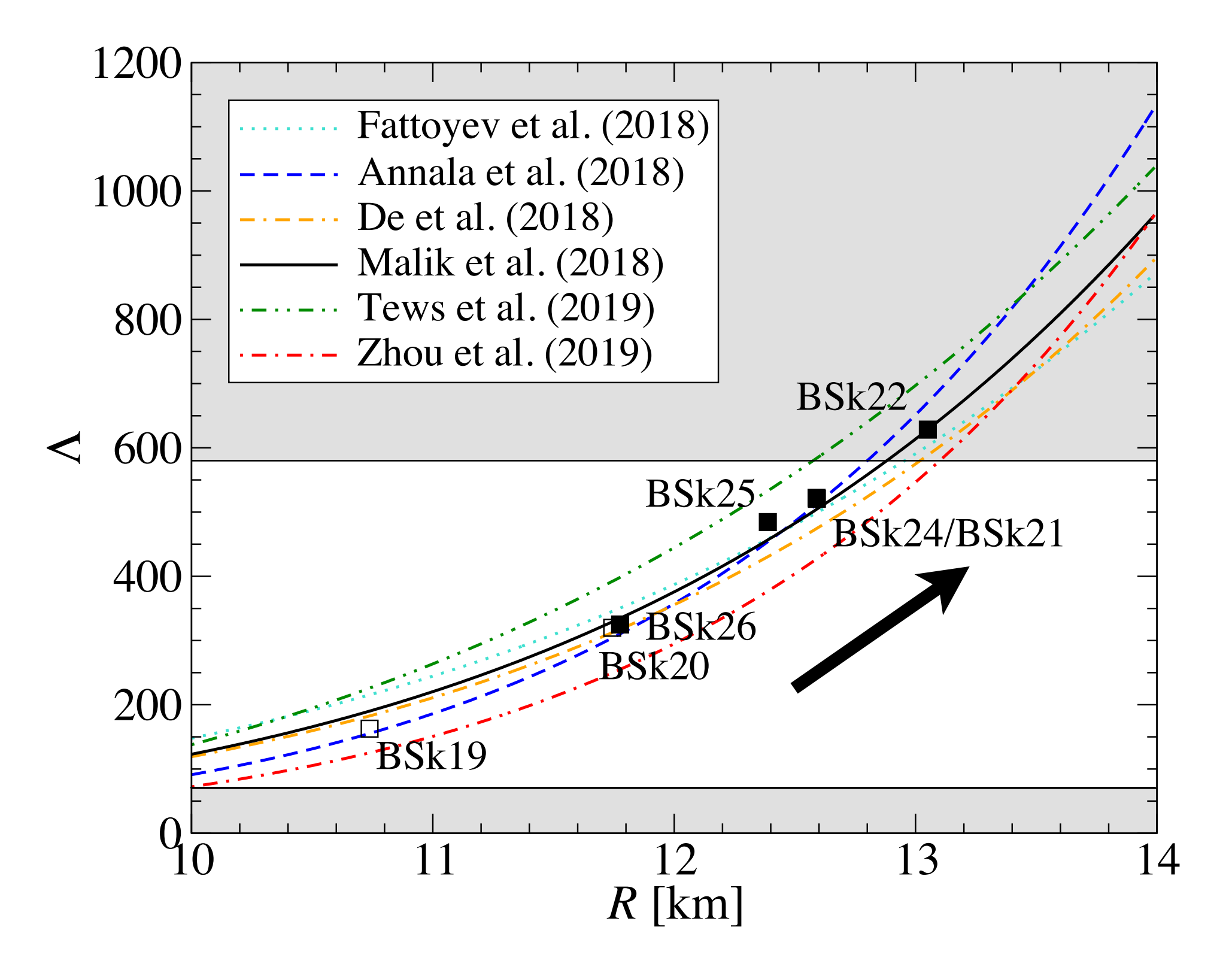


- From the existence of atomic nuclei, the density n_N must be $\gtrsim 0.2$ fm⁻³ while n_Q is usually freely adjusted
- However, requiring quark matter to be stable constrains n_O and leads to a *lower* maximum mass

Tidal deformability

The tidal deformability Λ of a 1.4 M_{\odot} neutron star is strongly correlated with R hence also with the symmetry energy:

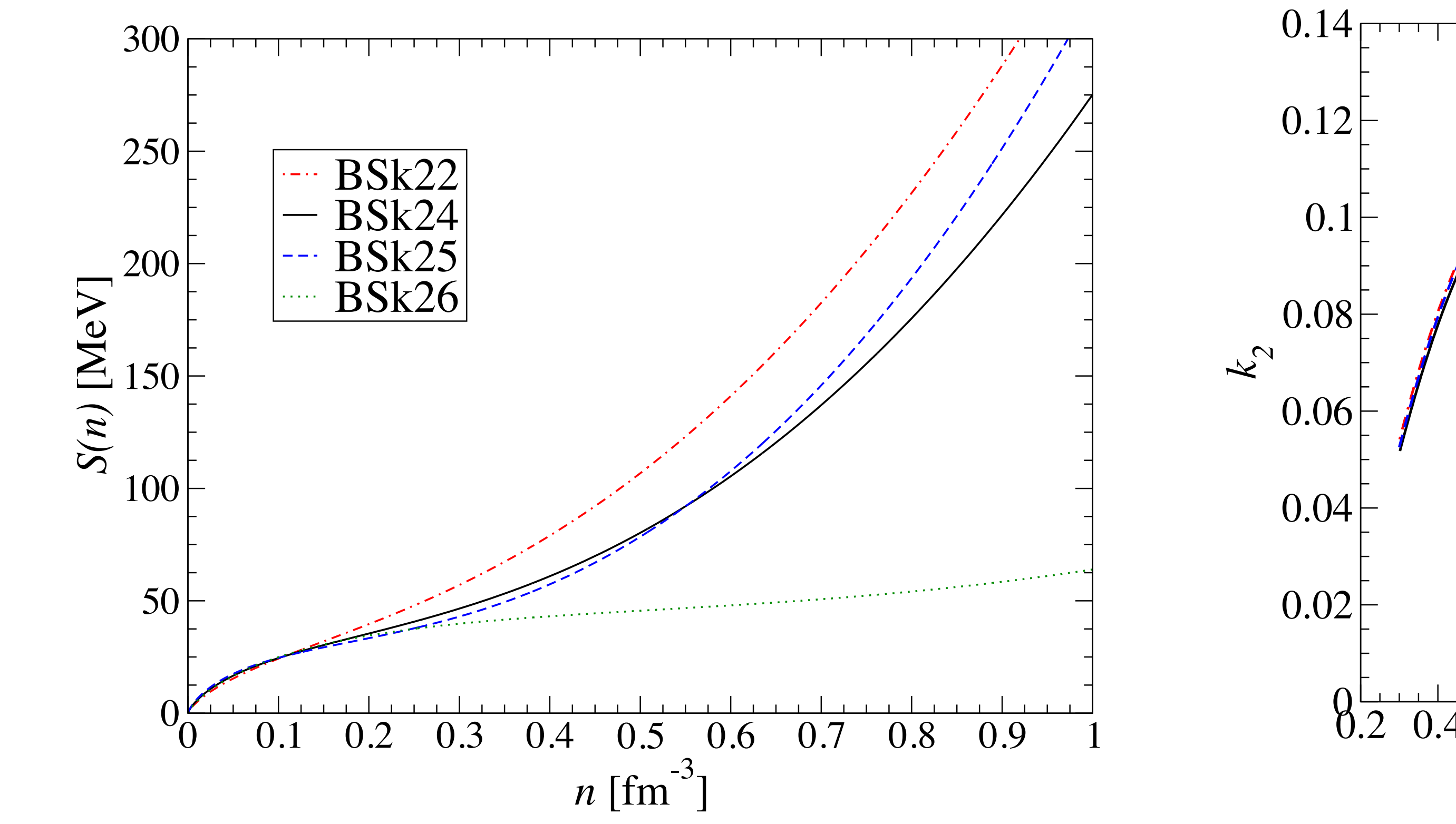


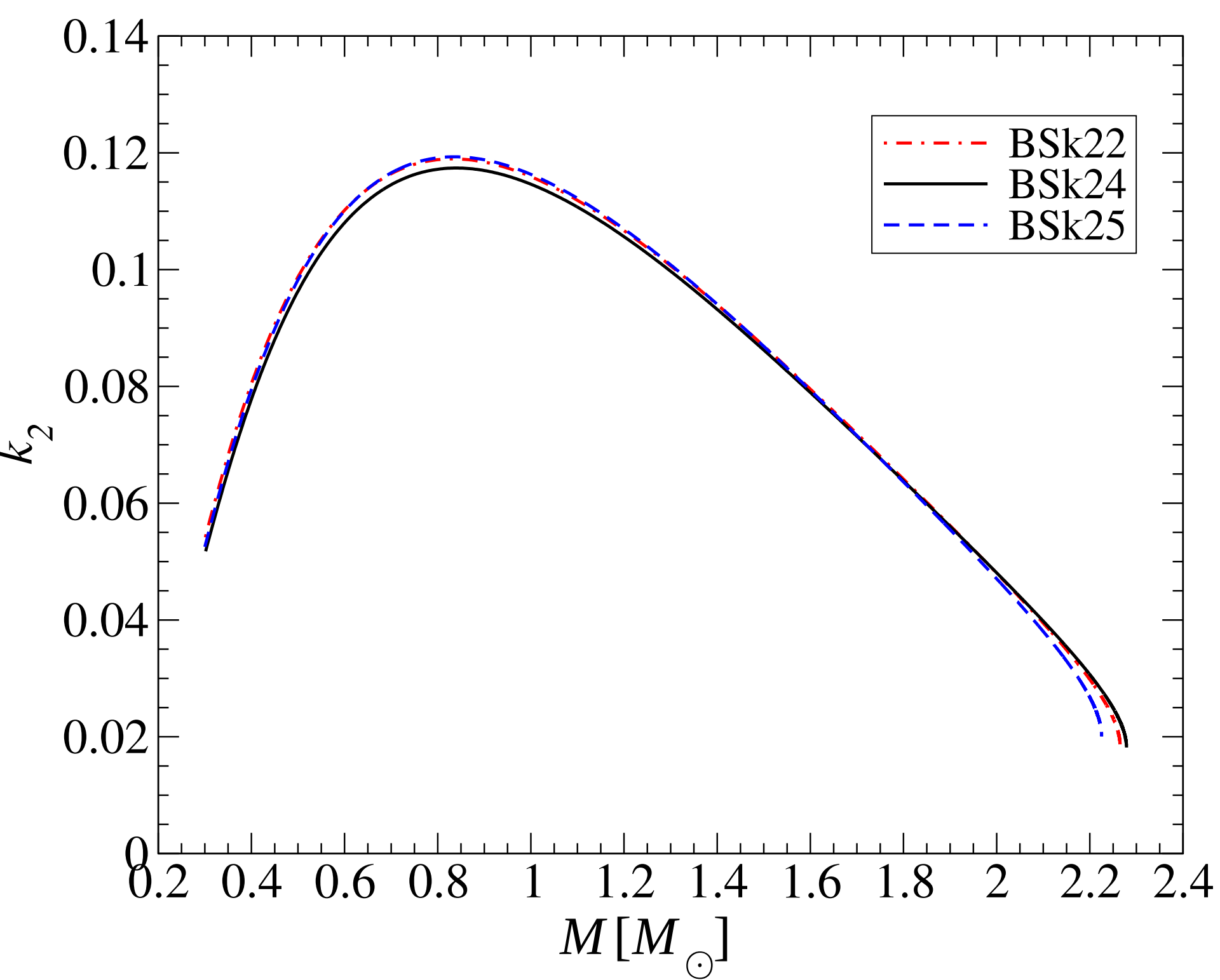


Perot, Chamel, Sourie (2019)

Symmetry energy and Love numbers

The Love number k_2 is insensitive to the symmetry energy:



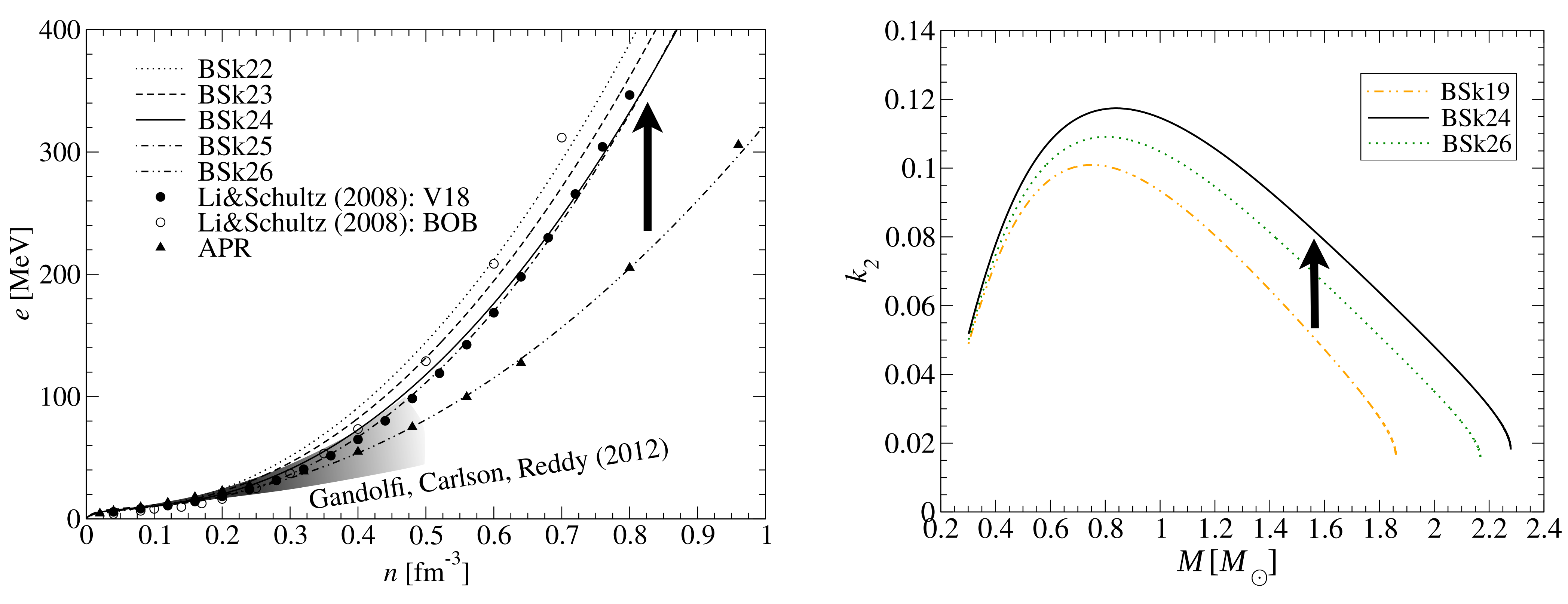


Perot, Chamel, Sourie (2019)

The dependence of $\Lambda = (2/3)k_2(Rc^2/GM)^5$ on the symmetry energy thus arises mainly from the factor R^5 .

Neutron matter and Love numbers

The Love number is mostly governed by the neutron-matter stiffness: the softer the equation of state, the lower k_2 is.



Perot, Chamel, Sourie (2019)

Similar behaviour for higher-order gravito-electric and magnetic Love numbers

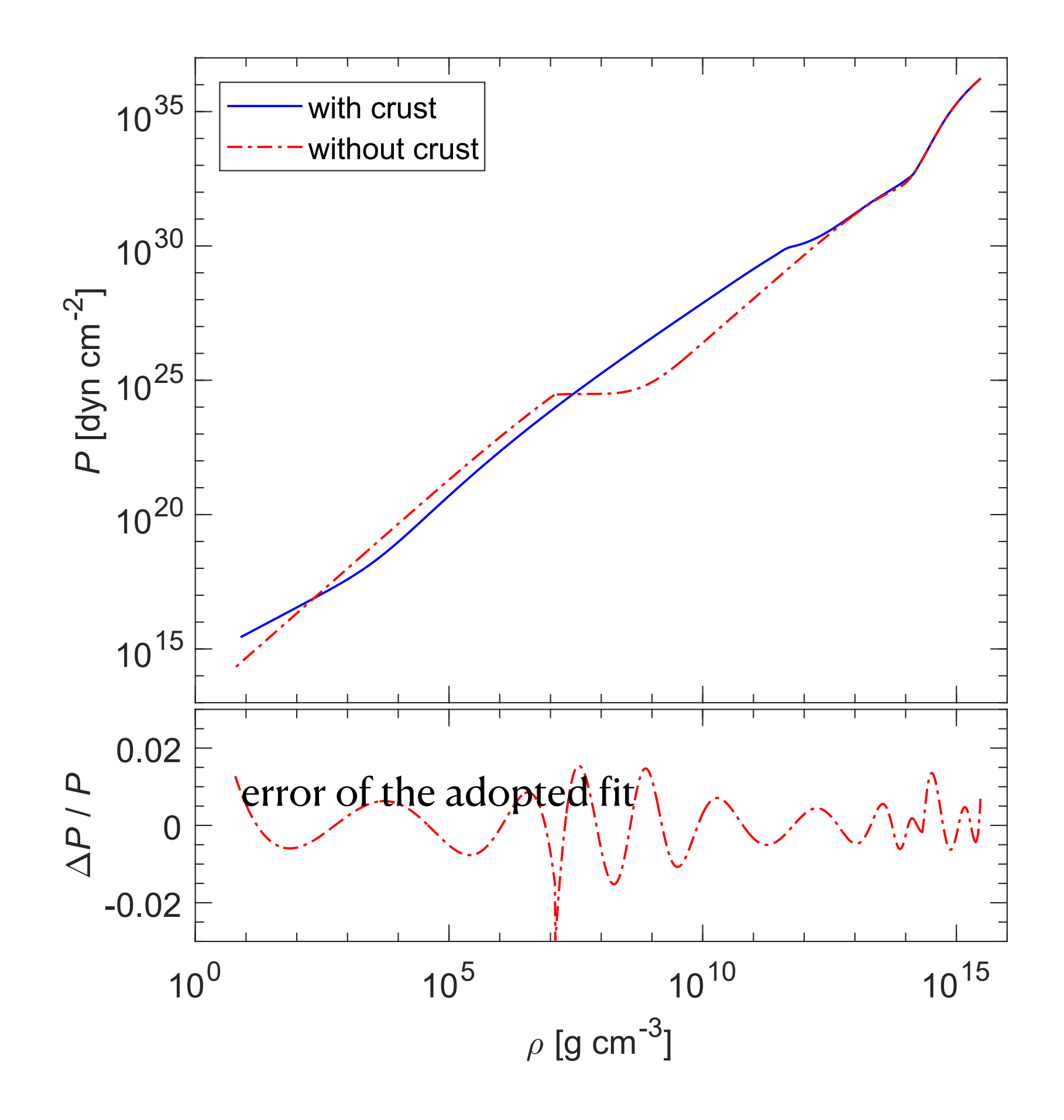
Perot & Chamel (2021)

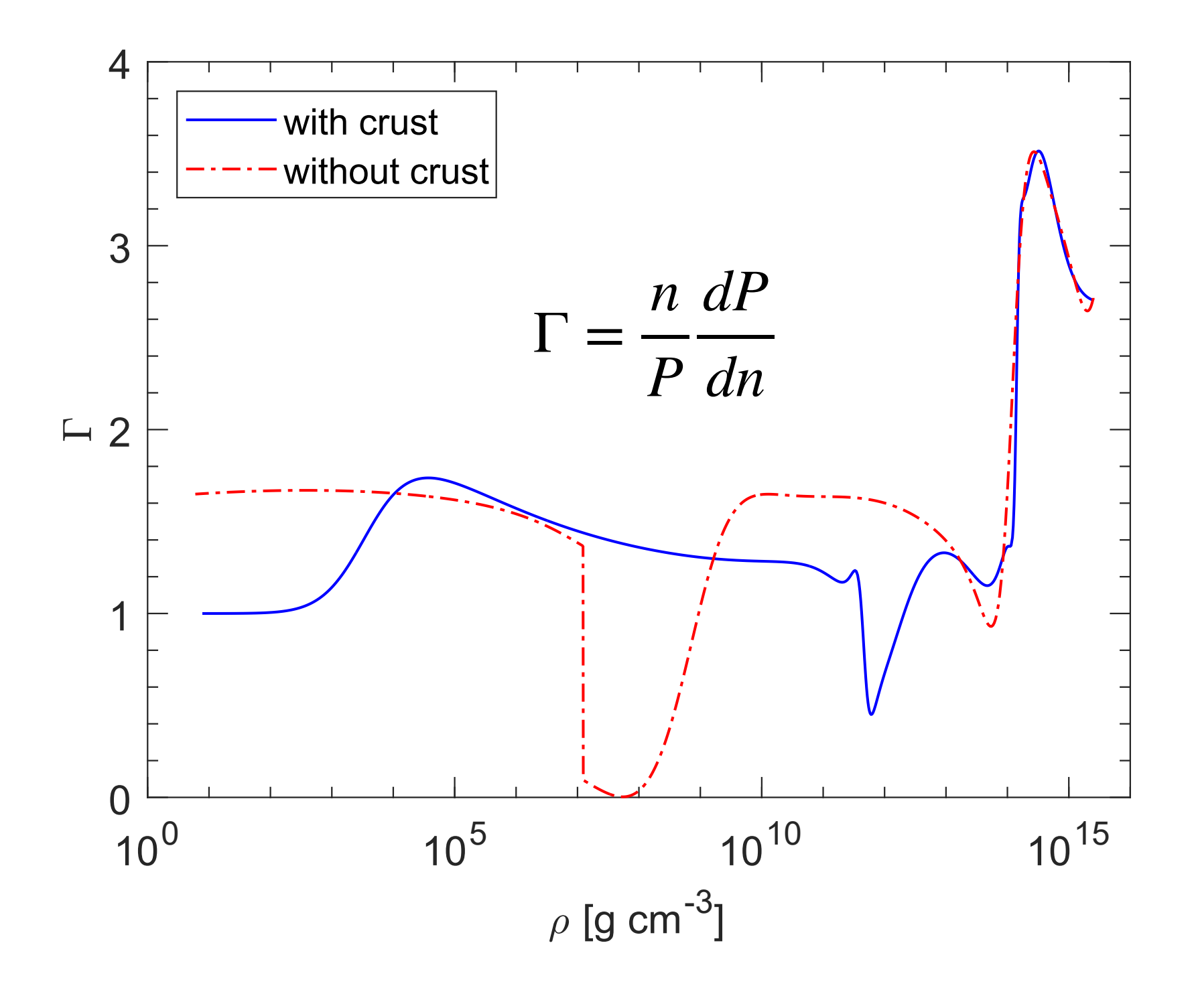
Crust and tidal deformability

Calculations based on different crust and core models yield $\delta \Lambda_{1.4}/\Lambda_{1.4} \sim 0.1-10\,\%$ depending on the matching conditions

Piekarewicz &Fattoyev (2019), Kalaitzis et al. (2019), Ji et al. (2019)

Unified equations of state with crust and "without crust" (replaced by homogeneous *n*, *p*, *e* matter):





Perot, Chamel, Sourie (2020)

Crust and tidal deformability

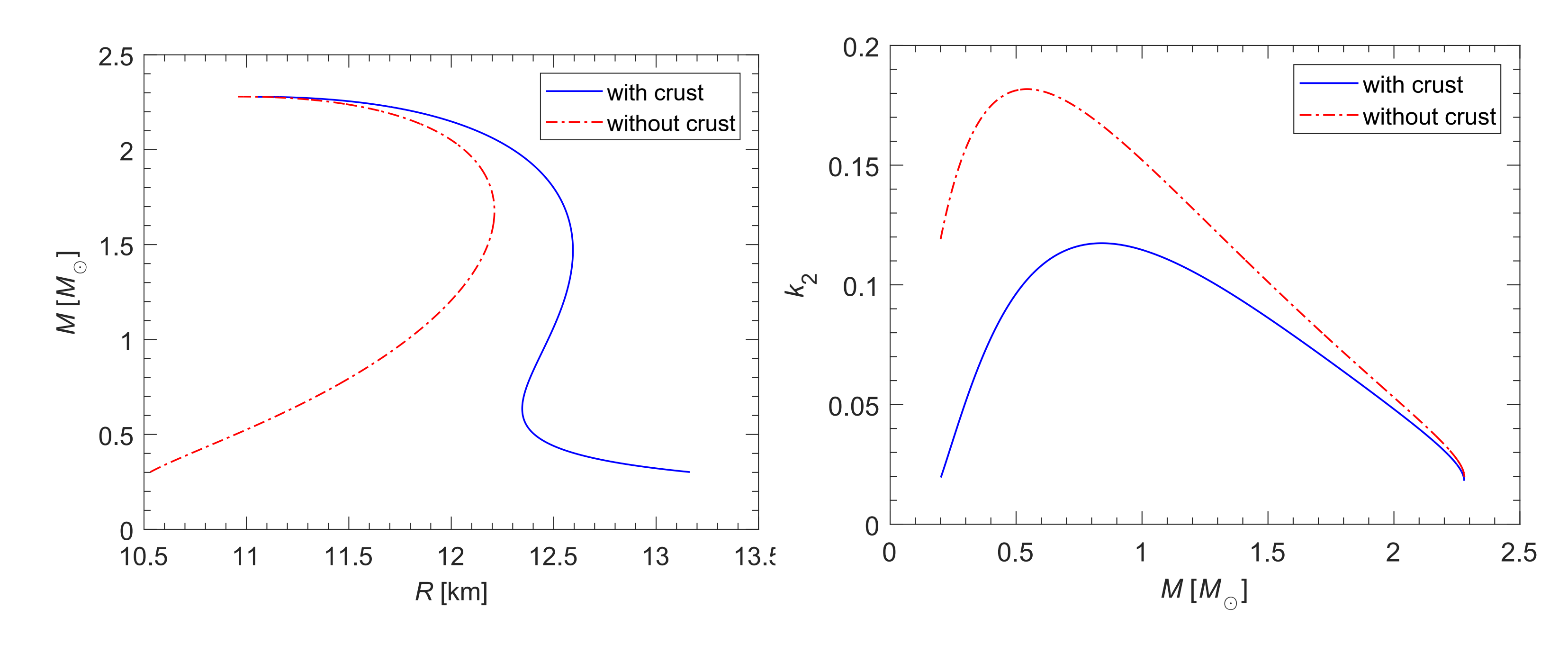
Calculations based on different crust and core models yield $\delta\Lambda_{1,4}/\Lambda_{1,4}\sim0.1-10\,\%$ depending on the matching conditions

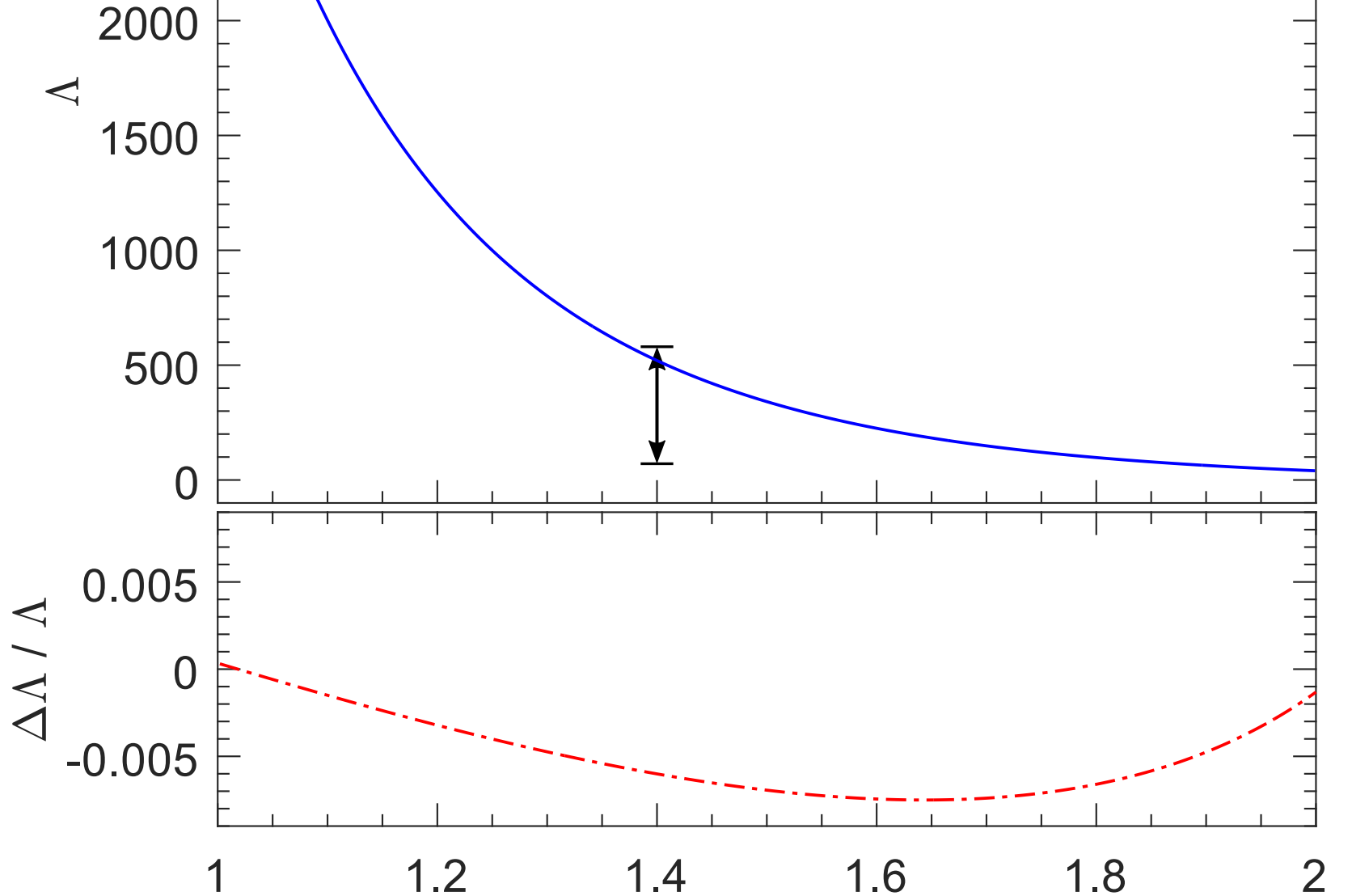
Piekarewicz &Fattoyev (2019), Kalaitzis et al. (2019), Ji et al. (2019)

3000

2500

Unified equations of state with crust and "without crust" (replaced by homogeneous *n*, *p*, *e* matter):





Note that elastic correction is completely negligible Gittins, Andersson, Pereira (2020)

Perot, Chamel, Sourie (2020)

 $M[M_{\odot}]$

Tidal deformability from homogeneous matter

The structure and tidal deformability can be inferred without the equation of state of the crust. It is enough to consider a neutron star made entirely of homogeneous n, p, e matter with the same mass M:

$$R = R_0 \left\{ 1 - \left[\left(\frac{m_{\rm H}}{m_{\rm Fe}} \right)^2 - 1 \right] \left(\frac{R_0}{R_s} - 1 \right) \right\}^{-1} \text{ where } R_0 \text{ is the radius from the TOV equations and } R_s = 2GM/c^2$$

$$Zdunik, \text{ Fortin, Haensel (2017)}$$

$$y(R) \approx \frac{1}{2} \left[-F_0 + \sqrt{F_0^2 - 4Q_0} \tanh \left(\frac{1}{2} \sqrt{F_0^2 - 4Q_0} \ln \frac{R}{R_0} + \tanh^{-1} \frac{2y_0 + F_0}{\sqrt{F_0^2 - 4Q_0}} \right) \right]$$

$$F_0 = \left(1 - \frac{R_s}{R_0} \right)^{-1} \qquad Q_0 = -6F_0 - F_0^2 \left(\frac{R_s}{R_0} \right)^2$$

$$F_0 = \left(1 - \frac{R_s}{R_0}\right)^{-1} \qquad Q_0 = -6F_0 - F_0^2 \left(\frac{R_s}{R_0}\right)^2$$

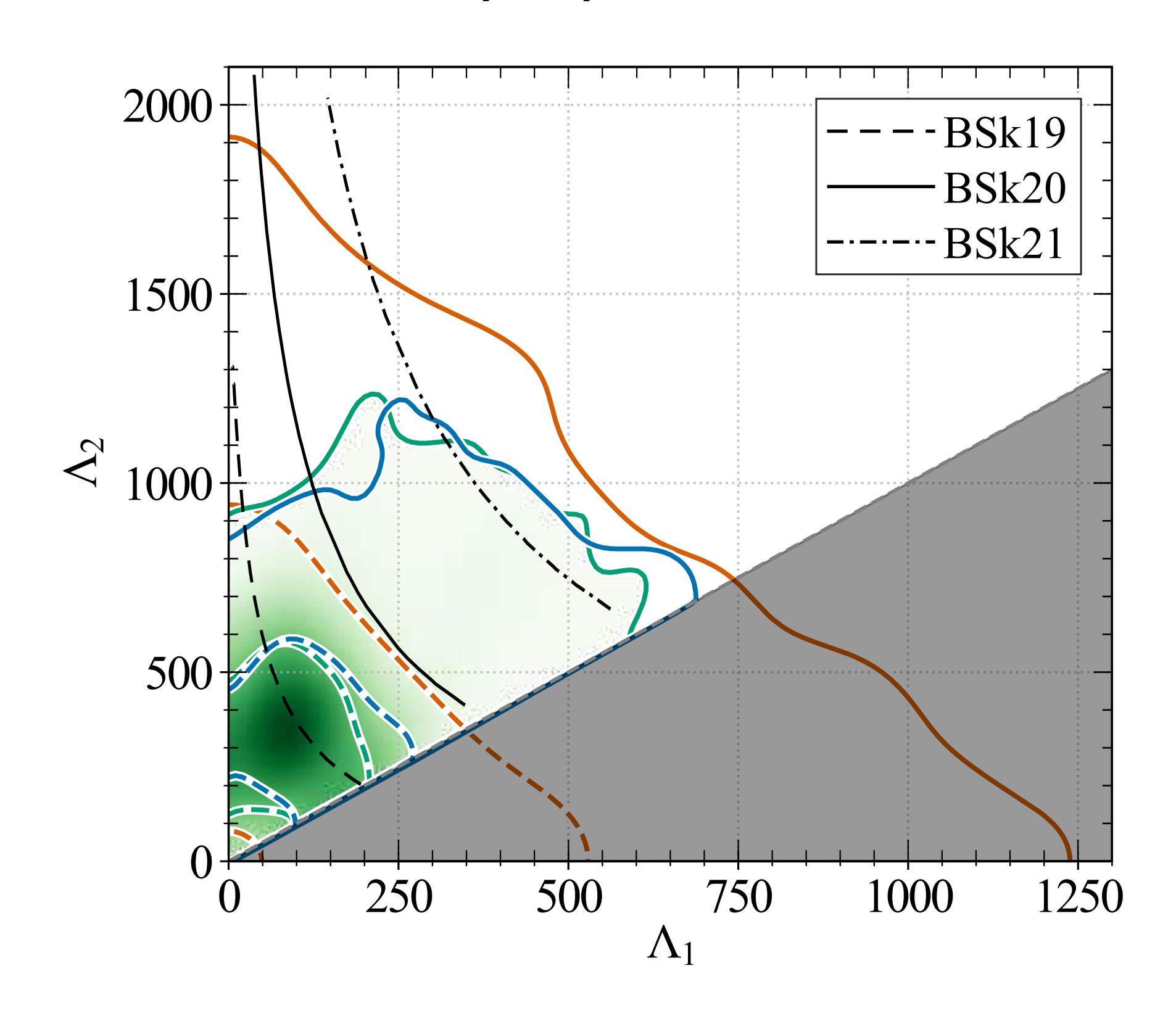
Here $y_0 \equiv y(R_0)$ is the solution of $ry'(r) + y(r)^2 + F(r)y(r) + Q(r) = 0$ from Postnikov, Prakash, Lattimer (2010)

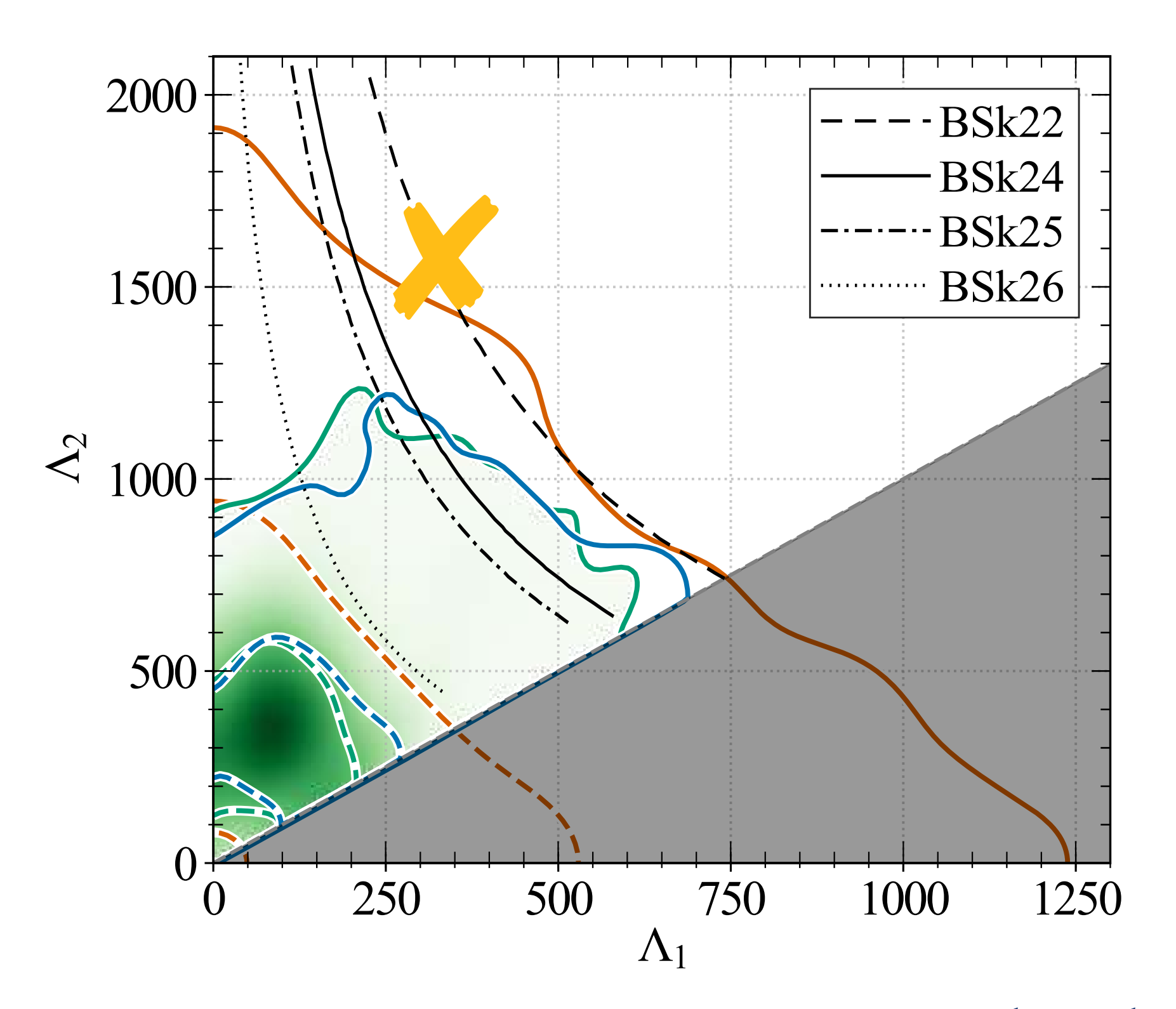
 k_2 can be obtained from y(R) using the usual formula from Hinderer et al.

The errors on R and k_2 are ~0.1 %

LIGO-Virgo observations

The detection of GW170817 has provided the first measurements of the tidal deformability of a neutron star:

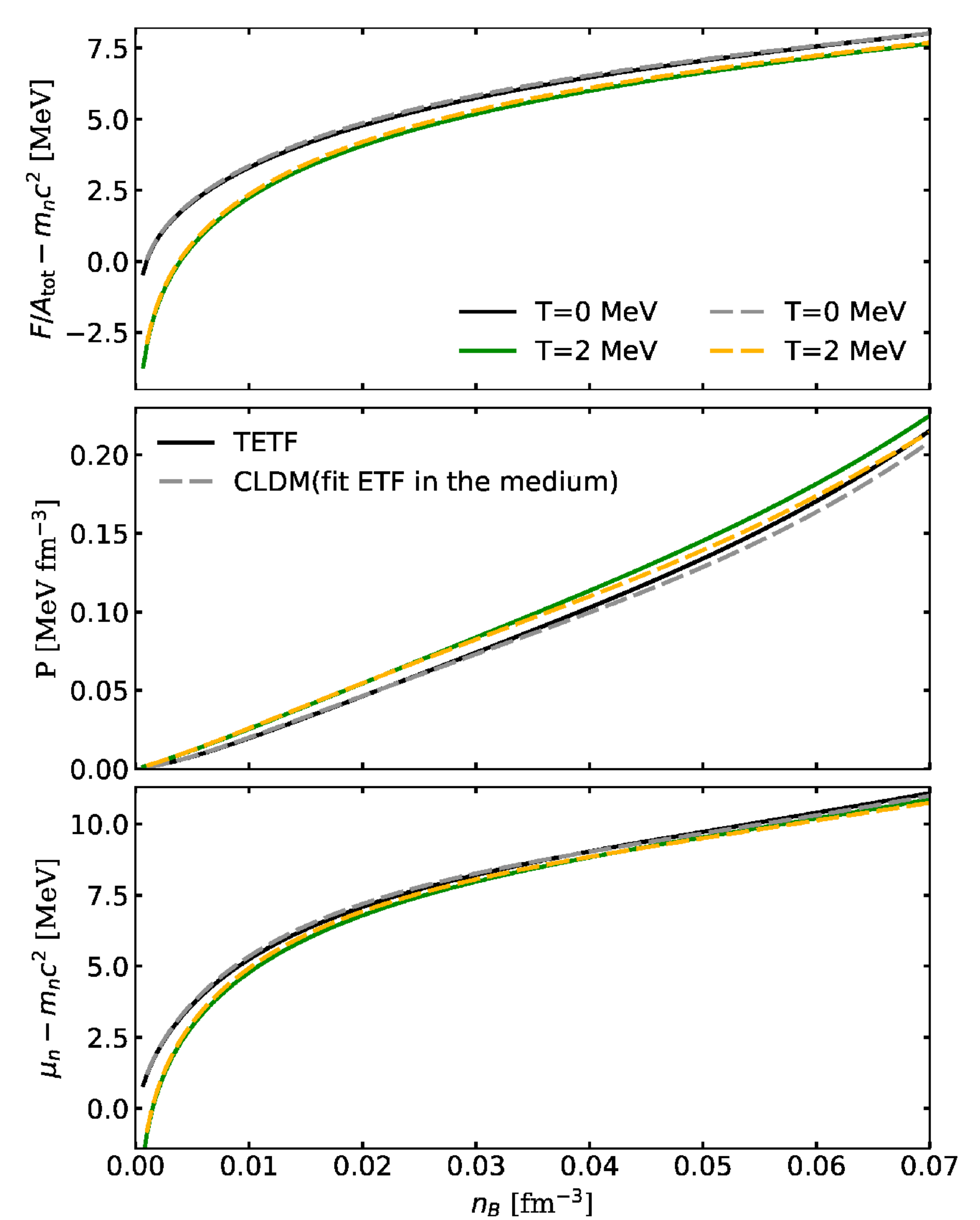




Perot, Chamel, Sourie (2019)

A stiff symmetry energy (BSk22) is marginally compatible.

Temperature-dependent Extended Thomas-Fermi (TETF) calculations with BSk24:



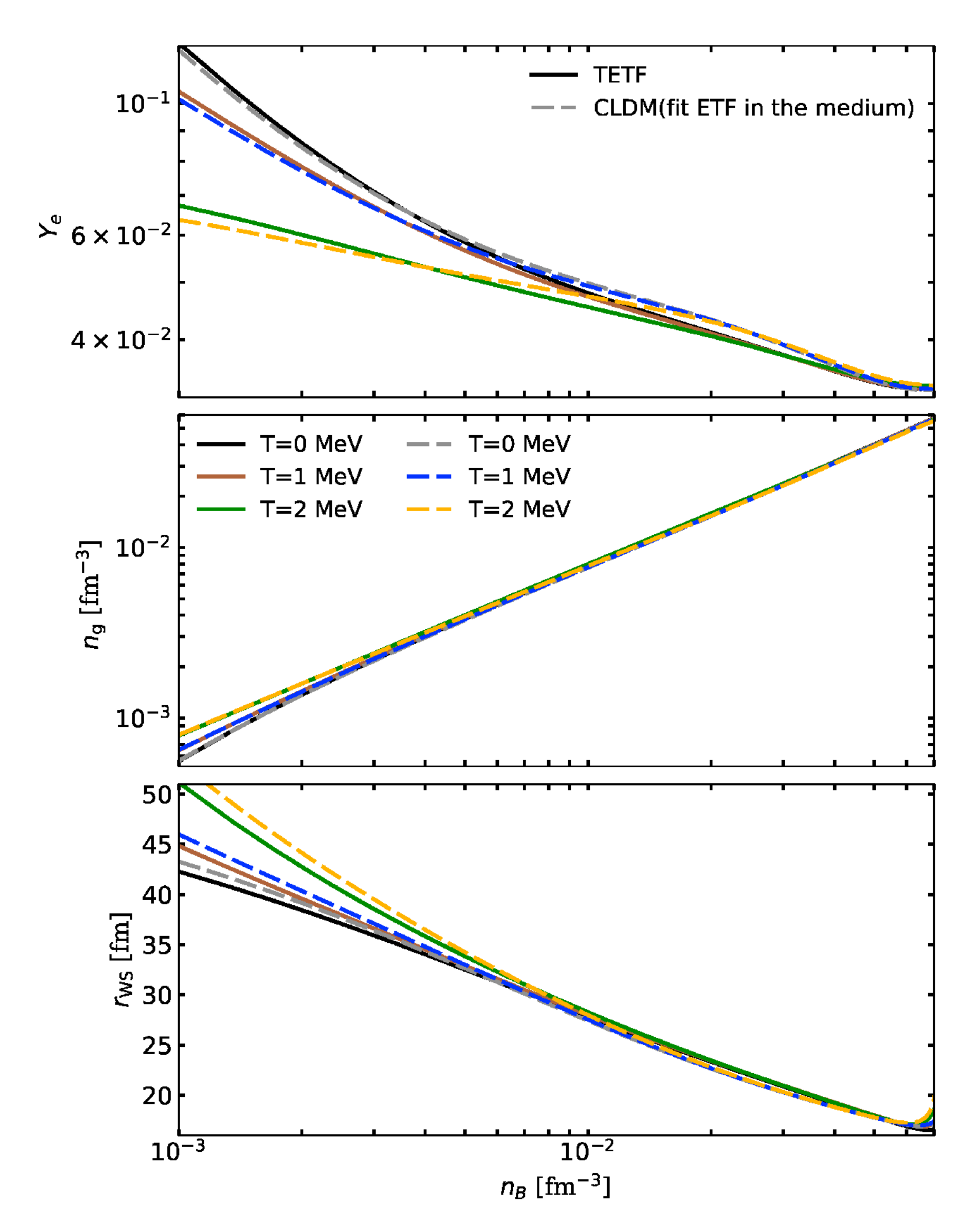
The equation of state can be well reproduced by a compressible liquiddrop model with surface parameters fitted to zero-temperature ETF calculations in the medium using the same functional



Guilherme Grams

Grams et al. (2025)

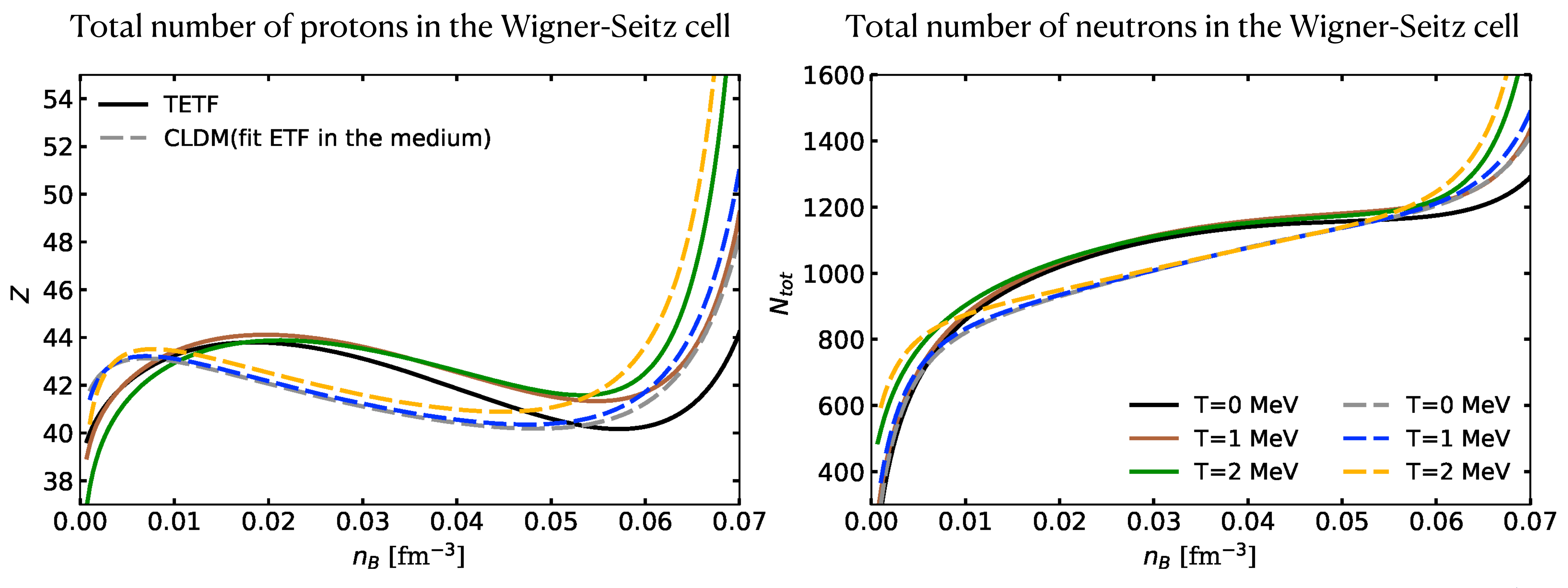
Temperature-dependent Extended Thomas-Fermi (TETF) calculations with BSk24:



The results from the liquid-drop model for the electron fraction, the density of the nucleon gas and the radius of the Wigner-Seitz cell remain close to the TETF predictions

Grams et al. (2025)

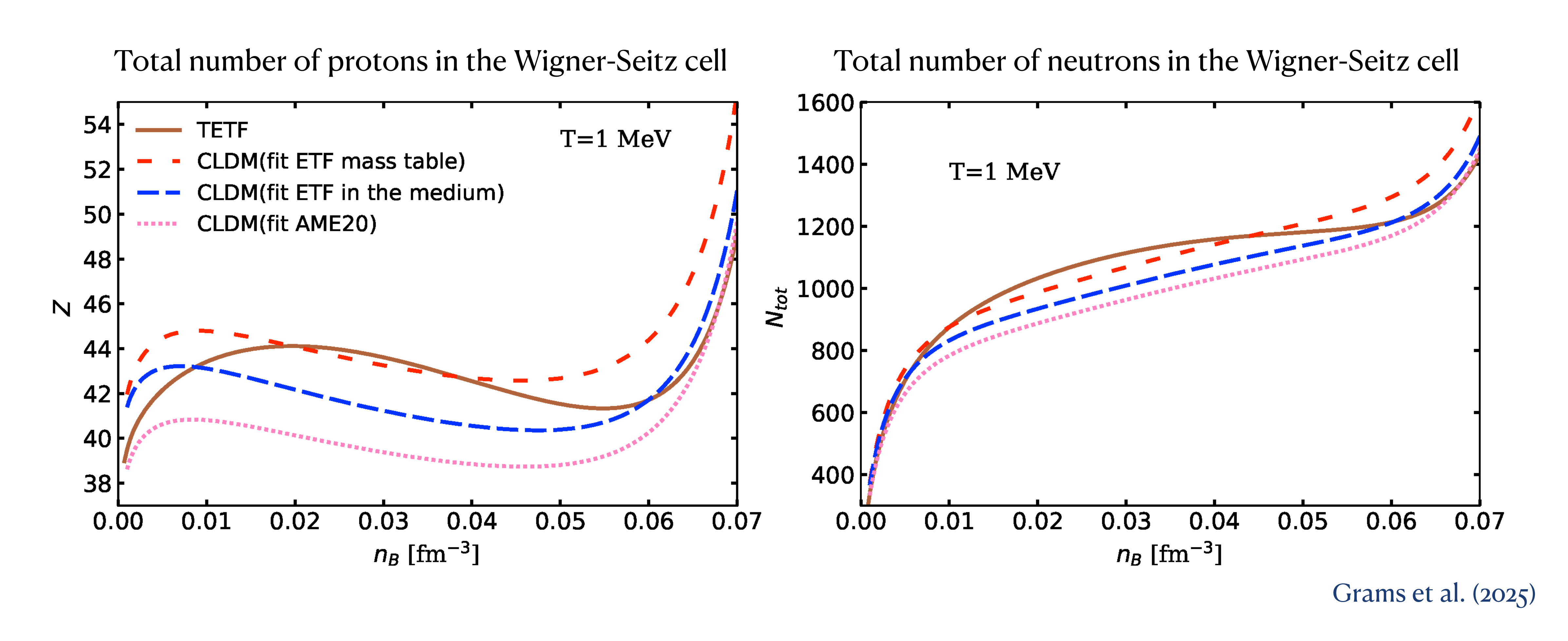
Temperature-dependent Extended Thomas-Fermi (TETF) calculations with BSk24:



Grams et al. (2025)

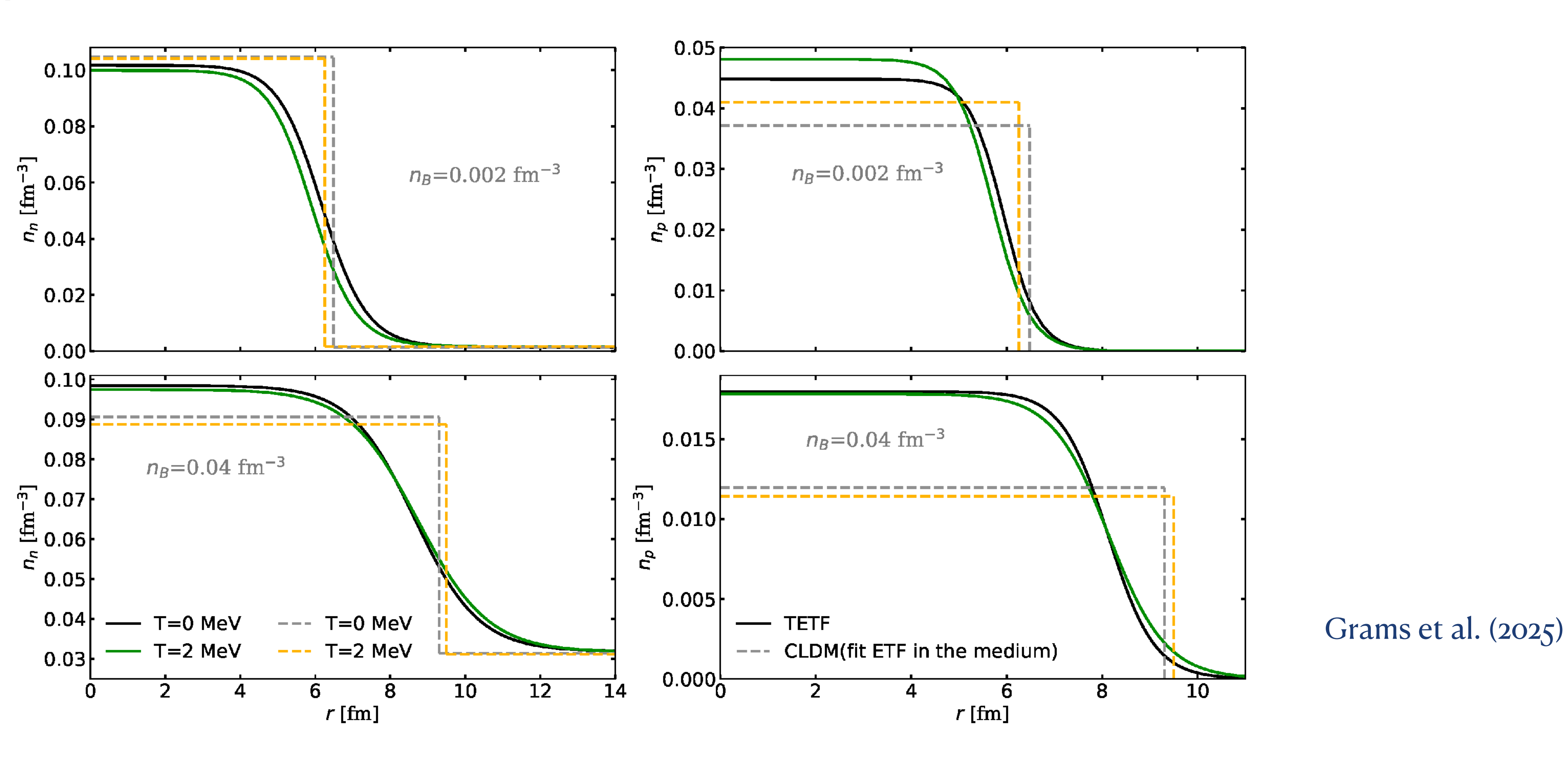
The composition obtained with the liquid-drop model is less accurate.

Temperature-dependent Extended Thomas-Fermi (TETF) calculations with BSk24:



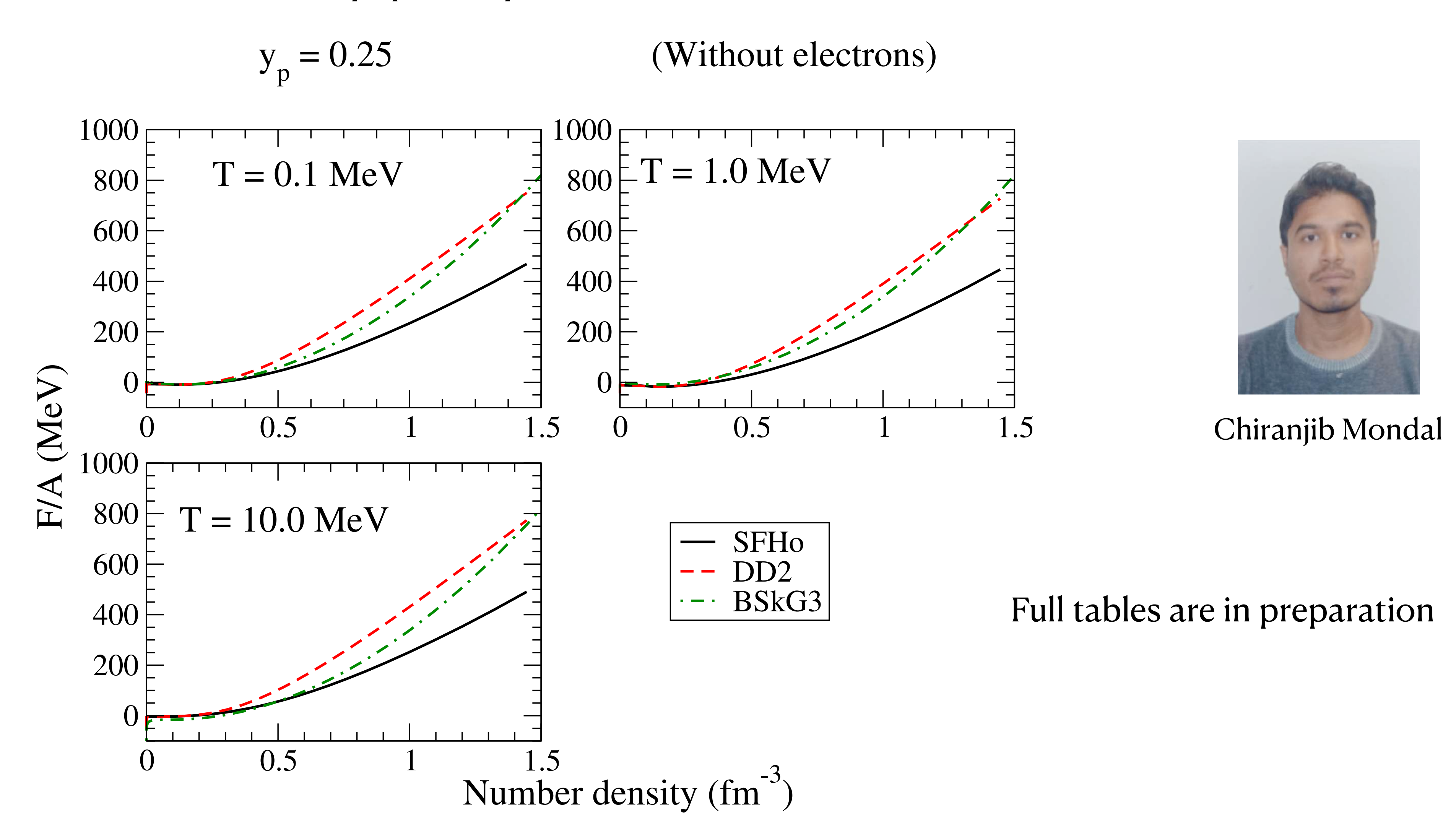
The predictions from the liquid-drop model are sensitive to the parametrisation of the surface energy.

Temperature-dependent Extended Thomas-Fermi (TETF) calculations with BSk24:



The nucleon density profiles can only be well determined in the TETF approach, especially at high densities

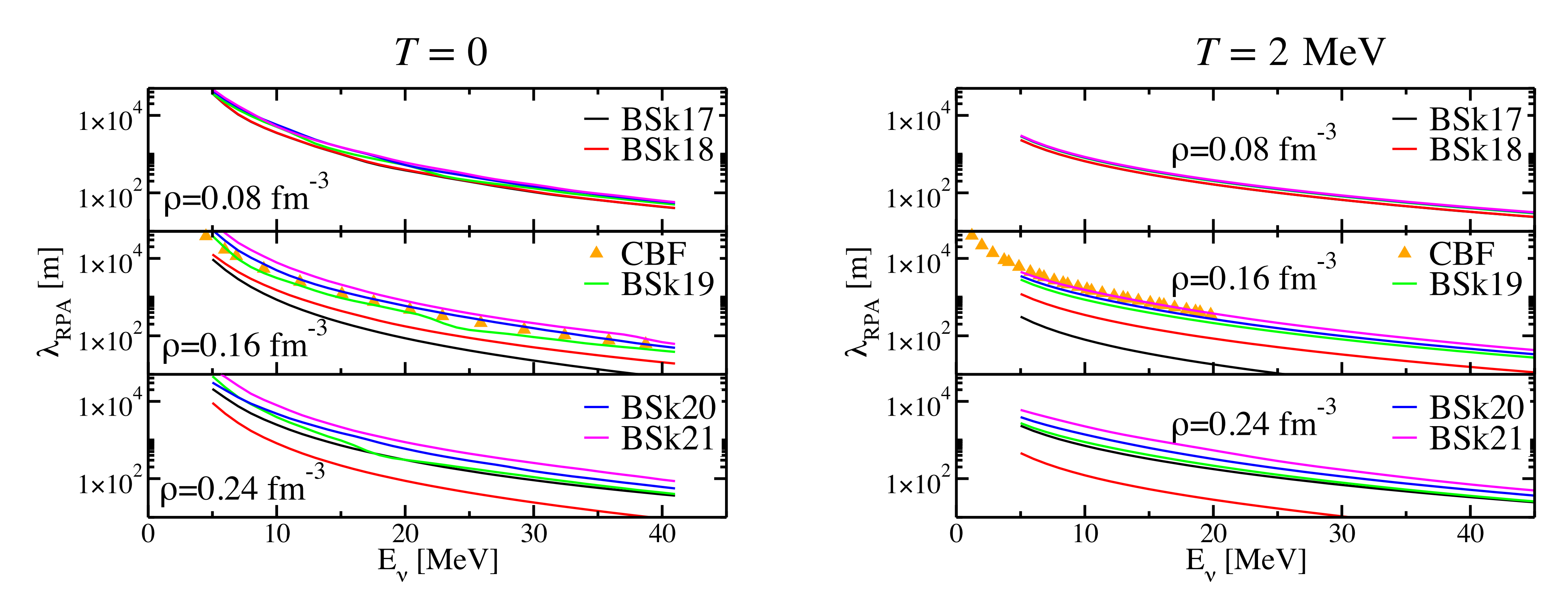
Comparison of our latest functionals with popular equations of state:



Neutrino transport in hot dense matter

The nuclear EDF theory allows for consistent calculations of response functions.

The neutrino mean free path is a key microscopic input for the binary neutron-star merger:



The predictions from BSk20-BSk21 in neutron matter are in good agreement with microscopic calculations

Superfluidity in neutron stars

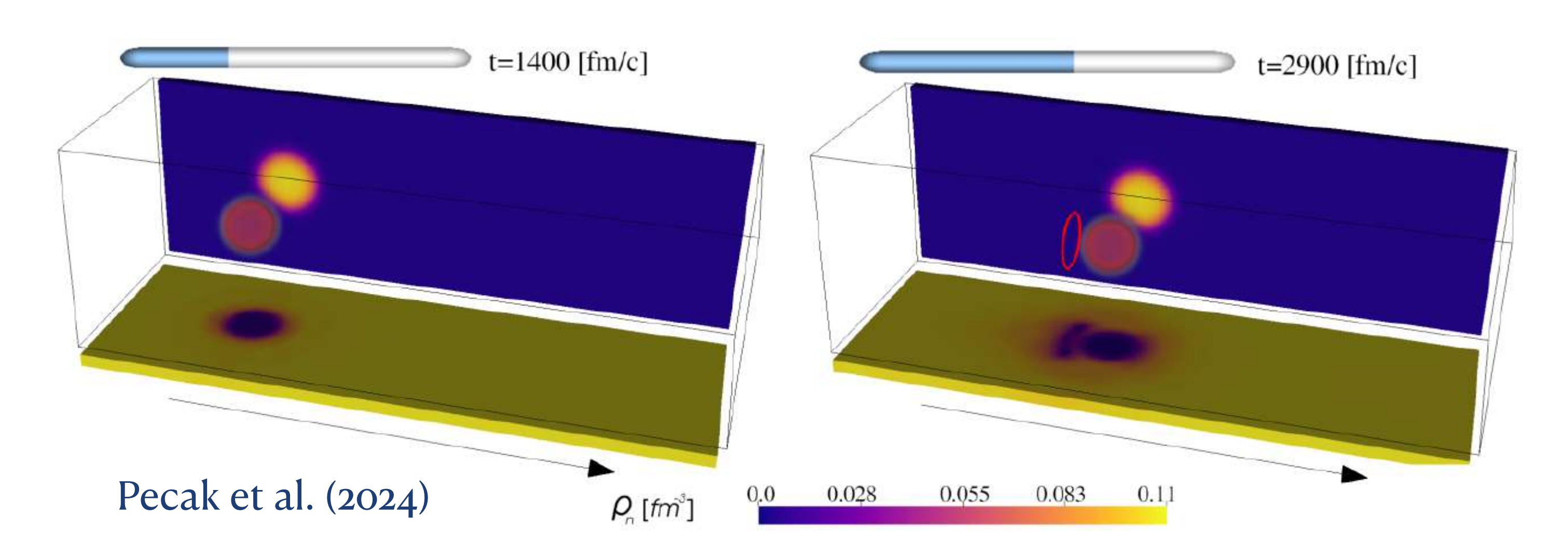
The nuclear EDF theory allows for consistent calculations of superfluid properties:

- Pairing gaps and critical temperatures in the crust and core Chamel et al. (2010), Allard & Chamel (2021)
- Neutron superfluid fraction in the crust Almirante & Urban (2024), Chamel (2025)
- Entrainment couplings of neutron-proton superfluid mixture in the core at arbitrary temperatures Chamel & Allard (2019), Allard & Chamel (2021)

Evidence of a gapless superfluid phase driven by the pinning of quantised vortices from observations of transiently accreting neutron stars

Allard & Chamel (2023), Allard & Chamel (2024)

The nuclear EDF theory allows for full quantum hydrodynamics simulations:



W-I3Sk Toolkit

Nucleation of quantised vortex rings: onset of quantum turbulence? glitch trigging mechanism?

Conclusions

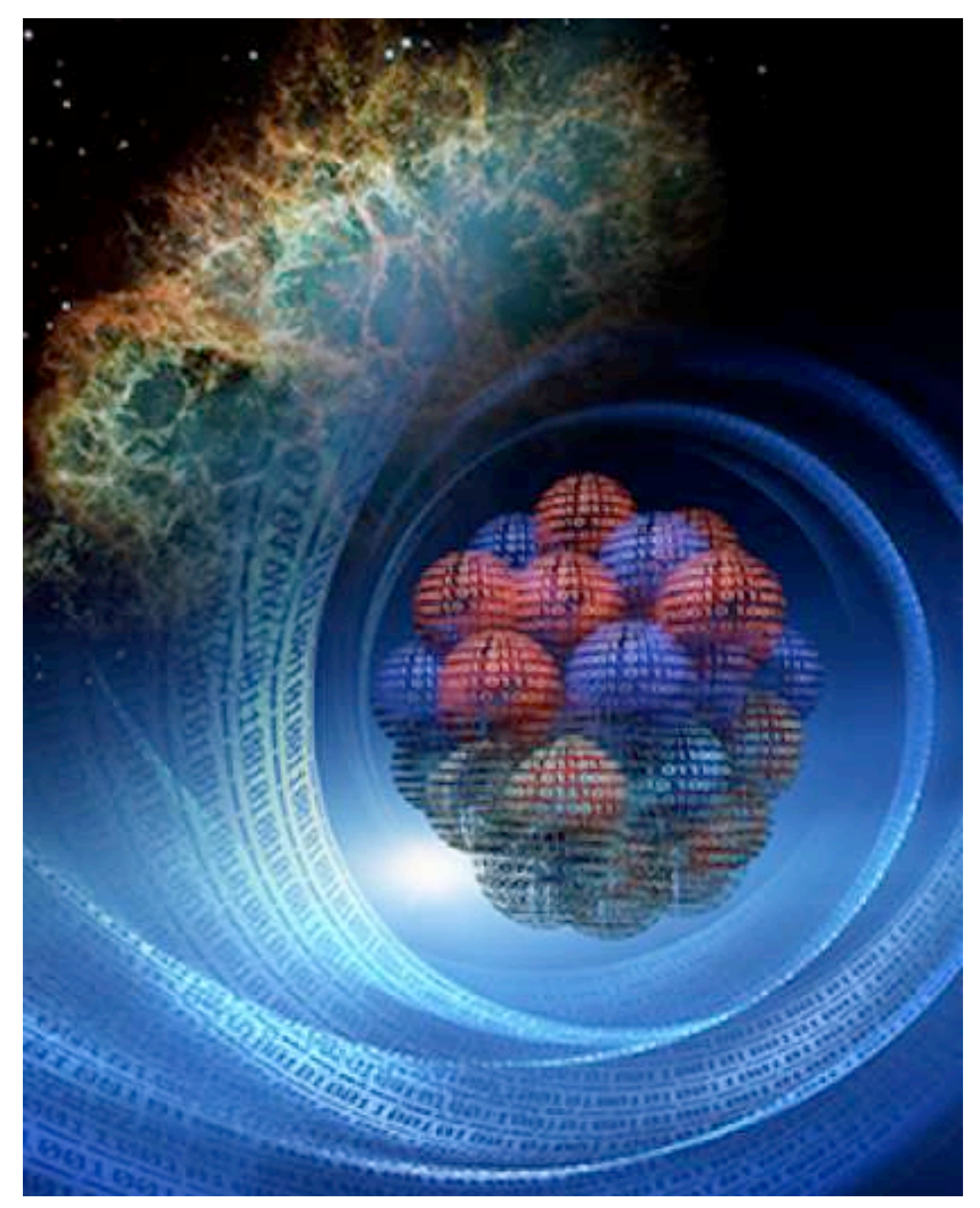
The nuclear EDF theory provides a quantum framework for determining consistently microscopic inputs for neutron stars, their merger, and the r-process nucleosynthesis from ejected material.

Available inputs:

- Properties (masses, radii, etc) of ~104 nuclei for nucleosynthesis http://www.astro.ulb.ac.be/bruslib/
- Unified equations of state for cold neutron stars and magnetars https://compose.obspm.fr
- Detailed composition of the crust and core https://www.ioffe.ru/astro/NSG/BSk/
- Impurity parameters in frozen crusts https://cdsarc.cds.unistra.fr/viz-bin/cat/J/A+A/633/A149
- Electrical and thermal conductivities in the crust https://www.ioffe.ru/astro/conduct/index.html
- ¹S_o pairing gaps and entrainment couplings in the core https://compose.obspm.fr

Work in progress:

- General purpose equations of state using latest BSkG functionals
- ¹S_o pairing gaps and superfluid fraction in the crust



Conceptual art by LeJean Hardin and Andy Sproles/ORNL

Looking ahead

To astrophysicists:

- Which microscopic inputs would like most or need to be improved?
- In which format?
 Tables? What kind of grid should be used?
 Analytical fits?
 Computer codes? In which language?
- Database collecting current astrophysical constraints (e.g. mass-radius measurements)?

To nuclear physicists:

- How to evaluate the errors induced by the form of the functional?
- Systematic comparisons between nonrelativistic and relativistic functionals calibrated to the same data
- How to match consistently hadronic and quark-matter equations of state?